Characterization of the role of Chp2/HP1 in heterochromatin assembly in fission yeast

Rahayu, Anisa Fitri

Department of Basic Biology

School of Life Science

The Graduate University for Advanced Studies, SOKENDAI

September 2023

Table of Contents

Summary

Heterochromatin protein 1 (HP1) is an evolutionarily conserved chromosomal protein that maintains a transcriptionally inert chromatin structure. HP1 family proteins share a basic structure consisting of an N-terminal disordered region, a chromodomain (CD), a disordered middle region called the hinge, and a C-terminal chromoshadow domain (CSD). The CD recognizes histone H3 lysine 9 methylation (H3K9me), a hallmark of heterochromatin, to target heterochromatic loci, while the CSD forms a dimer to provide an interacting surface for other chromosomal proteins. In some HP1 homologs, the CSD is important for heterochromatin targeting or nucleosome binding. HP1 proteins are therefore often referred to as crosslinker or adaptor proteins. HP1 proteins were first identified as one of the factors associated with a phenomenon called position effect variegation (PEV) in *Drosophila* and have subsequently been studied in many other organisms including *Schizosaccharomyces pombe* (*S. pombe*), *Drosophila*, *Xenopus laevis*, plants, and humans.

The fission yeast *S. pombe* is an excellent model organism to study the molecular mechanisms underlying heterochromatin assembly, because like higher eukaryotes, its heterochromatin is marked by di- or tri-methylation of histone H3K9 (H3K9me2/3) and it expresses two HP1 proteins, Swi6, and Chp2. While Swi6 is abundantly expressed and plays a dosage-dependent role in heterochromatin formation, Chp2 is expressed at low levels but plays a distinct role in the heterochromatin assembly. Chp2 recognizes H3K9me via the CD and recruits the Snf2/HDAC repressor complex (SHREC) via the CSD. Among the SHREC components, Chp2 interacts with the chromatin remodeler module protein, Mit1, and this interaction is thought to mediate the recruitment of the entire SHREC. Chp2 also plays a critical role in maintaining the subnuclear localization of the mating-type region. In addition, Chp2, but not Swi6, is tightly associated with a chromatin-enriched nuclear fraction independently of Clr4, which is thought to be related to their distinct properties and roles. However, how the distinct function of Chp2 contributes to the formation of a fully repressed chromatin state remains incompletely understood. To gain insight into the distinct function of HP1 proteins, I focused on *S. pombe* Chp2 and investigated its biochemical properties, in particular its DNA binding ability, and tried to identify Chp2-specific interacting partners by affinity purification.

To characterize the interaction between Chp2 and Mit1, I performed yeast two-hybrid assay and found that the N-terminus of Mit1 is critical for the interaction with Chp2. This conclusion is also supported by a structural study by another group that identified a CkIvV motif (residues 9-13) at the N-terminus of Mit1 interacts with the dimerized Chp2-CSD and also showed that the Mit1 I11R mutation ($Mit1^{I11R}$) disrupts the interaction with Chp2. Using this knowledge, I next generated *S. pombe* cells expressing $Mit1^{I11R}$ and examined the chromatin association of Chp2 by chromatin fractionation assay. Interestingly, I found that Chp2 in the chromatin-enriched fraction was not affected by *clr4*Δ or $mit1^{I11R}$ mutation, suggesting that Chp2 is tightly associated with a chromatin-enriched fraction independent of Clr4 and Mit1, and uses a different mechanism(s) for this association.

HP1 proteins bind to DNA or RNA via the hinge region, and this activity is thought to be involved in their stable chromatin binding. While a similar activity has been demonstrated for Swi6, it has not been clear whether Chp2 has DNA-binding ability and, if so, which domain contributes to the binding. To investigate the relationship between the tight chromatin association of Chp2 and its DNA-binding ability, I prepared recombinant proteins for each Chp2 and Swi6 domain, and performed electrophoretic mobility shift assays (EMSAs). I found that Swi6 binds DNA primarily with its N-terminus and hinge, whereas the hinge and CSD of Chp2 exhibit robust DNA-binding activities. Since DNA-binding activity associated with the CSD has not been described in other HP1 proteins so far, this activity involving the Chp2-CSD may contribute to Chp2-specific function. To further characterize the DNA-binding activities of Chp2, I introduced amino acid substitutions and found that a cluster of basic amino acid residues KRRRSR (residues 271-276) in the hinge and QKK (residues 320-322) at the N-terminus of the CSD cooperatively contribute to the DNA-binding activities of Chp2.

To investigate the importance of DNA binding in Chp2 *in vivo*, I generated *S. pombe* strains expressing mutant Chp2 defective in DNA binding and examined their effect by monitoring the silencing state of a marker gene inserted into a heterochromatic region in the mating type locus. Interestingly, I found that cells expressing mutant Chp2 containing combined mutations of the hinge and the mutations in the N-terminus of CSD showed a silencing defect, suggesting that the DNA-binding activities of the hinge and the N-terminus of CSD are important for the silencing at heterochromatic regions, and that these activities cooperate to maintain the silencing function of Chp2 *in vivo*. To further investigate the effect

of the DNA-binding activities of Chp2 on its localization to heterochromatic regions, I performed chromatin immunoprecipitation (ChIP) assays and found that Chp2 mutants lacking DNA-binding activities exhibited reduced association at heterochromatic regions, suggesting that the DNA-binding activities of Chp2 are required for its stable association with heterochromatic regions.

Next, I tested whether the DNA-binding activities of Chp2 were involved in its tight chromatin association. Interestingly, I found that mutants Chp2, which lack DNA-binding activities, were still tightly associated with the chromatin-enriched fraction, suggesting that Chp2 uses multiple modes in addition to the H3K9me2/3 recognition, DNA-binding activities, and the interaction with Mit1 to maintain stable association with chromatin. While Mit1 has been identified as a Chp2 interacting partner, it is possible that other interacting partner(s) mediate the Chp2-chromatin association. To identify novel interacting partner(s) of Chp2, I generated *S. pombe* strains expressing Chp2 with a tandem affinity purification (TAP) tag expressed under *swi6*$^{+}$ promoter, and performed affinity purification. Mass spectrometry analysis identified a number of novel Chp2 binding partners, including importin/karyopherin family proteins, RNA polymerase II components, factors involved in DNA replication/repair, and the H3K9 methyltransferase Clr4. This mass spectrometry analysis also identified potential phosphorylation sites on Chp2.

Although the physical interaction between HP1 proteins and H3K9 methyltransferases has been identified in other organisms, it remains unclear whether Chp2 or Swi6 interacts directly with Clr4. Since Clr4 has been identified as one of the Chp2 binding partners, I decided to comprehensively investigate the relationship between Chp2 and Clr4. I performed yeast two-hybrid assay and found that although Chp2 only weakly interacts with Clr4, it robustly interacts with either the N-terminus or C-terminus only of Clr4, suggesting that intra- or intermolecular interaction of Clr4 itself may be related to the interaction with Chp2. Interestingly, ChIP experiments revealed that the levels of H3K9me2 at heterochromatic regions are reduced in cells expressing mutant Chp2 defective in the DNA binding, suggesting that the physical interaction between Chp2 and Clr4 contributes to the read-and-write mechanisms underlying heterochromatin assembly.

Taken together, these results suggest that the cooperative DNA-binding activities of Chp2 are critical for its function in heterochromatin assembly. Furthermore, this study reveals the novel interacting partners of Chp2 and the functional link between Chp2 and Clr4.

Thus, these results have important implications for the distinct function of HP1 proteins and the molecular mechanisms underlying higher-order chromatin assembly.

Introduction

General introduction of heterochromatin

In eukaryotic cells, there are two distinct types of chromatin: heterochromatin and euchromatin. These chromosomal structures were first defined as differentially stained chromosomal regions by Emil Heitz in 1928. He described euchromatin as a region that is not stained after telophase and heterochromatin as a region that is stained throughout the cell cycle (Allshire & Madhani, 2018). Later studies have demonstrated that its "closed" state renders the transcriptionally silent region, whereas euchromatin is characterized as its "open" state, making the region accessible to the transcriptional machinery. In general, heterochromatic regions consist of repetitive DNA, including satellite repeats, transposable elements, and retroviruses, which must be transcriptionally silenced (Grewal & Elgin, 2002). Heterochromatin plays an important role in maintaining epigenetic gene regulation during development and chromosomal integrity, as some functional chromosomal domains such as centromeres and telomeres are tightly linked to the heterochromatin (Goto & Nakayama, 2012).

HP1 isoforms and heterochromatin assembly

Heterochromatin Protein 1 (HP1) family proteins localize to the heterochromatin regions and play an important role in maintaining higher-order chromatin structure called heterochromatin (Allshire & Madhani, 2018; James & Elgin, 1986; Vermaak & Malik, 2009). HP1 family proteins were first identified as heterochromatin-associated proteins. HP1 family proteins were also identified as Su(var)2-5, one of the factors associated with a phenomenon called position effect variegation (PEV) in *Drosophila* (Allshire & Ekwall, 2015; James & Elgin, 1986), and later shown to be a reader of the modification provided by another modifier called Su(var)3-9, which encodes a histone methyltransferase (HMTase) that selectively methylates histone H3 at lysine 9 (H3K9), a hallmark of heterochromatin (Schotta et al., 2002). HP1 proteins are evolutionarily conserved within eukaryotes and have subsequently been studied in many organisms including *S. pombe* (Nakayama et al., 2000), *Drosophila* (James & Elgin, 1986; Zhao et al., 2000), *Xenopus laevis* (Meehan et al., 2003), plants (Singh et al., 1991) and humans (Sugimoto et al., 1996). Many organisms express more than one

HP1 isoforms. For example, *S. pombe* has two HP1 isoforms (Swi6 and Chp2), *Xenopus* and humans have three isoforms (HP1α, HP1β, HP1γ), and *Drosophila* has at least five isoforms (HP1a, HP1b, HP1c, HP1d, HP1e) (Allshire & Madhani, 2018; Meehan et al., 2003; Tien et al., 2021; Vermaak & Malik, 2009).

HP1 family proteins share two evolutionarily conserved domains: an N-terminal chromodomain (CD) and a C-terminal chromoshadow domain (CSD) linked by an unstructured hinge region (H). HP1 family proteins recognize the H3K9me mark via their CD and recruit other proteins through their CSD-CSD dimer (Cowieson et al., 2000; Jacobs & Khorasanizadeh, 2002; Paro & Hogness, 1991). The CD is important for nuclear localization, chromatin binding and selective targeting of H3K9me (Paro & Hogness, 1991; Sadaie et al., 2008; Suso Platero et al., 1995). The dimerized CSD provides an interface to preferentially bind proteins with hydrophobic amino acid sequences such as the PxVxL motif. Mouse HPβ recognizes the PxVxL motif to bind its binding partners, and it is suggested that *S. pombe* Swi6 and *Drosophila* HP1 may recognize a similar motif (Cowieson et al., 2000; Thiru et al., 2004). Meanwhile, *S. pombe* Chp2 can recognize the CkIVv motif, suggesting that the recognition of the pentapeptide motif by the dimerized CSD is loosely conserved among different organisms (Leopold et al., 2019; Thiru et al., 2004).

In contrast to the well-conserved CD and CSD of HP1 proteins, the N-terminus (N) and the hinge region (H) connecting the CD and CSD, are structurally disordered and evolutionarily less conserved, but these regions contain some clusters of basic amino acid residues and are involved in binding to DNA or RNA. The hinge of HP1 proteins in some organisms such as *Drosophila*, *Xenopus*, and humans, can bind DNA directly (Meehan et al., 2003; Nishibuchi et al., 2014; Smothers & Henikoff, 2001). To bind the DNA, the hinge relies on basic residues or the conserved KRK motif, which is conserved among HP1 proteins. This positive charge of the basic residues also regulates the binding of CD to H3K9me3 by balancing the total PI value with other domains in the HP1 proteins (Mishima et al., 2013). This DNA binding of HP1 is also regulated by the phosphorylation in the N-terminus region. The N-terminus is known to be subjected for phosphorylation modification that can reduce HP1's DNA binding but increase the specificity to recognize H3K9me (Hiragami-hamada et al., 2011; Mishima et al., 2013; Nishibuchi et al., 2014).

HP1 proteins are also known to be subjected to a variety of modifications such as phosphorylation, SUMOylation, acetylation, or methylation, and a lack of modifications

leads to heterochromatin instability (LeRoy et al., 2009; Maison et al., 2011). However, the most studied modification is phosphorylation. Casein kinase II (CK2) is a ubiquitous and conserved kinase among organisms that is important for the phosphorylation of HP1 proteins (Hiragami-Hamada et al., 2011; Nishibuchi et al., 2014; Shimada & Murakami, 2010). HP1 proteins are also known to be phosphorylated by a mitotic-related kinase, Aurora B kinase (AURKB). This kinase helps HP1 proteins to detach from the chromatin specifically during chromosome condensation and segregation (Nishibuchi et al., 2019; Nozawa et al., 2010).

Heterochromatin establishment and HP1 isoforms in fission yeast

The fission yeast, *S. pombe*, is an excellent model organism to study heterochromatin assembly because the basic heterochromatin structure and the factors involved in heterochromatin assembly are similar to those found in other eukaryotes. Heterochromatin in fission yeast is found at centromeres, telomeres, the mating-type locus, and ribosomal DNA repeat regions. Since fission yeast lacks DNA methylation, therefore, the heterochromatin formation primarily relies on chromatin modification known as transcriptional gene silencing (TGS) and RNAi machinery known as post-transcriptional gene silencing in *cis* (Cis-PTGS) (Allshire & Ekwall, 2015; Goto & Nakayama, 2012).

During the establishment of heterochromatin, although this region is also known as a transcription-repressive region, a low level of transcription still occurs and is required for the propagation of a silent state along heterochromatic regions. Cis-PTGS is a regulation that involves nascent RNA transcription catalyzed by RNA polymerase II with subsequent processing by RDRC (RNA-dependent RNA polymerase complex) and the ribonuclease III enzyme, Dicer, to produce small interfering RNA(s) (siRNA: ~21 nt). This siRNA then acts as RNA machinery and is brought back to the transcription site by the RITS (RNA-Induced Transcriptional Silencing) complex for transcriptional silencing of the homologous transcripts (Fig 1A). Furthermore, this RNAi machinery recruits CLRC methyltransferase through the RITS complex and further increases the methylation level from mono- to di-, and tri-methylation of H3K9. The establishment of trimethylation in H3K9 is preferentially recognized by HP1 proteins and spreads the silent state of heterochromatin. As mentioned above, HP1 proteins will then recognize this H3K9me mark through their CD and subsequently maintain the integrity of heterochromatin (Fig. 1A) (Allshire & Madhani, 2018; Goto & Nakayama, 2012; Jih et al., 2017; Motamedi et al., 2004).

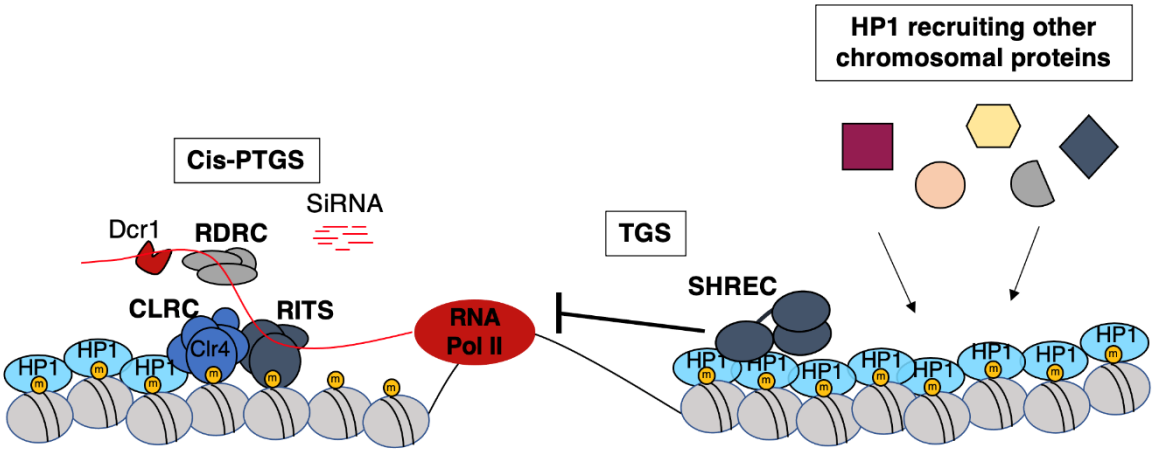

Fig. 1. Schematic model of heterochromatin establishment and maintenance in fission yeast. Nascent transcripts generated by RNA polymerase II are targeted by the RNA machinery consisting of RITS (RNA-induced transcriptional silencing) complex and RDRC (RNA-dependent RNA polymerase complex). RDRC is responsible for synthesizing dsRNAs from the transcripts, and the dsRNAs are subsequently cleaved by Dicer to generate mature siRNAs. These siRNAs are then processed into single-stranded siRNAs and loaded back into RITS to complete the loop. Subsequently, RITS then recruits the CLR4 complex (CLRC) for the spreading of methyl mark on H3K9 into adjacent regions. This process is known as post-transcriptional gene silencing in *cis* (Cis-PTGS). Then, HP1 will recognize the H3K9me and subsequently maintain the silencing of heterochromatin, which is known as transcriptional gene silencing (TGS).

Fission yeast expresses two HP1 isoforms, Swi6 and Chp2, which play distinct roles in the formation of higher-order chromatin structure, in part due to their ability to recruit different partners through their CSD-CSD dimers (Cowieson et al., 2000; Motamedi et al., 2008; M. Sadaie et al., 2008). Swi6 interacts with a diverse set of proteins involved in a variety of nuclear processes (Fischer et al., 2009; Iglesias et al., 2020; Motamedi et al., 2008), whereas Chp2 specifically recruits the Snf2/HDAC repressor complex (SHREC), a family of the nucleosome remodeling and deacetylation complexes (NuRDs) (Job et al., 2016; Leopold et al., 2019; Motamedi et al., 2008; Sugiyama et al., 2007). Deletion of *swi6+* or *chp2+* alleviates silencing at the heterochromatic regions, but the defect is not compensated by reciprocal expression under their original promoters, further emphasizing that Swi6 and Chp2 play distinct roles in the heterochromatin assembly (Motamedi et al., 2008; Sadaie et al., 2008). Nevertheless, Swi6 and Chp2 show similar localization to the same heterochromatin regions through their CD, which recognizes H3K9me2/3. Clr4, a homolog of mammalian SUV39H, is known to provide H3K9me2/3 as a hallmark of heterochromatin in fission yeast.

Swi6 is abundantly expressed and plays a dosage-dependent role in heterochromatin formation, whereas the expression level of Chp2 is low compared to Swi6 (Canzio et al., 2014; Isaac et al., 2017; Sadaie et al., 2008; Sadaie et al., 2004). Like other HP1 homologs, the hinge of Swi6 interacts with RNA to promote RNAi-mediated process or with DNA, presumably to facilitate its chromatin binding (Goto & Nakayama, 2012; Keller et al., 2012; Motamedi et al., 2008; Nishibuchi et al., 2014). Meanwhile, the N-terminus of Swi6 is phosphorylated by casein kinase II (CK2), and the phosphorylation affects its DNA binding and H3K9me-recognition (Nishibuchi et al., 2014).

A recent paper demonstrated the association of Swi6 with the Rix1 RNA processing complex, the nucleoporin, and the inner nuclear membrane (INM), further deciphering how heterochromatin is localized and regulated in cells (Iglesias et al., 2020). However, in contrast to Swi6, the contribution of Chp2 to heterochromatin assembly remains elusive. So far, Chp2 is known to recruit SHREC, a multifunctional protein complex that includes the nucleosome remodeler Mit1 and the histone deacetylase Clr3, to maintain the heterochromatin structure (Job et al., 2016; Motamedi et al., 2008). Further studies have shown that Chp2 specifically interacts with a specific motif in the N-terminal domain of Mit1 to recruit of SHREC complex to the heterochromatic region (Leopold et al., 2019).

The association of Chp2 with the heterochromatic regions is likely dependent on H3K9me recognition. In addition, Chp2, but not Swi6, is tightly associated with a chromatin-enriched nuclear subfraction, and Chp2-chromatin association remains in the *clr4*Δ, which is thought to be related to their distinct roles (Sadaie et al., 2008). These results suggest that Chp2 associates with the chromatin-enriched fraction independently of H3K9me. The mechanisms by which Chp2 tightly associates with the chromatin remain unclear. A possible explanation for the tight chromatin association of Chp2 is due to Chp2's DNA/RNA binding, its binding partner, or an unknown modification that regulates Chp2-chromatin association. Like other HP1 homologs, Chp2 may use all of these mechanisms to act as a cross-linking protein that brings together nucleosomal DNA, H3K9me, and other non-histone protein complexes to form higher-order chromatin structure.

Materials and methods

Plasmids construction

The coding sequence for Chp2 was amplified by PCR and cloned into the pGBKT7 vector (Clontech) to produce Chp2 fused to the Gal4 binding domain (Gal4-BD). The coding sequence for Mit1 was amplified by PCR and cloned into the pGADT7 vector (Clontech) to produce Chp2 fused to the Gal4 activation domain (Gal4-AD). The coding sequences of Mit1 domains (N; 1 – 505 aa, N-Helic; 1 – 1051 aa, Helic; 505 – 1051 aa, Helic-CID; 505 – 1418 aa, CID; 1051 – 10418 aa) were amplified by PCR and cloned into PGADT7 (Clontech) using NEBuilder HiFi DNA assembly master mix (NEB). The coding sequence for Clr4 was amplified by PCR and cloned into the pGADT7 vector (Clontech) to produce Clr4 fused to the Gal4-AD. The coding sequence for Clr4 mutants (CDΔ; Δ8 – 63 aa, NpreΔ; Δ193 – 330 aa, SETΔ: Δ331 – 452 aa) and Clr4 domains (N-H; 1 – 192 aa, N-Npre; 1 – 330 aa, Npre; 192 – 490 aa, SET; 330 – 490 aa) were PCR amplified and cloned into PGADT7 (Clontech) using NEBuilder HiFi DNA assembly master mix (NEB). All primers used to generate the above constructs for the yeast two-hybrid assay are listed in Table 1.

Plasmids for the expression of recombinant 6×His tagged Swi6 or Chp2 in *E. coli* cells have been described previously (Sadaie et al., 2008). Coding sequences for Chp2 domains (N; 1 – 164 aa, CD; 165 – 244 aa, H; 239 – 313 aa, CSD; 314 – 381 aa), and Swi6 domains (N; 1 – 80 aa, CD; 81 – 139 aa, H; 140 – 260 aa, and CSD; 261 – 329 aa) were PCR amplified and cloned into *Nde*I and *Bam*HI sites of pET15b using NEBuilder HiFi DNA assembly mix (NEB). All mutations in the coding sequences of Chp2 were introduced by site-directed mutagenesis using the primers listed in Table 1.

Strains and culture media

The strains used in this study are listed in Table 2. The media to culture *S. pombe* cells were prepared as described previously (Moreno et al., 1991). To create a strain carrying $mit1^{I11R}$, fthe $ura4^{+}$ gene was first introduced into the *mit1* coding region through homologous recombination (*mit1-N::ura4*$^{+}$). The *mit1* coding region was then amplified by PCR, cloned into pBluescript, and subjected to site-directed mutagenesis to generate the $mit1^{I11R}$ mutation. The *mit1* coding region containing the $mit1^{I11R}$ mutation was amplified by PCR, introduced

into cells harboring *mit1-N::ura4*$^{+}$, and stable clones in which *mit1-N::ura4*$^{+}$ was replaced by *mit1*^{I11R} were selected using counter-selective media containing 5-fluorotic acid (5-FOA). Strains expressing 3×FLAG-tagged, wild-type and mutant Chp2 were generated as described previously (Fennessy et al., 2014) using the *rpl42*^{P56Q} mutant and a *rpl42*$^{+}$ cassette to replace wild-type *chp2*$^{+}$ at the endogenous locus. Strain carrying *mit1*^{I11R} was crossed with strains carrying 3xFLAG-tagged, 3×FLAG-tagged, wild-type and mutant Chp2, or N-terminal TAP-tagged (NTAP-Chp2, wild type, and *CSD*Δ). *clr4*Δ in every strain was constructed through homologous recombination with hygromycin gene.

Antibodies

The following antibodies were used in this study: anti-myc, anti-HA (3F10; Sigma), anti-FLAG (A8592; Sigma), anti-tubulin (T5168; Sigma), anti-Swi6, anti-Chp2 (Sadaie et al., 2008), anti-H3K9me2 (m5.1.1, gift from Dr. Takeshi Urano), anti-H3K14Ac (ab52946; Abcam).

Yeast two-hybrid assay

Each of the pGBKT7-derived plasmid to express GAL4-BD-fused protein (bait) was introduced into *S. cerevisiae* AH109 strain and transformants were selected on SD/-Trp medium. Each of the pGADT7-derived plasmid to express GAL4-AD-fused protein (prey) was introduced into Y187 strain, and transformants were selected on SD/-Leu medium. The growing cells carrying either bait and prey were mated and dropped on YPDA medium and incubated for 5 – 6 hours at 30^{o}C. The mating strains were spread onto SD/-Trp/-Leu medium and incubated for 2 – 3 days at 30^{o}C. To detect protein-protein interactions, the diploid cells were grown on SD/-Trp/-Leu/-His medium containing gradient concentration from 0, 5, and 15 mM of 3-amino-1,2,4-triazole (3-AT).

Immunoblotting

Harvested cells (~2×10^{7}) were washed once with ice-cold water, resuspended in 75 µl of alkaline-2ME solution (1.85N NaOH and 1.07 M 2-mercaptoethanol) and incubated on ice

for 5 min. The cell suspension was mixed with 75 µl of 50% TCA and further incubated on ice for 5 min. Cellular proteins were precipitated by centrifugation, and the protein pellets were resuspended in SDS sample buffer, followed by boiling at 95°C for 5 min. Protein samples were resolved by SDS-polyacrylamide gel electrophoresis (PAGE) and subjected to Western blotting.

Chromatin fractionation assay

The chromatin fractionation assay was performed as previously described (Sadaie et al., 2008) with some modifications. Briefly, cells (2.5×10^8 cells) were harvested, washed once with stop buffer (150 mM NaCl, 50 mM NaF, 10 mM EDTA, 1 mM NaN_3), and placed on ice for 5 min. The cells were resuspended in PEMS (100 mM PIPES, 10 mM EGTA, 10 mM $MgSO_4$, 1.2 M sorbitol) containing 1 mg/ml lysing enzyme and 1 mg/ml Zymolyase 100T, and incubated at 37°C for 20 min. The cell suspensions were spun and the resulting cell pellet was washed twice with 1.2 M sorbitol and then lysed with HBS buffer (25 mM MOPS [pH7.2], 60 mM b-glycerolphosphate, 15 mM $MgCl_2$, 15 mM EGTA, 15 mM p-nitrophenylphosphate, 0.1 mM sodium vanadate) containing 1 mM phenylmethylsulfonyl fluoride (PMSF), protease inhibitor (Complete™ [Roche]), and 0.5% Triton X-100. The resulting lysate, whole-cell extract, was spun at 21,880 ×*g* for 15 min at 4°C to obtain supernatant and pellet fractions. The whole-cell extract, supernatant and pellet fractions. The whole-cell extract, supernatant and pellet fractions were resolved by SDS-PAGE and subjected to Western blotting.

Production of recombinant proteins

Recombinant 6×His-tagged Swi6 and Chp2 proteins were expressed in *E. coli* BL21 (DE3) and purified by immobilized metal affinity chromatography (TALON; Clontech) according to the manufacturer's instructions. Recombinant proteins were further purified by anion exchange chromatography (SOURCE 15Q; Cytiva) or cation exchange chromatography (SOURCE 15S; Cytiva). Full-length Chp2 dimers were further purified by size exclusion chromatography (Superdex 200 pg, Cytiva).

Electrophoretic mobility shift assays (EMSAs)

EMSAs were performed as previously described (Nishibuchi et al., 2014) with some modifications. Different concentrations of proteins were incubated with with 0.19 pmol of 203-bp double-stranded DNA corresponding to pericentromeric repeats in 10 µl of EMSA assay buffer (20 mM Tris-HCl [pH 7.5], 50 mM NaCl, 1 mM dithiothreitol [DTT], and 0.1 mg/ml bovine serum albumin [BSA]) for 15 min at 37°C. After incubation, 1 µl of 30% sucrose was added, and the samples were loaded onto 5% native polyacrylamide gels in 0.5× Tris-borate-EDTA. Gels were run at room temperature at 100 V for 1.5 h. Gels were stained with SYBR Gold (Invitrogen), visualized using a ChemiDoc Imaging System (Biorad), and quantified using Fiji. Binding curves were fitted with the following equation: fraction bound = 1 − fraction unbound. Curve fitting was performed using Igor Pro software.

Silencing assay

Silencing assays were performed as described previously with some modifications (Sadaie et al., 2008). Cells carrying a silencing marker (*mat3M::ura4*$^{+}$) were grown, and collected by centrifugation and resuspend in water. Serial dilutions (10-folds) were prepared and spotted on non-selective medium (YEA; yeast extract with adenine), minimal medium lacking uracil (PMG-Ura) or minimal medium with 5 fluoroorotic acid (5FOA) (PMG+5FOA). Plates were then incubated at 30ºC for 2 – 4 days.

Chromatin immunoprecipitation (ChIP) and quantitative PCR (qPCR)

For all chromatin immunoprecipitation (ChIP) experiments, the cells were grown at 30°C in YEA until the cell density reached 1×10^{7} cells/ml. For Swi6 and Chp2 ChIP experiments, cells were incubated for 2 h at 18°C and fixed with 1% formaldehyde for 30 min at 18°C. For the H3K9me2 and H3K14ac ChIP experiments, the cells were immediately fixed with 1% formaldehyde for 20 min at 25°C. The fixed cells were harvested by centrifugation, washed twice with ice-cold phosphate-buffered saline (PBS), transferred to a 1.5 ml tube, frozen in liquid nitrogen, and stored at -80°C before use. Antibodies were preincubated with 20 µL IgG-conjugated or Protein A-conjugated magnetic beads (Dynabeads; Thermo Fisher Scientific). Cells were lysed with ChIP lysis buffer (50 mM HEPES-KOH [pH 7.5], 140 mM

NaCl, 1 mM EDTA, 1% Triton-X, 0.5% Na-Deoxycholate) containing protease inhibitor (Complete™; Roche) and 1mM PMSF, and disrupted using Multi-Beads Shocker (Yasui Kikai). Chromatin was sheared by sonication using Bioruptor (Cosmobio) and incubated with antibody-bound magnetic beads overnight at 4°C. Beads were washed twice with ChIP lysis buffer, twice with ChIP lysis buffer containing 0.5 M NaCl, twice with wash buffer (10 mM Tris-HCl [pH 8.0], 250 mM LiCl, 1 mM EDTA, 0.5% NP-40, 0.1% Na-deoxycholate), and twice with TE buffer (10 mM Tris-HCl [pH 8.0] and 1 mM EDTA). Precipitated chromatin was incubated with RNase A, eluted from the beads by incubating with TES buffer (50 mM Tris-HCl [pH 8.0] and 10 mM EDTA, 1% SDS), and reverse cross-linked by incubation at 65°C overnight. DNA samples were purified using NucleoSpin gel and PCR clean-up (Macherey-Nagel). Quantitative PCR (qPCR) was performed using Luna qPCR master mix (NEB) and a real-time PCR machine (StepOnePlus™; ABI). Primers used for qPCR are listed in Table 1.

Fluorescence microscopy of *S. pombe* cells

For observation of GFP-Chp2 cellular localization, cells were cultured overnight on EMM medium plate at 30°C to obtain the logarithmic growth phase. The cells were suspended in EMM liquid medium and mounted on a slide glass. The fluorescence images were taken using a DeltaVision Personal microscopy system (Cytiva) equipped with a 100× oil-immersion objective lens (PlanApo, NA = 1.45, Olympus) and a chilled CCD camera (CoolSNAP HQ2, Photometrics) at 25˚C. The images were taken at 10 focal planes with 0.3 μm intervals for observation of Chp2 foci. Quantification of the fluorescence signal was performed using the Fiji software. Chp2 foci were manually marked as ROI in the Z-stack images. The fluorescent intensity was measured by 3D Objects Counter after the subtraction of the background.

Tandem affinity purification (TAP)

Tandem affinity purification (TAP) was performed as previously described (Buker et al., 2007) with some modifications. Cells (2.0×10^{10} cells) were harvested and washed once with stop buffer (150 mM NaCl, 50 mM NaF, 10 mM EDTA, 1 mM NaN_3). The cell pellet was resuspended in iso-volume lysis buffer (50 mM HEPES [pH 7.6], 300 mM potassium acetate,

5 mM magnesium acetate, 20 mM b-glycerol phosphate, 1 mM EGTA, 1 mM EDTA, 0.1% (v/v) Nonidet P-40 [NP-40]) containing protease inhibitors (1 mM PMSF, 1× Complete™ [Roche]), and 35 g glass beads were added to the cell suspension. Cells were disrupted using Multi Beads Shocker (Yasui Kikai). Whole cell lysates were harvested by centrifugation for 20 min. The cell lysates were transferred to a 50-mL Falcon tube and incubated with 400 mL of pre-washed IgG Sepharose 6 Fast Flow beads (Cytiva) for 3 h at 4ºC. The beads and immobilized proteins were collected by centrifugation and washed twice with lysis buffer with rotation for 15 min at 4ºC. The beads were then loaded onto a Bio-Rad poly prep column and washed once with lysis buffer and twice with TEV buffer (10 mM Tris-HCl [pH 8.0], 150 mM NaCl, 1 mM $Mg(oAc)_2$, 0.5 mM EDTA, 0.5 mM dithiothreitol [DTT], 0.1% NP-40). After washing, the beads were transferred to 5 mL Lobind screw-caps tubes (Eppendorf) and mixed with 1 mL TEV buffer, 10 µl DTT, and 10 µl TEV protease, and incubated overnight at 4ºC. The TEV eluates were transferred to the new tubes, added 3× elution volume of calmodulin-binding buffer (10 mM Tris-HCl [pH 8.0], 150 mM NaCl, 1 mM $Mg(oAc)_2$, 1 mM imidazole, 2 mM $CaCl_2$, 10 mM 2-mercaptoethanol, 0.1% NP-40) and 3/1000 volume of 1 M $CaCl_2$, and incubated with 200 µL of calmodulin beads (Agilent) for 2 h at 4ºC. The beads were washed twice with calmodulin binding buffer with rotation for 15 min at 4ºC. The beads were transferred to the Muromac column or Bio-Rad poly prep column and washed twice with calmodulin binding buffer supplemented with 0.02% NP-40. Bound proteins were eluted with calmodulin elution buffer (10 mM Tris-HCl [pH 8.0], 150 mM NaCl, 1 mM $Mg(oAc)_2$, 1 mM imidazole, 20 mM EGTA, 10 mM 2-mercaptoethanol, 0.02% NP-40). The proteins in the elution fractions were precipitated with 2× volume of ethanol, and incubated overnight at −25ºC. The precipitated proteins were dissolved in 2× SDS sample buffer, resolved on an 8% SDS-PAGE gel, and analyzed by immunoblotting. Alternatively, the gels were stained using SilverQuest Silver Staining Kit (Invitrogen) and subjected to LC-MS/MS analysis.

Table 1. Primer list

Primer Name	gene	Sequence (5'-3')	Description
mit1_GA_Fw	*mit1*$^+$	CATATGGCCATGGAGGCCGAAATGCCAAAAGAAGAT GATTCTTTATG	
mit1_GA_Rv	*mit1*$^+$	TGCGGCCGCTGCAGGTCGACGCTAAAGAGTTTTTGCT TCATTAATTATG	
Mit1_R1_Rv	*mit1*$^+$	TGCGGCCGCTGCAGGTCGACGCTAATCTGTTTCTTTA GGAGGTGGTTC	
Mit1_R2_Fw	*mit1*$^+$	CATATGGCCATGGAGGCCGAAGAAACAGATAGAAAT CGCTGGAAAGCG	
Mit1_R2_Rv	*mit1*$^+$	TGCGGCCGCTGCAGGTCGACGCTATTCATCACCAGCC TCTTCAAATAATGC	
Mit1_R3_Fw	*mit1*$^+$	CATATGGCCATGGAGGCCGAAGAGGCTGGTGATGAA CCGTCTATTAAG	
Mit1_Nter_Rv	*mit1*$^+$	TGCGGCCGCTGCAGGTCGACGCTAAGCTTTATTATCG TTTTCTGTGGA	Yeast two hybrid assay of *mit1*$^+$
Mit1_ZNF_Fw	*mit1*$^+$	CATATGGCCATGGAGGCCGAAGCTCCTTATTTCTCAC TTCTTTAC	
Mit1_ZNF_Rv	*mit1*$^+$	TGCGGCCGCTGCAGGTCGACGCTAATCACAAGGATG CATAGAACATTC	
Mit1_CD_Fw	*mit1*$^+$	CATATGGCCATGGAGGCCGAAGTTTGTAATGAATGTT CTATG	
Mit1_CD_Rv	*mit1*$^+$	TGCGGCCGCTGCAGGTCGACGCTAATTTCTATCTGTT TCTTTAGG	
Mit1_Nter-UP_Rvx	*mit1*$^+$	GTCGTGACTGGGAAAACCCTGGCGCTGTGTATTTGGA GTTGTCCT	
Mit1_Nter_Fwy	*mit1*$^+$	TCCTGTGTGAAATTGTTATCCGCTTCTTCATCTGATAC AAATAAG	
Mit1_I11R_SDM	*mit1*$^+$	CTTTATGTAAAAGAGTAGTACGTCGTG	*mit1*$^+$ mutant
Mit1_UP_fw	*mit1*$^+$	ATGCTATGAATGCTGCTGCATTC	
Mit1_seq_545	*mit1*$^+$	CGGAAATTGAGTCCACAGAAAAC	
Mit1_seq_1157	*mit1*$^+$	CGGACTTGAGCTTTTGGTCTAGA	
Mit1_seq_1657	*mit1*$^+$	GGTGGTACACTAATGCCATATC	
Mit1_seq_2261	*mit1*$^+$	CGGAAAAGGTGACTGAACTTCATC	
Mit1_seq_2912	*mit1*$^+$	CTCATCAAGACATGCAAGCGAT	
Mit1_seq_3427	*mit1*$^+$	GCACACCACAAAATCCATTATGGC	*mit*$^+$ sequencing and mutant strain construction
Mit1_seq_4007	*mit1*$^+$	GTGGAACACCTCACTTTAGTGGA	
Mit1_Nter880_Rv	*mit1*$^+$	GGATAACTAGATCCTGTCCAGA	
Mit1_UP_fw2	*mit1*$^+$	GTATCCGCAAATACCTATATGGCTC	
Mit1_seq_Nter42_Fw	*mit1*$^+$	TCGTGAACCGCTTGATGTTTTAC	
Mit1_UP_Check	*mit1*$^+$	ATGCTTATGCGTTTCCTCGTAAG	
T7	T7	TAATACGACTCACTATAGGG	
T7 terminator	T7	GCTAGTTATTGCTCAGCGG	
ura4-5'-RV	*ura4*$^+$	CATATAGCCAGTGGGATTTGTAGC	
Chp2-N_pET15b_Fw (NdeI)	*chp2*$^+$	CTGGTGCCGCGCGGCAGCCATATGATGGTCAAAAGT GCCGACCTT	*chp2*$^+$ and *swi6*$^+$ recombinant proteins
Chp2-N_pET15b_Rv (BamHI)	*chp2*$^+$	CGGGCTTTGTTAGCAGCCGGATCCACTAGCAATATAC TCAAACCCTTC	

Chp2-CD_pET15b_Fw (NdeI)	*chp2*$^+$	CTGGTGCCGCGCGGCAGCCATATGTCTGGTAGTGAA GATAAAAATTCAGAT	
Chp2-CD_pET15b_Rv (BamHI)	*chp2*$^+$	CGGGCTTTGTTAGCAGCCGGATCCTCGCGTCAATCGT ATTAAAGACGAAAG	
Chp2-H_pET15b_Fw (NdeI)	*chp2*$^+$	CTGGTGCCGCGCGGCAGCCATATGTTAATACGATTGA CGCGAAGCCGC	
Chp2-H_pET15b_Rv (BamHI)	*chp2*$^+$	CGGGCTTTGTTAGCAGCCGGATCCTTTTGAAGATTTA TCAGATTTCATATATTTCTC	
Chp2-CSD_pET15b_Fw (NdeI)	*chp2*$^+$	CTGGTGCCGCGCGGCAGCCATATGAATTTTAAACCTC CTTTTCAGAAGAAAAG	
Chp2-CSD_pET15b_Rv (BamHI)	*chp2*$^+$	CGGGCTTTGTTAGCAGCCGGATCCTTATGTAAATTTA ATATGAGCCTC	
Swi6-CD_pET15b_Rv (BamHI)	*swi6*$^+$	TCGGGCTTTGTTAGCAGCCGGATCCTGGTCTTCCTCC ATGTTCATTCC	
Swi6-CD_pET15b_Fw (Nde1)	*swi6*$^+$	CTGGTGCCGCGCGGCAGCCATATGTATGTTGTAGAA AAGGTTTTAAAACACCGTATGGC	
Swi6-Nter_pET15b_Fw (NdeI)	*swi6*$^+$	CTGGTGCCGCGCGGCAGCCATATGATGAAGAAAGGA GGTGTTCGATCT	
Swi6-H_pET15b_Rv (BamHI)	*swi6*$^+$	TCGGGCTTTGTTAGCAGCCGGATCCAACCGTCAGCTC TCTGTTGTC	
Swi6-H_pET15b_Fw (NdeI)	*swi6*$^+$	CTGGTGCCGCGCGGCAGCCATATGGAACCTTCTAAA AGAAAGAGGACTGCAAGAC	
pET15b-Swi6-CSD_Fw	*swi6*$^+$	GCCGCGCGGCAGCCATATGAAACAAGTAGAAAACTA TGATTCTTGGGAAGAC	
pET15b-Swi6-CSD_Rv	*swi6*$^+$	GCTTTGTTAGCAGCCGGATCCTTATTCATTTTCACGG AACGTTAAGTGGC	
Chp2 KR271-276A	*chp2*$^+$	GATGACTCTATATCTTATGCTGCTGCTGCTAGCGCTA ATGCAGCAAATCGTATTAC	
Chp2-PPFQAA	*chp2*$^+$	AATTTTAAACCTCCTTTTCAGGCTGCTAGCTGGGAAG ATTTGGTTGAT	
Chp2-CSD-PPFQAA	*chp2*$^+$	ATCAACCAAATCTTCCCAGCTAGCAGCCTGAAAAGG AGGTTTAAAATTCAT	
Chp2-PPFAAA mutant	*chp2*$^+$	TCTTCAAAAAATTTTAAACCTCCTTTTGCTGCTGCTA GCTGGGAAGATTTGGTTGATTGT	
Chp2-CSD PPFAAA mutant	*chp2*$^+$	ACAATCAACCAAATCTTCCCAGCTAGCAGCAGCAAA AGGAGGTTTAAAATTCATATG	
chp2-RV	*chp2*$^+$	AGATATCCCTTCTGCTTTGGTTTGTGA	*chp2*$^+$ mutants and sequencing
Chp1/g-up	*chp2*$^+$	AACTTACACAACCACCCAGA	
SpChp2_5'check Fw	*chp2*$^+$	ATGTTGGTATATCTGGAAAGTCT	
Chp2_DW_Rv	*chp2*$^+$	CACTGTAAAAGCGTTGAACGAG	
SpChp2-check_Fw	*chp2*$^+$	CCAGCATCAAATTAATTAGAGCAG	
Chp2-N-Rv (EcoRI)	*chp2*$^+$	CGAATTCAATTTTTATCTTCACTACCAG	
Chp2 check 5utr_Fw	*chp2*$^+$	CTGTTGATTAACCAAGCATAG	
Rpl42 DW-RV	*rpl42*$^+$	CCGAAATCACAACACCTGTCTTC	
Rpl42 g-up	*rpl42*$^+$	TGGGAAATACTGCTTAGCCTGACT	
Rpl42_Rv	*rpl42*$^+$	GCTCCAATATTGAGAACAGACCT	
Sp_SIRE1/4_Rv	perincentromeric	TGTGCGGAATGTCTACTTCAA	EMSA DNA probe
Sp_SIRE1/4_Fw	Perincentro	AGCCTCAAGTGACTGCATTAAAG	

	meric		
SpClr4-pFw2	*clr4*$^+$	TGGTTTTGCGCATTTATC	Δ*clr4* amplification and checking
spClr4-DW-Rv	*clr4*$^+$	GCTCCTTCTATAGCTTCTGAAGG	
TEFt check	drug resistance gene	CGATTCGATACTAACGCCGCCATCCA	
clr4-DW-Rv3	*clr4*$^+$	CTGCAGCTACTAATGAAGAGAGTG	
act1 RT-Fw1	*act1*$^+$	CGTGCCCCTGAAGCTCTTT	qPCR of ChIP
act1 RT-Rv1	*act1*$^+$	CTCATGAATACCGGCGTTTTC	
SpCen-dgF-Fw	*dgF*	CTGCGGTTCACCCTTAACAT	
SpCen-dgF-Rv	*dgF*	CAACTGCGGATGGAAAAAGT	
cenH dh Rv	*cenH*	GCTAAGATCGATTGGTGACG	
cenH dh Fw	*cenH*	AAGTTCACTGTTCTTATACACTGG	
SPAC212.11RT-Fw2	telomere	GTCGTGGTCATAAACGCACATAC	
SPAC212.11RT-Rv2	telomere	CCAACACTACCATGAACACGATTC	
ura4 RT-Fw1	*ura4*$^+$	GGCCTCAAAGAAGTTGGTTTACC	
ura4 RT-Rv1	*ura4*$^+$	GAAGACATTTCAGCCAAAAGCA	
NTAP-Chp2-DCSD_pAL2_Fw	*chp2*$^+$	TAAGCTCATATTAAATTTACATAA	*NTAP-chp2*$^+$
NTAP-Chp2-DCSD_pAL2_Rv	*chp2*$^+$	AGGTTTAAAATTTTTTGAAG	
Chp2_H-CSD_Fw	*chp2*$^+$	CATATGGCCATGGAGGCCGAATTGACGCGAAGCCGCGCACG	
Clr4_GA_Fw	*clr4*$^+$	CATATGGCCATGGAGGCCGAAATGTCGCCTAAACAAGAGGAG	Yeast two hybrid screen of *clr4*$^+$
Clr4_GA_Rv	*clr4*$^+$	TGCGGCCGCTGCAGGTCGACGTTAACCGAAAAGCCAGCCACGACA	
Clr4-H_GA_Fw	*clr4*$^+$	CATATGGCCATGGAGGCCGAACTAAAGGGAAGTAACTCCGACTCG	
Clr4-H_GA_Rv	*clr4*$^+$	TGCGGCCGCTGCAGGTCGACGAGGGTTTCGCGGTTTTGTGAGAATTGA	
Clr4-Npre_GA_Rv	*clr4*$^+$	TGCGGCCGCTGCAGGTCGACGAAGCGGAAGAGTTCTACCACGTTG	
Clr4-Npre_GA_Fw	*clr4*$^+$	CATATGGCCATGGAGGCCGAAAAACTTGACTCTTATACCCATCT	
Clr4-SET_GA_Fw	*clr4*$^+$	CATATGGCCATGGAGGCCGAAGAAATATTTAAAACAAAAGAAAAAGGA	

Table 2. Strain list

Strain name	Genotype	Source
SPM2267	*h+ ade6-216 ura4DS/E leu1-32 his7 chp2::3F-chp2+*	This study
SPAF40	*h+ ade6-M2 ura4DS/E leu1-32 his7 chp2::3F-chp2+ clr4Δ::KanMX6*	This study
SPAF43	*h+ ade6-216 ura4DS/E leu1-32 his7 chp2::3F-chp2+ mit1::mit^{I111R}*	This study
SPAF111	*h90 ade6-216 ura4DS/E leu1-32 mat3-M(EcoRV)::ura4+ chp2::3x3F-chp2ΔCSD rpl42::rpl42^{P56Q}*	This study
SPM1468	*h- ade6-210 ura4DS/E leu1-32 otr1R::ura4+*	This study
SPM1557	*h- ade6-210 ura4DS/E leu1-32 otr1R::ura4+ swi6::NTAP-chp2+-pAL2BP*	This study
SPM4157	*h- ade6-210 ura4DS/E leu1-32 otr1R::ura4+ swi6::NTAP-chp2+-pAL2BP mit1::mit^{I111R}*	This study
SPAF53	*h- ade6-210 ura4DS/E leu1-32 otr1R::ura4+ swi6::NTAP-chp2DCSD-PAL2*	This study
PG1783	*h90 (?) ade6-210 ura4DS/E leu1-32 mat3-M(EcoRV)::ura4+ chp2Δ::LEU2*	(Thon & Verhein-Hansen, 2000)
SPAF110	*h90 ade6-216 ura4DS/E leu1-32 mat3-M(EcoRV)::ura4+ chp2::3x3F-chp2 rpl42::rpl42^{P56Q}*	This study
SPAF99	*h90 ade6-216 ura4DS/E leu1-32 mat3-M(EcoRV)::ura4+ chp2Δ::rpl42+kanMX6 rpl42::rpl42^{P56Q}*	This study
SPAF119	*h90 ade6-216 ura4DS/E leu1-32 mat3-M(EcoRV)::ura4+ chp2::3x3F-chp2^{5KRA} rpl42::rpl42^{P56Q}*	This study
SPAF100	*h90 ade6-216 ura4DS/E leu1-32 mat3-M(EcoRV)::ura4+ chp2Δ::rpl42+kanMX6 rpl42::rpl42^{P56Q}*	This study
SPAF125	*h90 ade6-216 ura4DS/E leu1-32 mat3-M(EcoRV)::ura4+ chp2::3x3F-chp2^{3QKA} rpl42::rpl42^{P56Q}*	This study
SPAF135	*h90 ade6-216 ura4DS/E leu1-32 mat3-M(EcoRV)::ura4+ chp2::3x3F-chp2^{2KA} rpl42::rpl42^{P56Q}*	This study
SPAF126	*h90 ade6-216 ura4DS/E leu1-32 mat3-M(EcoRV)::ura4+ chp2::3x3F-chp2$^{5KRA-2KA}$ rpl42::rpl42^{P56Q}*	This study
SPAF130	*h90 ade6-216 ura4DS/E leu1-32 mat3-M(EcoRV)::ura4+ chp2::3x3F-chp2$^{5KRA-3QKA}$ rpl42::rpl42^{P56Q}*	This study
SPAF154	*h90 ade6-216 ura4DS/E leu1-32 mat3-M(EcoRV)::ura4+ chp2::3x3F-chp2+ rpl42::rpl42P56Q clr4Δ::Hygr*	This study
SPAF246	*h- ade6-210 ura4-D18 leu1-32 chp2Δ::ura4^{+} pREP41-GFP-Chp2$^{5KRA-2KA}$*	This study
SPAF250	*h- ade6-210 ura4-D18 leu1-32 chp2Δ::ura4^{+} pREP41-GFP-Chp2$^{5KRA-3QKA}$*	This study
SPAF262	*h- ade6-210 ura4-D18 leu1-32 chp2Δ::ura4^{+} pREP41-GFP-Chp2*	This study
AH109 (Budding yeast)	*MATa trp1-901 leu2-3 112 ura3-52 his3-200 gal4Δ gal80Δ LYS2::GAL1$_{UAS}$-GAL1$_{TATA}$-HIS3 GAL2$_{UAS}$-GAL2$_{TATA}$-ADE2 URA3::MEL1$_{UAS}$-MEL1$_{TATA}$-LacZ*	(P. James et al., 1996); A. Holtz, unpublished
Y187 (Budding yeast)	*MATα ura3-52 his3-200 ade2-101 trp1-901 leu1-32 112 gal4Δ met^{-} gal80Δ URA3::GAL1$_{UAS}$-GAL1$_{TATA}$-Lacz*	(Wade Harper et al., 1993)

Results

Mit1 interacts with Chp2 via its N-terminal region

The chromatin remodeler, Mit1, is identified as one of the binding partners of Chp2 (Motamedi et al., 2008) and fails to localize to the centromeric region in the absence of Chp2 (Fischer et al., 2009; Motamedi et al., 2008). Mit1 is one of the components of snf2/HDAC repressor complex (SHREC), which consists of a chromatin remodeler module and HDAC module (Fig. 2A). While chromatin remodeler module relies on catalytic domain of Mit1, the HDAC module relies on histone deacetylase Clr3 supported by other components, such as the MBD-like protein Clr2, and the scaffolding subunit, Clr1, that links the remodeler module with HDAC module (Fig. 2A). When I started my Ph.D. study, the mechanisms underlying how Chp2 recruits Mit1 remained unclear. To understand the role of Chp2 in heterochromatin assembly in fission yeast, I first tried to characterize the interaction between Mit1 and Chp2 using yeast two-hybrid assay.

In this assay, the interaction between prey and bait is evaluated by the expression of the reporter gene HIS3 (Fig. 2B). Full-length Chp2 fused to a GAL4 DNA binding domain (BD) was used as the bait, while full-length Mit1 fused to a GAL4 DNA activation domain (AD) was used as the prey (Fig. 2B). The diploid yeast cells expressing both bait and prey grew well on the minimum medium lacking histidine (SD-TLH) and also on SD-TLH medium containing 3-amino-1,2,4-triazole (3AT), an inhibitor of the HIS3 gene product (Fig. 2C), indicating that Mit1 interacts robustly with Chp2. Since the direct interaction between Chp2 and Mit1 was unknown, to confirm that the growth of diploid cells in Mit1-Chp2 was not a false positive result, I used negative control which was consisted empty vector as bait and pray for a comparison (Fig. 2C).

To investigate which domain(s) of Mit1 is responsible for the binding to Chp2, a series of truncated Mit1 domains were expressed as prey (Fig. 3A, Fig, 4A and B) and their ability to interact with full-length Chp2 was examined (Fig. 3B – F). The diploid cells expressing Mit1-N containing the PHD zinc finger domain and the chromodomain as the bait, grew well of on SD-TLH medium containing 15 mM 3AT, indicating its robust interaction with Chp2 (Fig. 3B). While the diploid cells expressing Mit1-N-Helic including a downstream helicase domain, grew well on SD-TLH medium, the growth on SD-TLH

medium containing 3AT was less than that of cells expressing Mit1-N (Fig. 3B and C). Thus, the helicase domain appeared to inhibit the interaction between Mit1-N and Chp2. On the other hand, the diploid cells expressing either Mit1 helicase domain (Mit1-Helic) (Fig. 3D), helicase domain and CID (Helic-CID) (Fig. 3E), or CID only (Fig. 3F) did not grow well on SD-TLH medium containing 3AT, indicating that these central and C-terminal domains are not involved in the interaction with Chp2. Taken together, these results clearly demonstrated that Chp2 interacts with the N-terminal region of Mit. Protein expressions of Chp2 and Mit1 full-length and truncated-domains in yeast two-hybrid assay were also checked by immunoblotting (Fig. 4).

While I could successfully identify N-terminal region of Mit1 as a Chp2 interacting domain by yeast two-hybrid assay, a recent structural study showed that Chp2 binds to the terminus of Mit1 with an extensive interface and that CkIvV motif located at the N-terminus of Mit1 (9-13 aa) is critical for the interaction with Chp2, as I11R mutation of Mit1 abolished the interaction with Chp2.

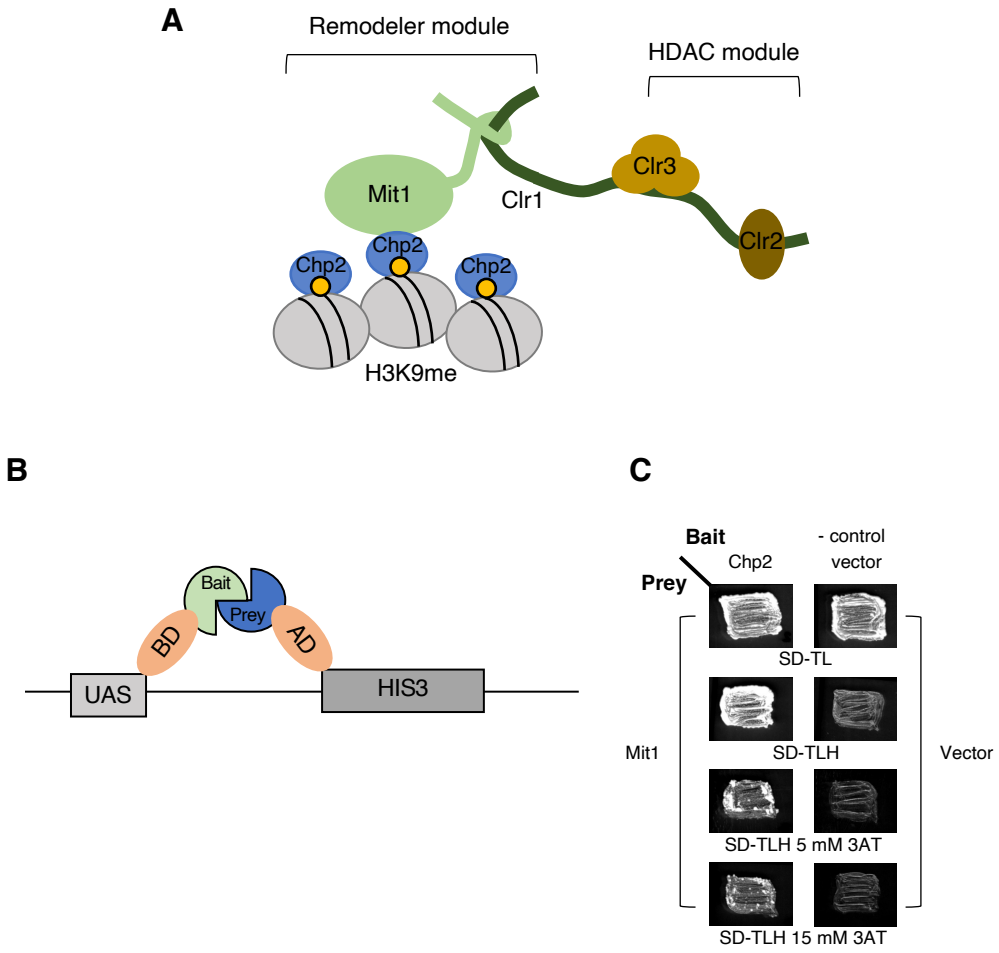

Fig. 2. Chp2 recruits SHREC complex through interaction with Mit1. (A) Schematic model of the Snf/Hdac repressive complex (SHREC) (adopted from Job et al., 2016). **(B)** Schematic Representative of Yeast two-hybrid system. The target protein will function as bait and prey when fused with the BD (DNA Binding-domain) and AD (Activation-domain), respectively. HIS3 gene was used as a reporter of bait and prey interaction. Clones with positive interaction will grow on the medium without histidine or in stringent condition with the addition of 3AT (3-amino-1,2,4-triazole), an inhibitor of HIS3 gene product. **(C)** Yeast two-hybrid assay of full-length Chp2 and Mit1. Yeast cells were streaked on SD-TL: SD/-Trp/-Leu; SD-TLH: SD/-Trp/-Leu/-His; 3AT: 3-amino-1,2,4-triazole. Negative control was empty vector as bait and prey.

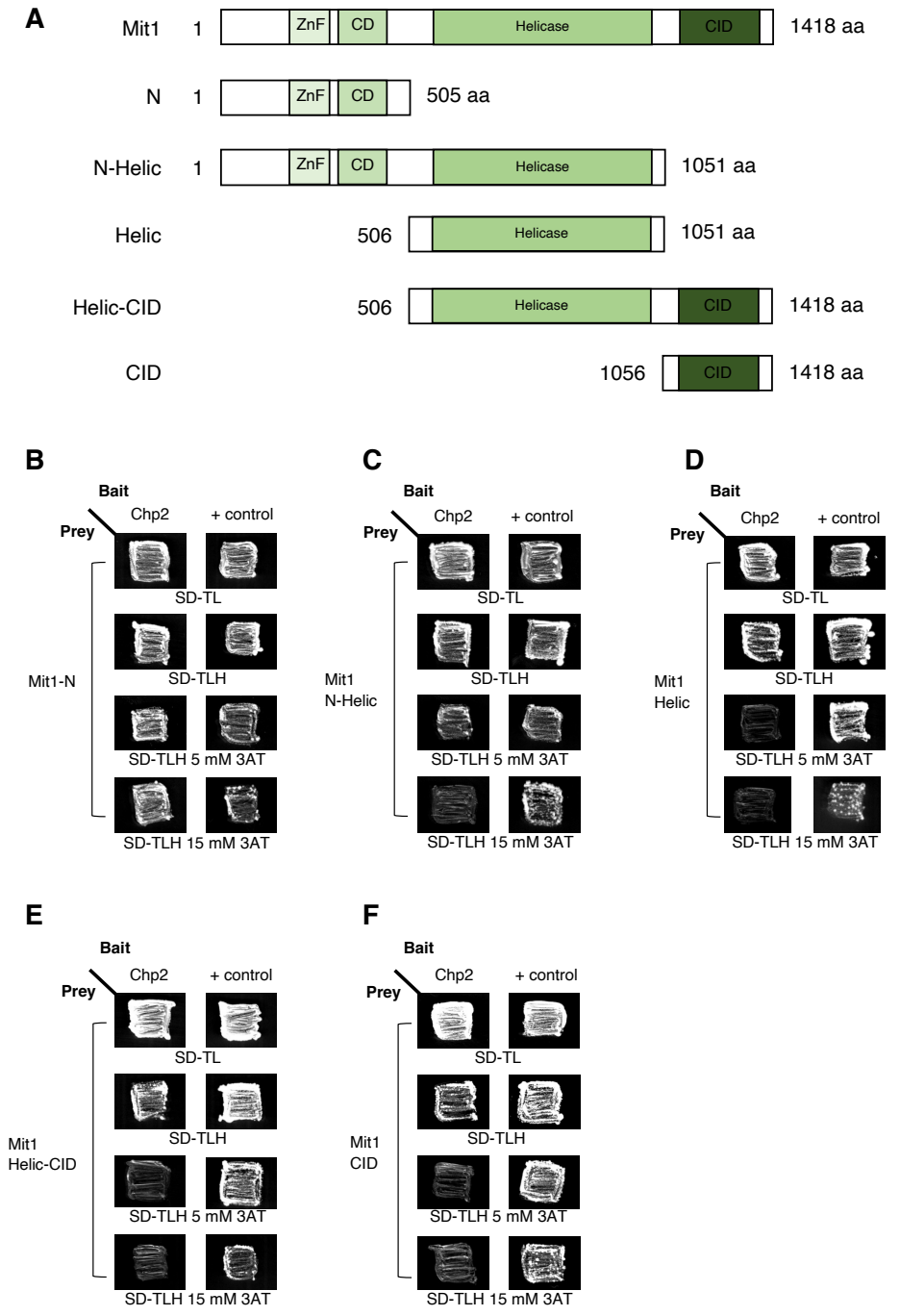

Fig. 3. The N-terminus of Mit1 is critical for the interaction with Chp2. (A) Schematic illustration of Mit1 full-length and Mit1 truncated domains for yeast two-hybrid assay. Mit1 protein consists of the PHD zinc finger motif (ZnF), chromodomain (CD), helicase, and CID (Clr1 interaction domain). **(B)** Yeast two-hybrid assay of full-length Chp2 and Mit1-N (ZnF and CD). **(C)** Yeast two-hybrid assay of full-length Chp2 and Mit1-N-Helic (ZnF, CD, and helicase), **(D)** Chp2 and Mit1-Helic (helicase domain), **(E)** Chp2 and Mit1-Helic-CID (helicase domain and CID), **(F)** Chp2 and Mit1-CID. Yeast cells were streaked on SD-TL: SD/-Trp/-Leu, SD-TLH: SD/-Trp/-Leu/-His, SD-TLH with 3AT: 3-amino-1,2,4-triazole. Positive control was Chp2 and Mit1 full-length same as Fig. 1C.

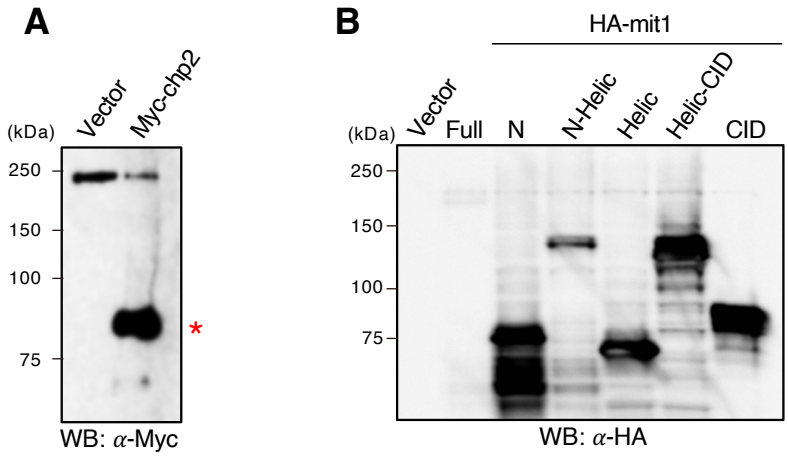

Fig. 4. Protein expression of Chp2 and Mit1 in *S. cerevisiae* for yeast two-hybrid assay. (A) Protein expression of the backbone vector (pGBKT) and Chp2 was checked by western blot analysis using anti-myc. Red asterisk represents the Chp2 protein, with later migrated band with ~250 kDa size are non-specific band that also presents in empty vector pGBKT. **(B)** Protein expression of the backbone vector (pGADT7), Mit1 full-length, and Mit1 truncated domains was checked by western blot analysis using anti-HA.

Chp2 is tightly associated with a chromatin-enriched fraction independently of Clr4 and Mit1

Although it is known that Swi6 and Chp2 localize to heterochromatic regions through Clr4-mediated H3K9me2/3 (Nakayama et al., 2001; Sadaie et al., 2004), Chp2 remains associated with chromatin-enriched fractions, and this association persists even in the absence of Clr4 (Sadaie et al., 2008) (Fig. 5B), suggesting that an additional mechanism(s) beyond H3K9me2/3 recognition contributes to Chp2-chromatin association. Since Chp2, like other HP1 proteins, acts as an adaptor as well as a crosslinker protein that recruits chromatin regulatory proteins, Chp2 may associate with the chromatin-enriched fraction through interaction with other binding partner(s) such as Mit1. Chp2 has been shown to interact specifically with SHREC, a family of nucleosome remodeling and deacetylation complexes (NuRDs). Among the SHREC components, Chp2 directly binds the N-terminus of chromatin remodeler Mit1 with an extensive interface, and this interaction is important for the function of Chp2 in recruiting SHREC to heterochromatic regions. To test whether the persistent chromatin association of Chp2 is mediated by its interaction with Mit1, I generated a strain expressing Mit1 with the I11R ($Mit1^{I11R}$), which has been shown to disrupt the interaction with Chp2 (Leopold et al., 2019), and performed a chromatin fractionation assay.

As previously reported, in wild-type cells, Swi6 was present in both the soluble (S) and chromatin-enriched pellet (P) fractions, with approximately 40% of total Swi6 protein detected in the pellet fraction, and most of the Swi6 in the pellet fraction was redistributed to the soluble fraction in *clr4*Δ cells (Fig. 5A). In contrast, Chp2 was preferentially present in the chromatin-enriched pellet fraction in wild-type cells, and the Chp2 in this fraction was not altered by the $clr4^{+}$ depletion (Fig. 5B). Interestingly, Chp2 association in the chromatin-enriched pellet fraction was not affected by the Mit1 I11R mutation (Fig. 5B). Additionally, the combination of both Clr4 and Mit1 depleted mutant was also not altered Chp2-chromatin association (Fig. 5C). These results suggest that Chp2 is tightly associated with a chromatin-enriched fraction independently of Clr4 and Mit1, and relies on a different mechanism(s) for this association.

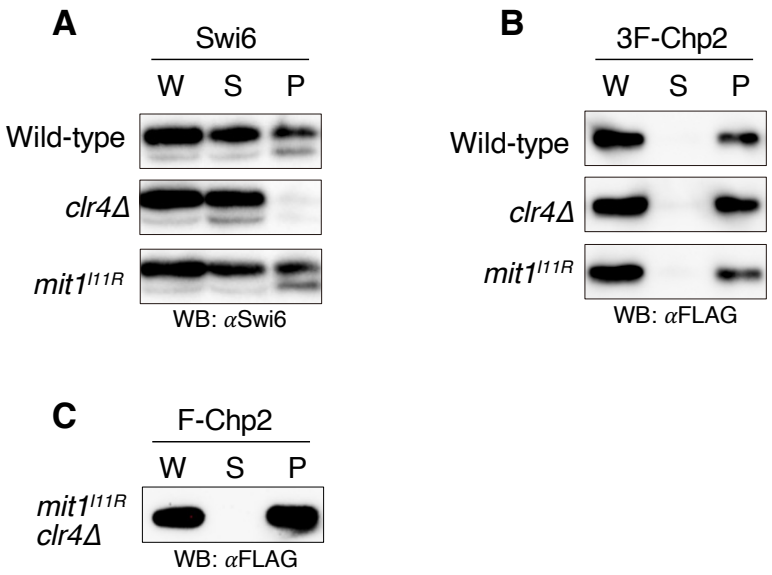

Fig. 5. Chp2 and Swi6 bind the chromatin-enriched nuclear fraction in different ways. (A) Chromatin fractionation assays of Swi6 **(A)** and Chp2 **(B)** in wild-type, *clr4*Δ or *mit1*^{I11R} strain and **(C)** combination between *clr4*Δ and *mit1*^{I11R}. Proteins from whole cell extract (W), soluble supernatant (S), and chromatin-enriched pellet faction (P) were separated by SDS-PAGE, and subjected to Western blotting.

Chp2 binds to DNA through its hinge and chromoshadow domains

HP1 proteins bind to DNA or RNA via the hinge region, and this activity is thought to be involved in their stable chromatin association (Keller et al., 2012; Meehan et al., 2003; Nishibuchi et al., 2014; Smothers & Henikoff, 2001). While a similar activity has been demonstrated for Swi6, it has not been clear whether Chp2 has DNA binding ability and, if so, which domain contributes to the binding (Fig. 7A). To investigate the relationship between the tight chromatin association of Chp2-chromatin and its DNA binding ability, recombinant Chp2 and Swi6 as a control were prepared, to perform electrophoretic mobility shift assays (EMSAs).

A previous study using size exclusion chromatography showed that recombinant Swi6 eluted as a single peak, whereas recombinant Chp2 eluted as two distinct peaks; the second peak corresponded to that of Chp2 ($Chp2^{I370E}$), which is defective in dimer formation. These results suggest that Swi6 forms stable dimers, whereas Chp2 dimers are less stable (Sadaie et al., 2008). To prepare stable dimer-formed Chp2 for EMSAs, recombinant Chp2 was loaded onto the size exclusion chromatography and the first peak was pooled (Fig. 6A). interestingly, in the fractions for the second peak, peptides with molecular mass less than 10 kDa were eluted in the slower eluted fraction (Fig. 6A), and mass spectrometric analysis revealed that these peptides corresponded to Chp2-CSD (data not shown). This result suggests that Chp2 was detected in two distinct peaks in size exclusion chromatography, not because the monomeric form of Chp2 was detected due to instability of the Chp2 dimer, but because Chp2 was degraded or truncated in the vicinity of the CSD, and a heterodimer of full-length Chp2 and CSD alone was detected as the second peak. The labile nature of Chp2 revealed in the *in vitro* experiment may be related to the *in vivo* function of Chp2.

Using purified full-length, dimerized Chp2 and Swi6, I performed EMSAs using 203-bp pericentromeric double-stranded DNA as a probe. Consistent with previous results, Swi6 bound DNA efficiently (Fig. 8A), and Chp2 also showed similar DNA binding activity (Fig. 7B). To investigate which domain of Chp2 and Swi6 is responsible for the DNA binding, each domain of Chp2 and Swi6 was purified (Fig. 7A, 7H and 8F) and their ability to bind DNA was examined. As previously reported, the hinge region of Swi6 (Swi6-H) bound strongly to DNA (Fig. 8D) (Keller et al., 2012), and the activity appeared to be stronger than that of full-length Swi6 (Fig. 8A and 8G). The DNA binding of Swi6-H might be suppressed by other domains as shown for human HP1α, in which DNA binding of the HP1α hinge is

suppressed by CSD (Mishima et al., 2013). The N-terminal disordered region of Swi6 (Swi6-N) bound weakly to DNA (Fig. 8B), whereas no DNA binding activity was detected for Swi6-CD or Swi6-CSD (Fig. 8C, 8E, and 8G). The hinge and the N-terminal disordered regions of Chp2 (Chp2-H and Chp2-N) also bound DNA (Fig. 7C, 7E, and 7H), and no detectable DNA-binding activity was observed for Chp2-CD (Fig. 7D). Interestingly, we found that Chp2-CSD exhibited a robust DNA binding activity (Fig. 7F and 7G), in contrast to Swi6-CSD (Fig. 8E and 8H). Since DNA-binding activity associated with CSD has not been described in other HP1 proteins, the activity involving Chp2-CSD may contribute to Chp2-specific function. Furthermore, the unique DNA-binding activity of Chp2-CSD may also provide insights into the evolution of HP1 proteins and their functions in different organisms.

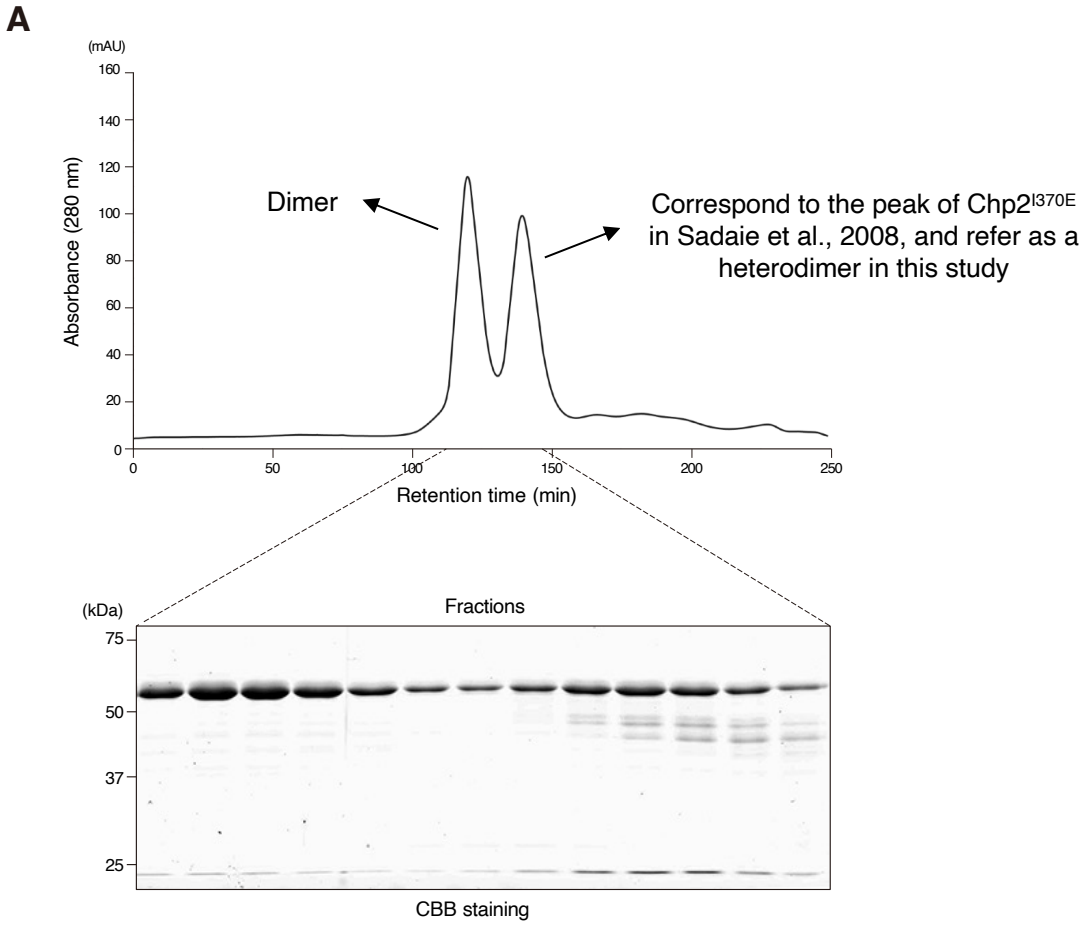

Fig. 6. Recombinant Chp2 protein presents in dimer and heterodimer formation. (A) The Chromatogram of the Chp2 wild-type showed a clear separation of the dimer and heterodimer that eluted at different retention times. The faster-eluted peak corresponds to the dimer, while the slower-eluted peak corresponds to the heterodimer. This heterodimer consists of Chp2 full-length dimerized with truncated-CSD of Chp2. The elution profiles from both fractions were checked by SDS-PAGE and stained by CBB.

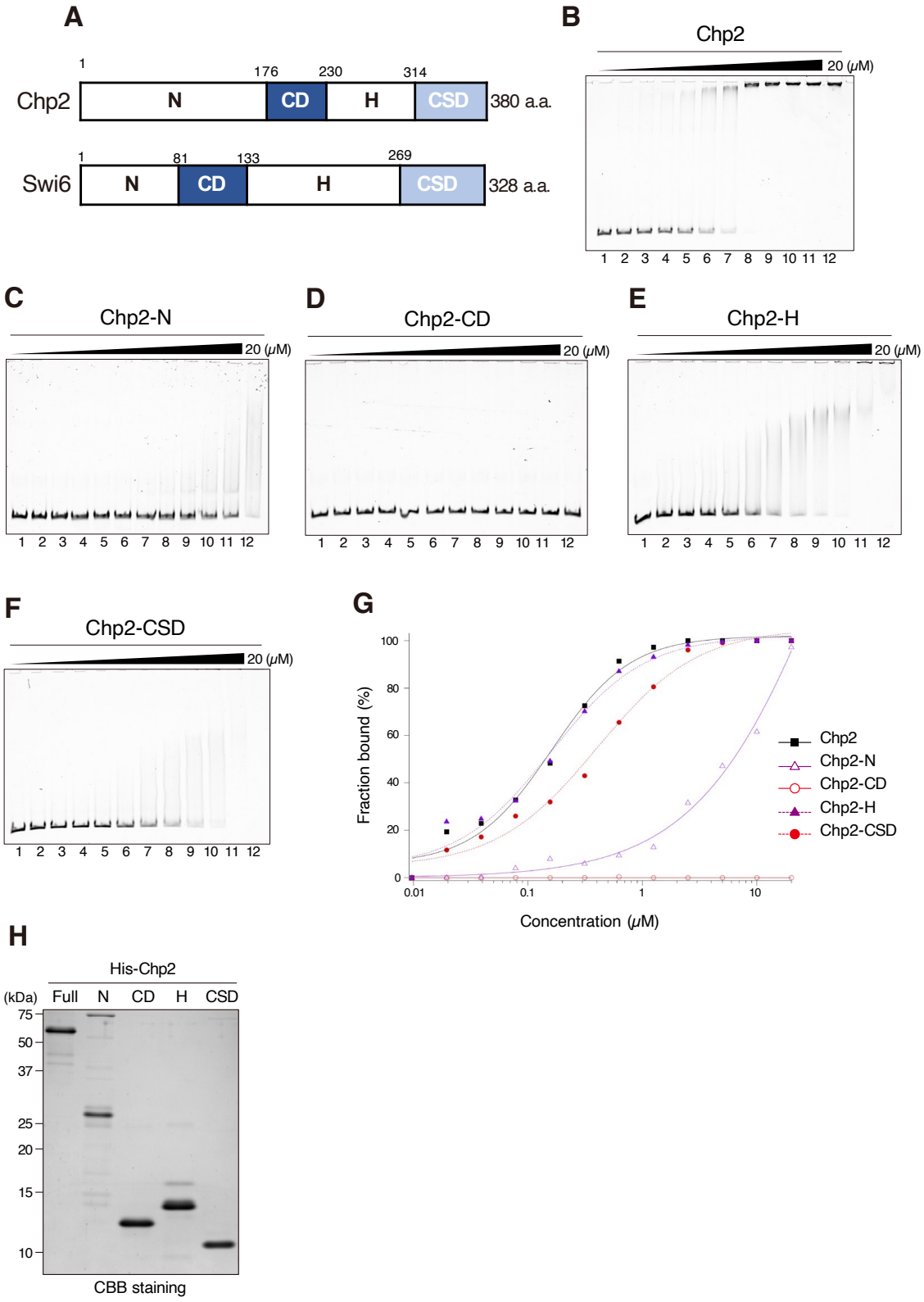

Fig. 7. Chp2's hinge and chromoshadow domain are predominantly contributed to the DNA-binding. (A) Schematic illustration of Chp2 and Swi6 protein. Both proteins share the same protein domains consisting of disordered region N-Terminus (N), and Hinge region (H) that connect Chromodomain (CD) and (CSD) Chromoshadow domain. **(B)** Representative EMSAs of Chp2 full-length with 203-bp fission yeast's pericentromeric dsDNA sequence as a probe. The highest concentration used in

this assay is 20 μM with 1:2 dilution. **(C)** Representative EMSAs of Chp2's N, **(D)** CD, **(E)** H, (**F**) CSD. **(G)** Quantification of EMSAs using Chp2 full-length and Chp2 truncated domains. The fraction of retarded DNA probes from **(B)** to **(F)** was plotted against the protein concentrations. **(H)** CBB staining of his-tagged Chp2 full-length and Chp2 truncation domains that were used for EMSA.

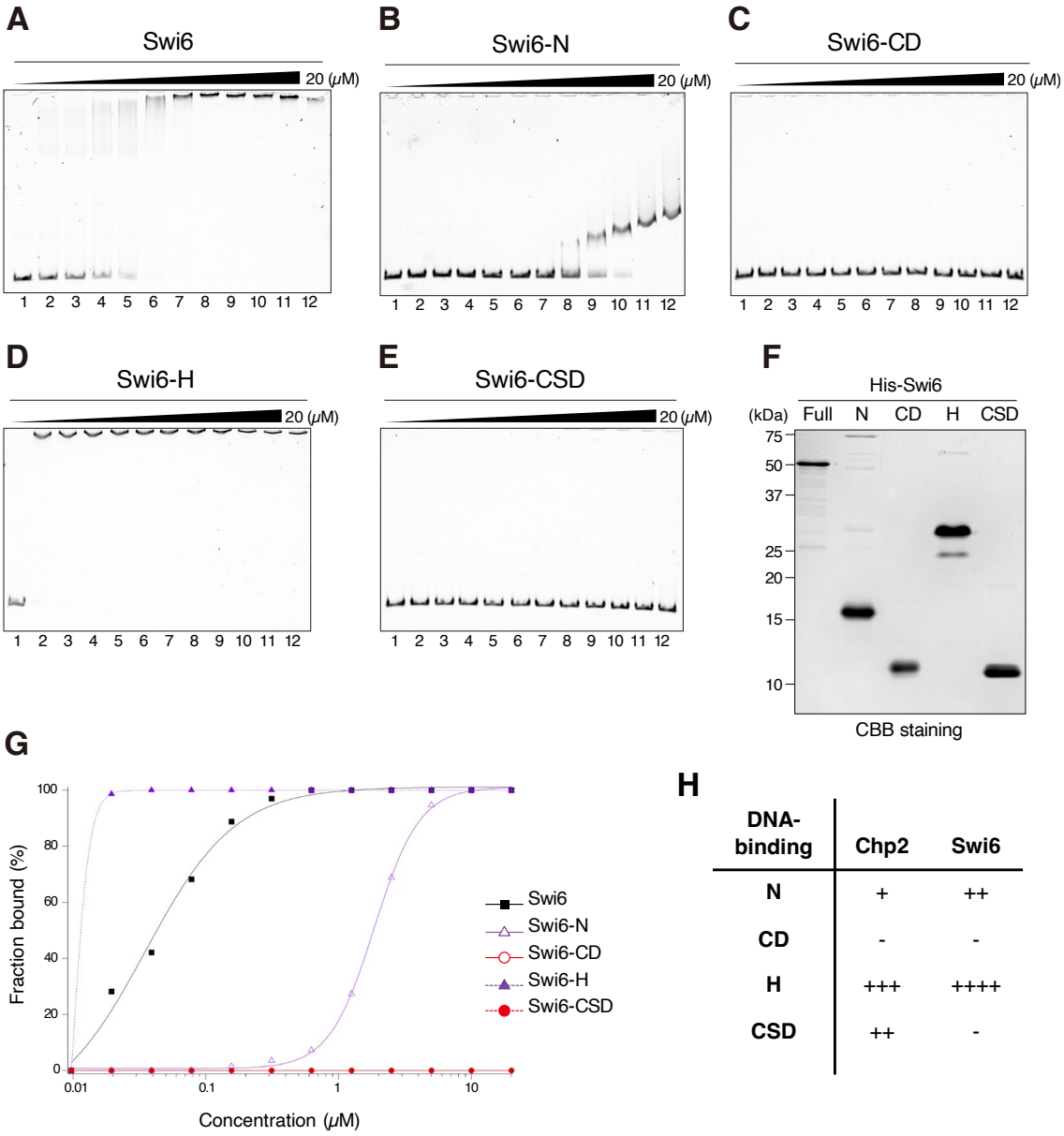

Fig. 8. Swi6's N-terminus and hinge are critical for DNA binding. (A) Representative EMSAs of Swi6 full-length with 203-bp fission yeast's dsDNA pericentromeric sequence as a probe. The highest concentration used in this assay is 20 µM with 1:2 dilution. **(B)** Representative EMSAs of Swi6's N, **(C)** CD, **(D)** H, **(E)** CSD. **(F)** CBB staining of his-tagged Swi6 full-length and Swi6 truncation domains that were used for EMSA. **(G)** Quantification of EMSAs using Swi6 full-length and Swi6 truncated domains. The fraction of retarded DNA probes from **(A)** and **(E)** was plotted against the protein concentration. **(H)** Table summary of DNA binding ability contributes by each domain of Chp2 and Swi6. (-) indicates no DNA binding observed by EMSA, and (+) indicates the strength of DNA binding with the higher number of (+) representing the higher strength of the binding.

Basic residues in the hinge and the N-terminus of CSD are involved in the DNA binding activity of Chp2

To gain insight into the amino acid residues involved in the DNA binding activity of Chp2, amino acid substitutions were introduced in the hinge and CSD domains, respectively. Previous studies using human HP1α have shown that a cluster of basic amino acid residues is critical to the DNA binding activity of the hinge region (Mishima et al., 2013; Nishibuchi et al., 2014), In the Chp2-hinge region, there is a cluster of basic amino acid residues, KRRRSR (271–276 aa) (Fig. 9A) and when these were replaced by alanine (Fig. 9A), the resulting in Chp2-H mutant (Chp2-H^{5A}) no longer able to bind DNA (Fig. 9B, 9C, and Fig. 10A, 10D), suggesting that these positively charged residues are involved in the DNA binding of the Chp2-hinge.

The CSD is an evolutionarily conserved module consisting of three β-sheets followed by two α-helixes. The overall structure of Swi6-CSD and Chp2-CSD is similar, but the structure of their N-terminus region is different and consists of a loop (Fig. 20A and 20B). In addition, while there is no obvious cluster of basic amino acid residues in the Chp2-CSD, there are two lysine residues found in the N-terminal region of the CSD (321–322 aa), that are not present in the corresponding region of Swi6. While these residues also face the solvent part in the structure, presumably will help to accommodate DNA. When these lysine residues in Chp2-CSD were replaced by alanine, the mutant Chp2-CSD (Chp2-CSD^{2A}) exhibited only a very weak DNA binding activity compared to wild-type Chp2-CSD wild-type (Fig. 9D, 9E, 10B and 10E). When an additional alanine substitution was introduced into the neighboring glutamine residue (Q320) that is also facing the solvent part in the structure, mutant Chp2-CSD (Chp2-CSD^{3A}) no longer bound DNA (Fig. 9F, 10B, and 10E), suggesting that these three residues are involved in the DNA binding activity associated with Chp2-CSD.

To confirm the involvement of these residues in the DNA-binding activity of full-length Chp2, mutant Chp2 proteins with amino acid substitutions in either the hinge or the CSD, or both, were generated (Fig. 9G and 10C), and their DNA-binding activity was examined by EMSAs. Full-length version of Chp2 with H^{5A} mutation in the hinge (Chp2-mut1) or with either CSD^{2A} or CSD^{3A} mutation in the CSD (Chp2-mut2 and Chp2-mut4) exhibited weaker DNA-binding activity compared to wild-type Chp2 (Fig. 9H, 9I, 9J, and 9L, and 10F). Interestingly, when amino acid substitutions in the hinge and CSD were combined,

the resulting Chp2 mutants (Chp2-mut3 and Chp3-mut5) were no longer bound to DNA (Fig. 9K and 9M, and 10F). I confirmed that mutant Chp2 proteins with these amino acid substitutions form a stable dimer, as judged by elution profiles in the size exclusion chromatography (Fig. 12D). These results clearly indicate that basic residues in the hinge and the N-terminal region of the CSD cooperatively contribute to the DNA-binding activities of full-length Chp2.

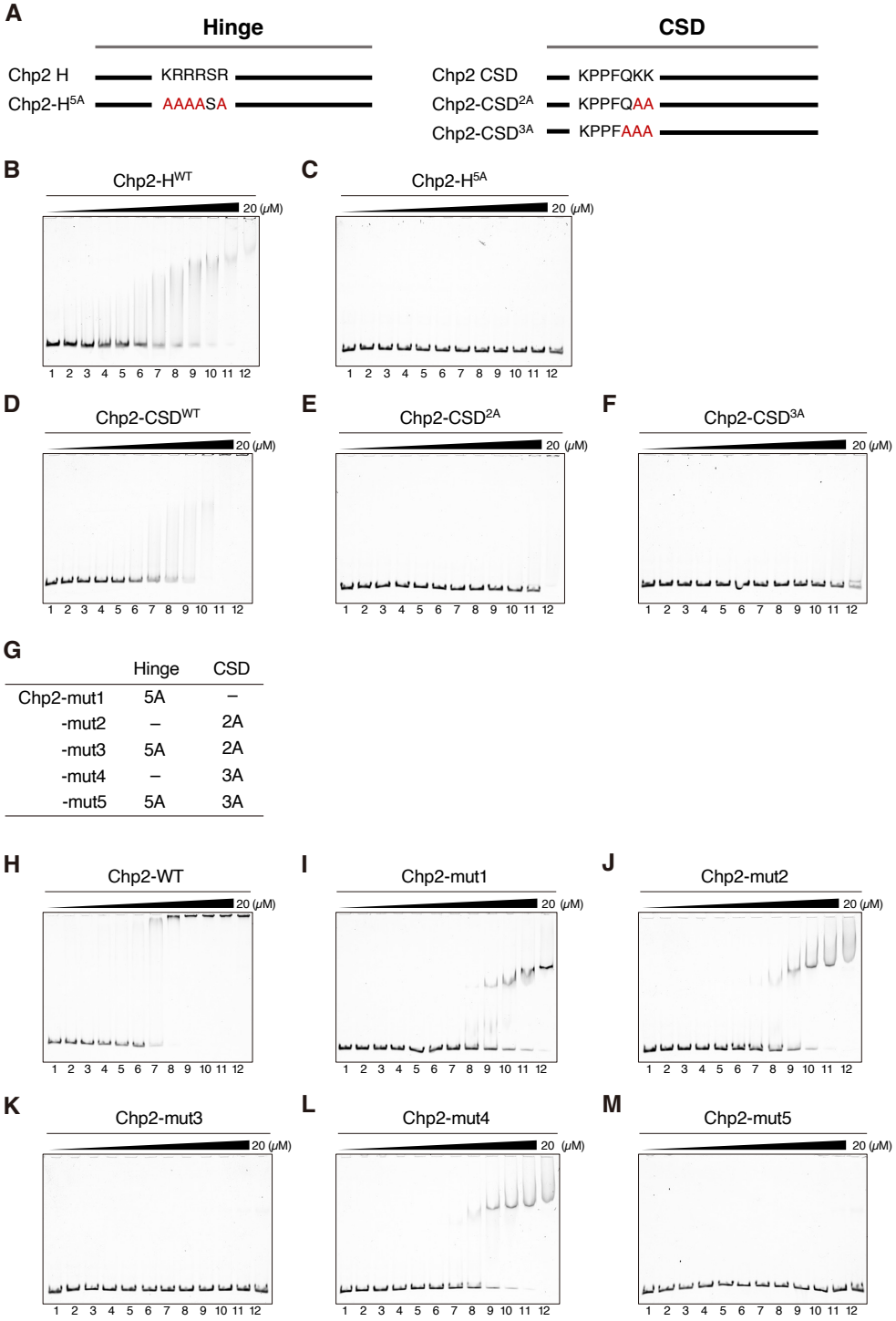

Fig. 9. Chp2's DNA binding mainly relies on basic residues at the hinge and the N-terminus of the chromoshadow domain. **(A)** Schematic illustration of amino acid substitutions at the hinge and the N-terminus of CSD to evaluate critical residues for DNA binding. **(B)** Representative EMSAs of Chp2-H^{WT} in comparison to **(C)** mutations of basic residues at truncated H, Chp2-H^{5A}. **(D)** Representative EMSAs of Chp2-CSD^{WT} in comparison to mutations of basic residues at truncated CSD, **(E)** Chp2-CSD^{2A}, and **(F)** Chp2-CSD^{3A}. **(G)** Schematic diagram of the full-length version of 5A, 2A, and 3A mutations labeled as mut1, mut2, and mut4 respectively, with combined mutations between 5A-2A (mut3) and 5A-3A (mut5). **(H)** Representative EMSAs of full-length Chp2-WT compared to **(I)** Chp2-mut1, **(J)** Chp2-mut2, **(K)** Chp2-mut3, **(L)** Chp2-mut4, and **(M)** Chp2-mut5.

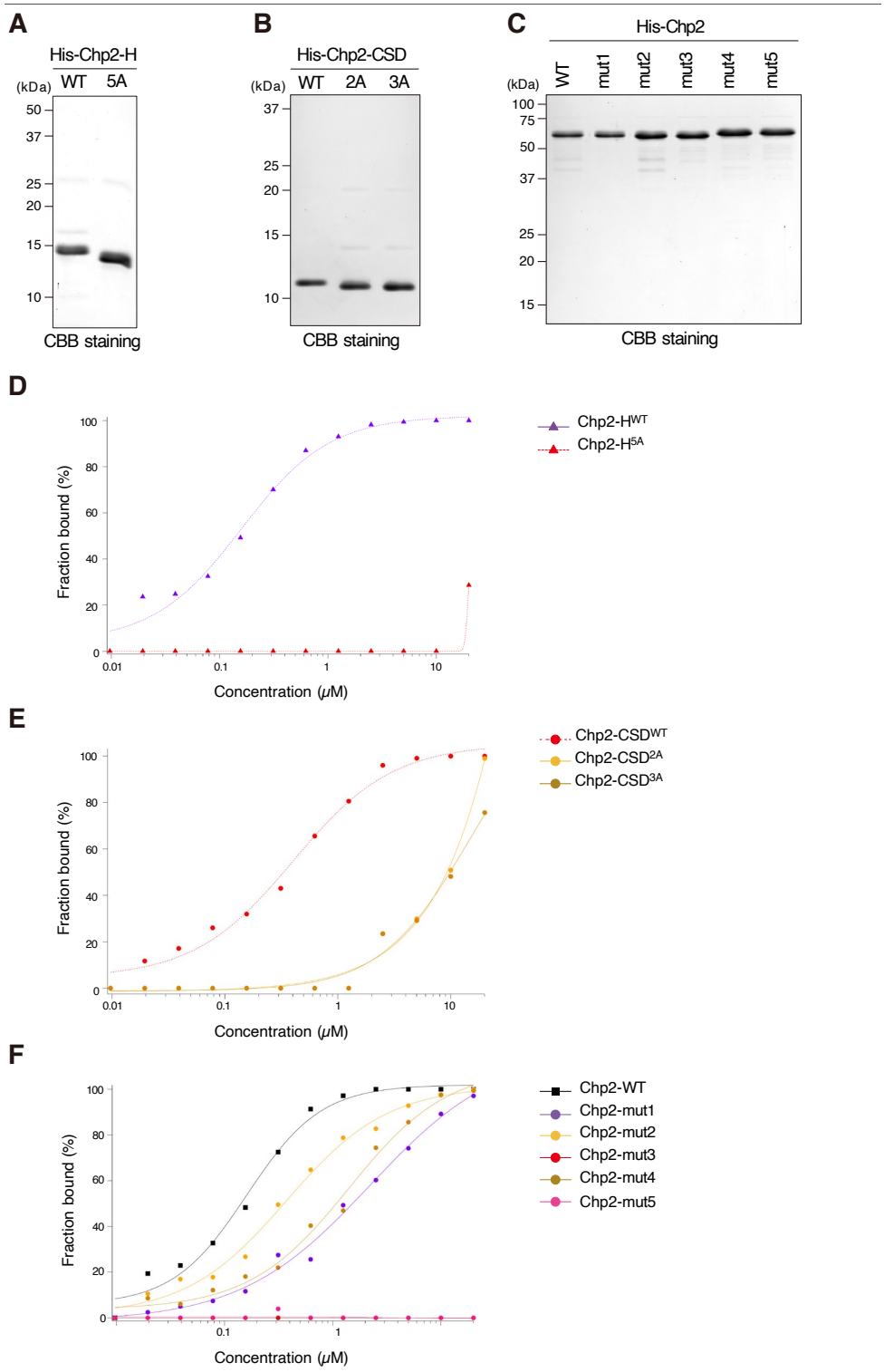

Fig. 10. Chp2 mutants show lower binding affinity and lose binding affinity to DNA. **(A)** CBB staining of his-tagged Chp2-H wild-type and Chp2-H with 5A mutations. **(B)** CBB staining of his-tagged Chp2-CSD wild-type and Chp2-CSD with 2A and 3A mutations. **(C)** CBB staining of his-tagged Chp2 wild-type and mut1 – mut5. **(D)** Quantification of EMSAs using Chp2-H (Fig. 9B) and Chp2-H^{5A} (Fig. 9C). **(E)** Quantification of EMSAs using Chp2-CSD (Fig. 9D), Chp2-CSD^{2A} (Fig. 9E), and Chp2-CSD^{3A} (Fig. 9F). **(F)** Quantification of EMSAs using Chp2 wild-type and mut1 – mut5 (Fig. 9H – M). The fraction of retarded DNA probes was plotted against the protein concentrations.

DNA binding activities of Chp2 are required for heterochromatic silencing

To investigate the importance of DNA binding in Chp2 function *in vivo*, the above mutant Chp2 proteins were expressed from the endogenous *chp2*$^{+}$ locus with N-terminal FLAG tag, and its effects on the mating-type *mat3M::ura4*$^{+}$ silencing were examined by using *chp2*Δ cells as control (Fig. 11A) (Thon & Verhein-Hansen, 2000). Immunoblotting assay showed that the expression levels of mutant Chp2 protein were comparable to the wild-type Chp2 and additionally, tubulin was also checked as control of the input samples (Fig. 11B). Cells expressing mutant Chp2 containing either the hinge mutation (mut1) or one of the mutations in the N-terminus of CSD (mut2 or mut4) showed silencing comparable to the cells expressing wild-type Chp2 (Fig. 11C). However, the cells expressing mutant Chp2 containing combined mutations of the hinge and one of the mutations in the N-terminus of CSD (mut3 and mut5) showed a silencing defect (Fig. 11C). Although the cells expressing Chp2-mut3 or Chp2-mut5 grew well on the PMG-Ura plates with comparable efficiency to the *chp2*Δ cells, they also grew robustly on the PMG+5FOA plates (Fig. 11C), indicating that the heterochromatic silencing is partially impaired in the cells expressing Chp2-mut3 and Chp2-mut5. Taken together, these results suggest that the DNA-binding activities of the hinge and the N-terminus of CSD are important for the silencing at the mating-type locus and presumably at other heterochromatic regions, and that these activities cooperate to maintain the silencing function of Chp2 *in vivo*.

DNA binding activities of Chp2 are involved in its *in vivo* stability

Next, I tested whether the DNA binding activities of Chp2 are involved in its tight chromatin association by the chromatin fractionation assay. Mutant Chp2 proteins lacking DNA-binding activities at both the hinge and the N-terminus of CSD (mut3 and mut5) were predominantly detected in the chromatin-enriched pellet fraction (P) (Fig. 12A). These results suggest that the DNA-binding activity of Chp2 plays a minor role in its tight association with chromatin-enriched fraction. However, when Chp2-mut3 and Chp2-mut5 were detected by immunoblotting, faster-migrating Chp2 bands were routinely detected in both whole-cell lysates (W) and chromatin-enriched pellet (P) fractions, which were not present in the immunoblotting of wild-type Chp2 (Fig. 12A) and were only weakly detected in the immunoblotting of samples prepared with alkaline and TCA (Fig. 11B). Since the FLAG tag

was introduced at the N-terminus of Chp2, the smaller Chp2 protein appeared to be a C-terminally truncated Chp2 species.

To further characterize this faster-migrating Chp2 species, a strain expressing mutant Chp2 with CSD deletion was created and its migration was compared with that of Chp2-mut3 and Chp2-mut5 (Fig. 12B). Immunoblotting results showed that the faster-migrating Chp2 species migrated slightly faster than that of Chp2ΔCSD, suggesting that mutant Chp2 lacking DNA-binding activities associated with both the hinge and the N-terminus of CSD (mut3 and mut5) were susceptible to cleavage at a specific position just upstream of CSD, corresponding to a region sandwiched between two regions with mutations. Regarding the stability of Chp2 proteins, the hinge mutation (mut1) caused an increased amount of truncated Chp2 products, although the effect was milder than that of mut3 or mut5 (Fig. 12C). On the other hand, one of the mutations in the N-terminus of the CSD (mut2 and mut4) had a minor effect on the stability of the mutant proteins; the banding patterns are comparable to those of wild-type Chp2 (Fig. 12C). Thus, the stability of Chp2 is also determined by the cooperative action of the hinge and the N-terminus of the CSD.

Although the physiological significance of the cleavage of the C-terminus of Chp2 is not yet clear, these results appear to be related to the behavior of recombinant Chp2 in size exclusion chromatography (Fig. 12D). As described above, when recombinant Chp2 prepared by the immobilized metal ion affinity chromatography was applied to the gel filtration chromatography, two distinct peaks were detected: the faster and slower eluting peaks appear to correspond to the homodimer of Chp2 and the heterodimer with Chp2 and truncated CSD, respectively (Fig. 6). For wild-type Chp2, the elution profile for the homo- and heterodimer were comparable, and a similar pattern was observed for mutant Chp2, mut1, mut2, or mut4 (Fig. 12D). However, when Chp2-mut3 or Chp2-mut5 was applied, the faster-eluting peak become higher than that of slower-eluting peak, suggesting that the population of the homodimer was higher in the preparation for Chp2-mut3 and Chp2-mut5 compared to wild-type. The balance between homo- and heterodimer could be altered either by the increased stability of dimer formation or by the decreased level of CSD in the preparation due to resistance to degradation. Although it remains unclear how these mutations affect the balance of Chp2 homodimer and heterodimer, it is clear that mutant Chp2 with the hinge mutation and one of the mutations in the N-terminus of the CSD forms a dimer at a level comparable to that of wild-type Chp2 (Fig. 12D).

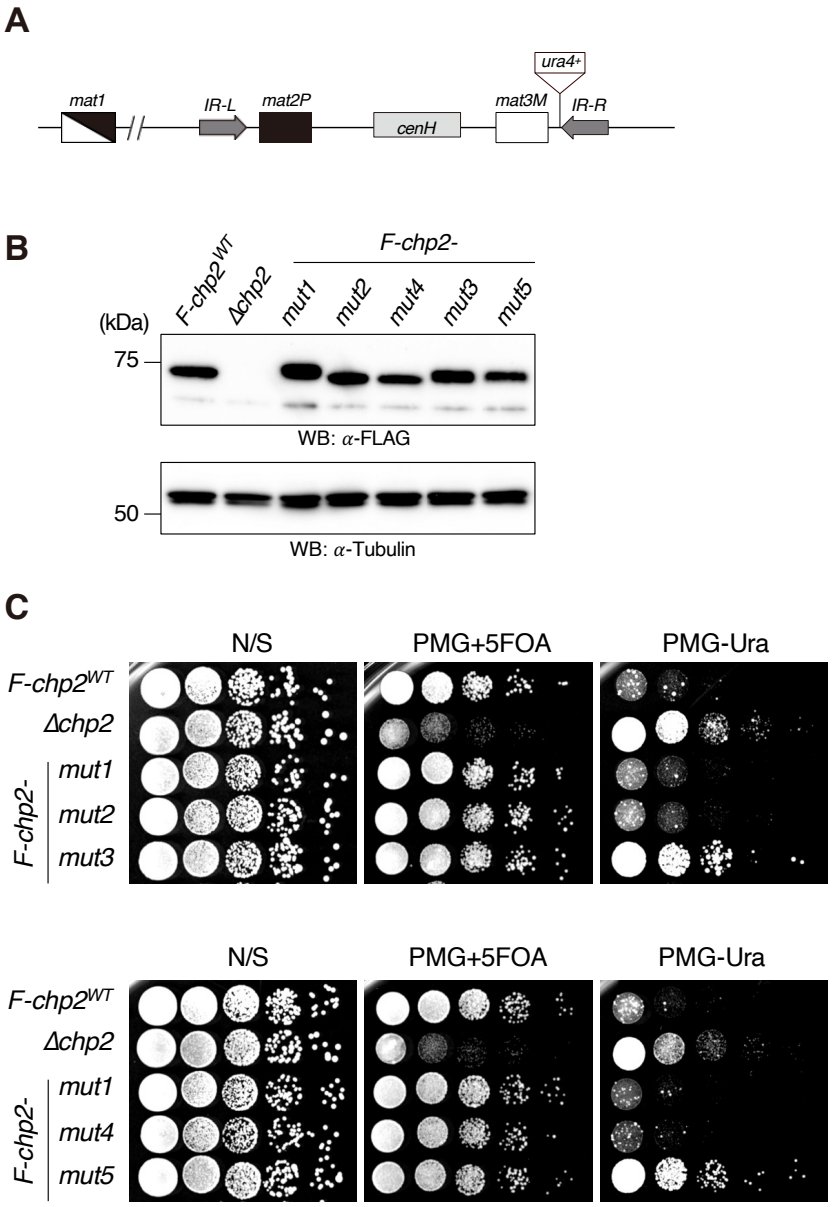

Fig. 11. DNA-binding of Chp2 is essential for heterochromatin formation. (A) Schematic illustration of *mat3M::ura4*$^{+}$ reporter for silencing assays. **(B)** Western blot analysis shows protein expression of Chp2 wild-type tagged with 3×3Flag (F-), F-Chp2 mut1 – mut5, and Chp2 deletion as a positive control, with tubulin being examined as a control of input samples. **(C)** Silencing assays of F-Chp2, Δ*chp2*, and F-Chp2 mut1 – mut5 in a *mat3M::ura4*$^{+}$ reporter. A 20-fold serially diluted culture of the indicated strains was spotted onto a nonselective medium (N/S), PMG-Ura medium, and PMG containing 5-FOA (5-fluorotic acid).

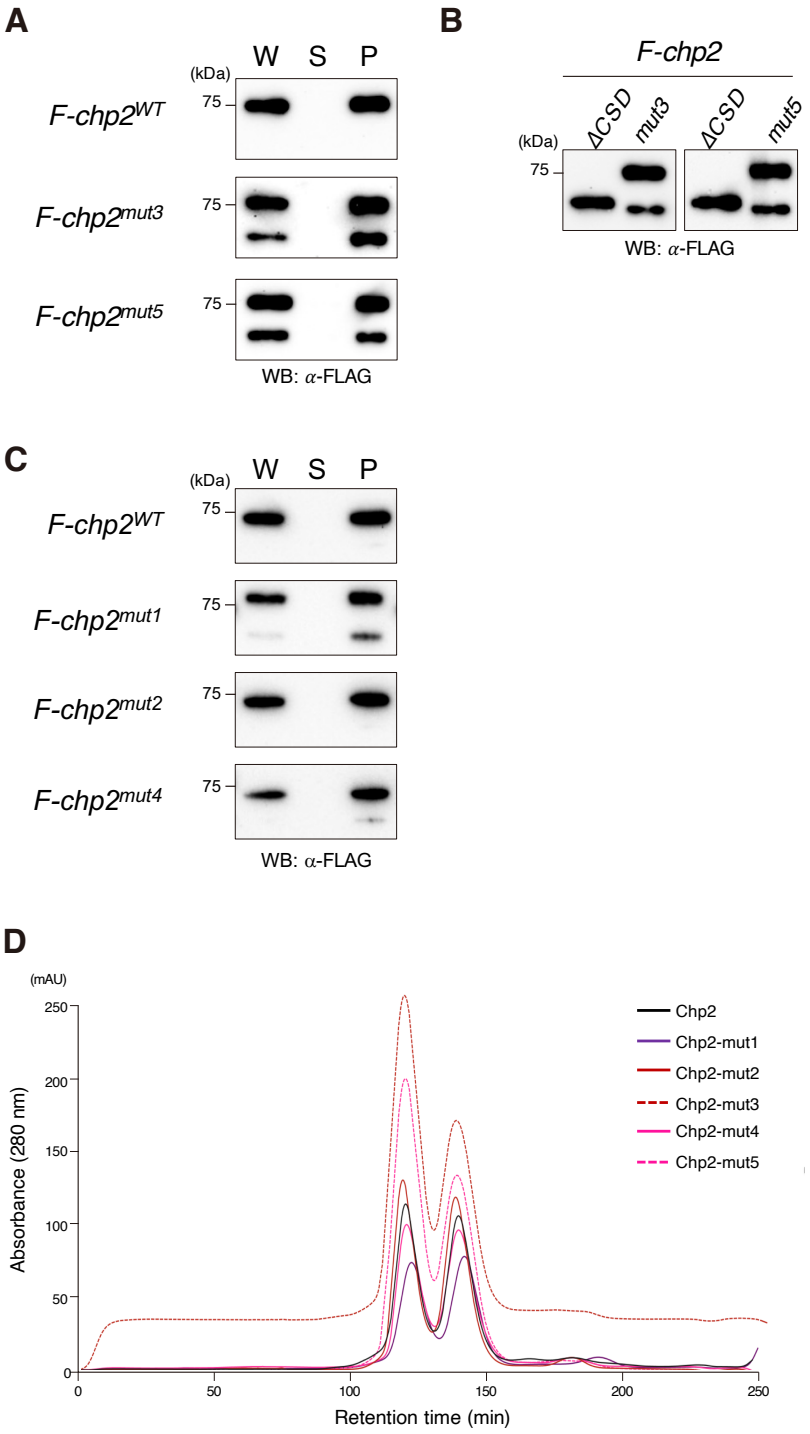

Fig. 12. DNA-binding activities of Chp2 are involved in its *in vivo* stability. (A) Chromatin fractionation assays of FLAG-tagged, wild-type and mutant Chp2. A degraded Chp2 protein is detected below 75 kDa for mutant 3 and mutant 5. W: whole-cell extract, S: soluble supernatant, P: chromatin-enriched pellet fraction. **(B)** Western blotting of Chp2ΔCSD protein compared to degraded Chp2 protein detected for mutant 3 and mutant 5. **(C)** Chromatin fractionation assays of FLAG-tagged, wild-type and mutant Chp2 (mut1, mut2 and mut4). **(D)** The chromatogram of wild-type and mutant Chp2 showed the dimer and heterodimer that eluted at different retention times. The faster-eluting peak corresponds to the dimer, while the slower-eluting peak corresponds to the heterodimer consisting of full-length Chp2 dimerized with the truncated CSD of Chp2.

DNA binding activities of Chp2 are required for its stable association with heterochromatic regions

To investigate the effect of the DNA binding activities of Chp2 on its localization to heterochromatic regions, chromatin immunoprecipitation (ChIP) assays were performed. Chp2 mutants lacking DNA-binding associated with both the hinge and the N-terminus of CSD (mut3 and mut5) exhibited reduced heterochromatin association compared to wild-type Chp2 at representative heterochromatic regions (centromeric *dg*, the mating-type *cenH*, telomere, and *mat3M::ura4*$^{+}$), and the reduction was more severe for Chp2-mut3 compared to Chp2-mut5 (Fig. 13A). These results suggest that the DNA-binding activities of Chp2 are required for its stable association with heterochromatic regions. Swi6 localization was moderately reduced at some heterochromatic regions in the cells expressing Chp2-mut3, but not evident in the cells expressing Chp2-mut5 (Fig. 13B). The reduction of Swi6 at some of the heterochromatic regions seems to follow a similar trend as that of Chp2 (Fig. 13A). This result may suggest their cooperative function in localizing to these heterochromatic regions.

Although Chp2 has been shown to bind the chromatin remodeler Mit1 and recruit the SHREC complex containing the H3K14 deacetylase Clr3, the levels of H3K14ac were not noticeably changed from the ChIP experiments in cells expressing Chp2-mut3 and -mut5 (Fig. 13C). This result is likely because the SHREC complex could be recruited to the heterochromatic regions via an alternative mechanism involving the Clr2 component (Job et al., 2016; Maksimov et al., 2018). Furthermore, although H3K9me2 levels were slightly reduced at the examined heterochromatin regions in cells expressing Chp2-mut5, this reduction was not statistically significant (Fig. 13D). Taken together, these results suggest that the silencing defect observed in cells expressing Chp2-mut3 and -mut5 is primarily due to reduced heterochromatin localization of Chp2. The ChIP-qPCR experiment also was confirmed by fluorescence microscopy using widefield DetlaVision. In agreement with ChIP-qPCR results, reduction intensity of GFP-Chp2 in mut-3 and mut-5 was observed (Fig 14). This result further explains the distinct defect in mut-3, may be due to the dysfunctional recruitment of Chp2 to heterochromatin.

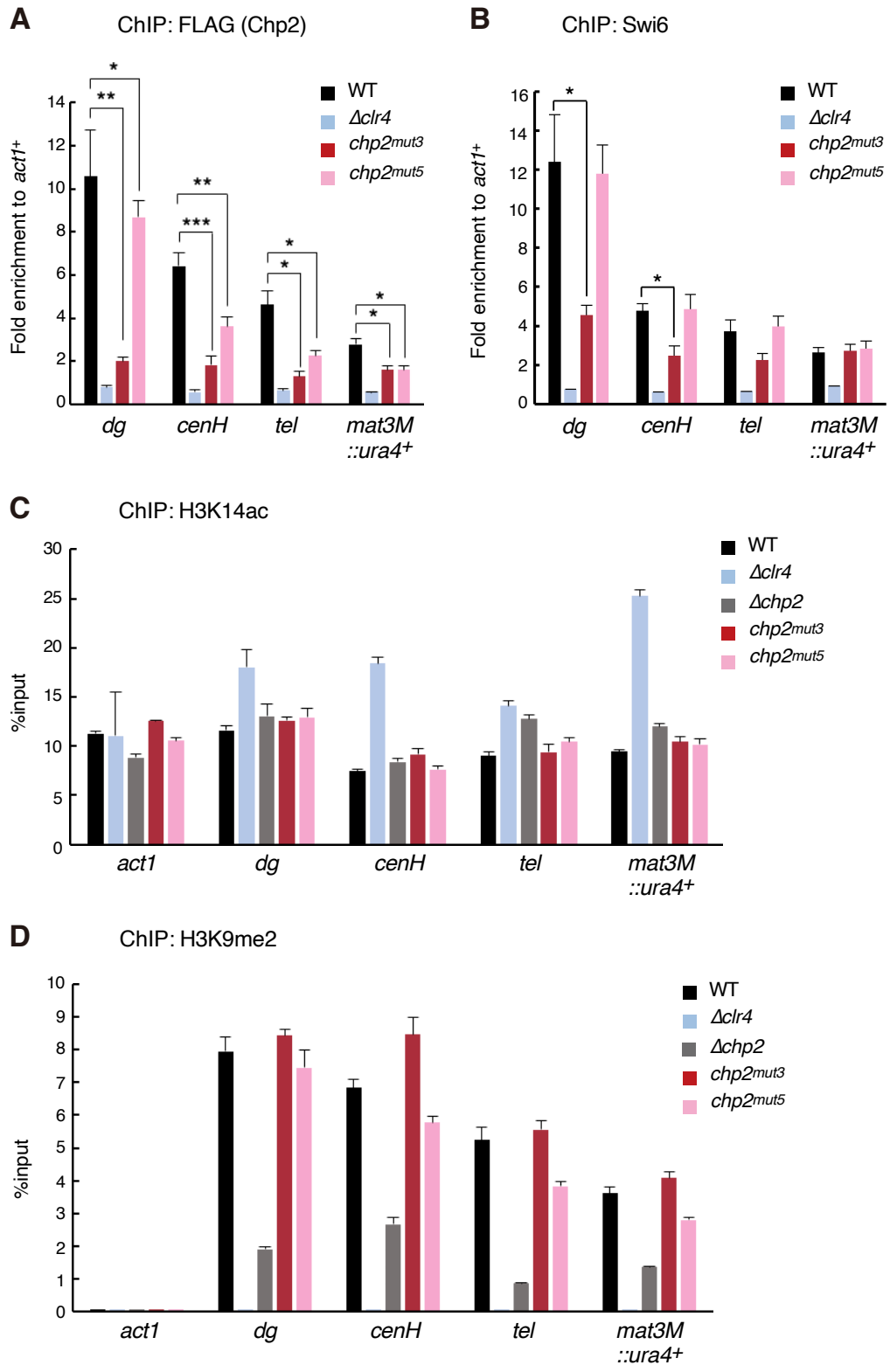

Fig. 13. DNA binding of Chp2 is required to support Chp2 association with heterochromatin. (A) ChIP-qPCR analysis of Chp2 in representative heterochromatic loci *dg*, *cenH*, telomere, and reporter *mat3M::ura4*$^{+}$. Fold enrichment of Chp2 was normalized to *act1* locus. Error bars were calculated from three technical replicates. *** $p < 0.001$, ** $p < 0.01$, * $p < 0.05$. **(B)** ChIP-qPCR analysis of Swi6. The Fold enrichment of Swi6 was normalized to the *act1* locus. Error bars were calculated from three technical

replicates. **(C)** ChIP-qPCR analysis of H3K14ac. Values are shown as percentage of input and error bars were calculated from three technical experiments. **(D)** ChIP-qPCR analysis of H3K9me2. Values are shown as percentage of input and error bars were calculated from three technical experiments.

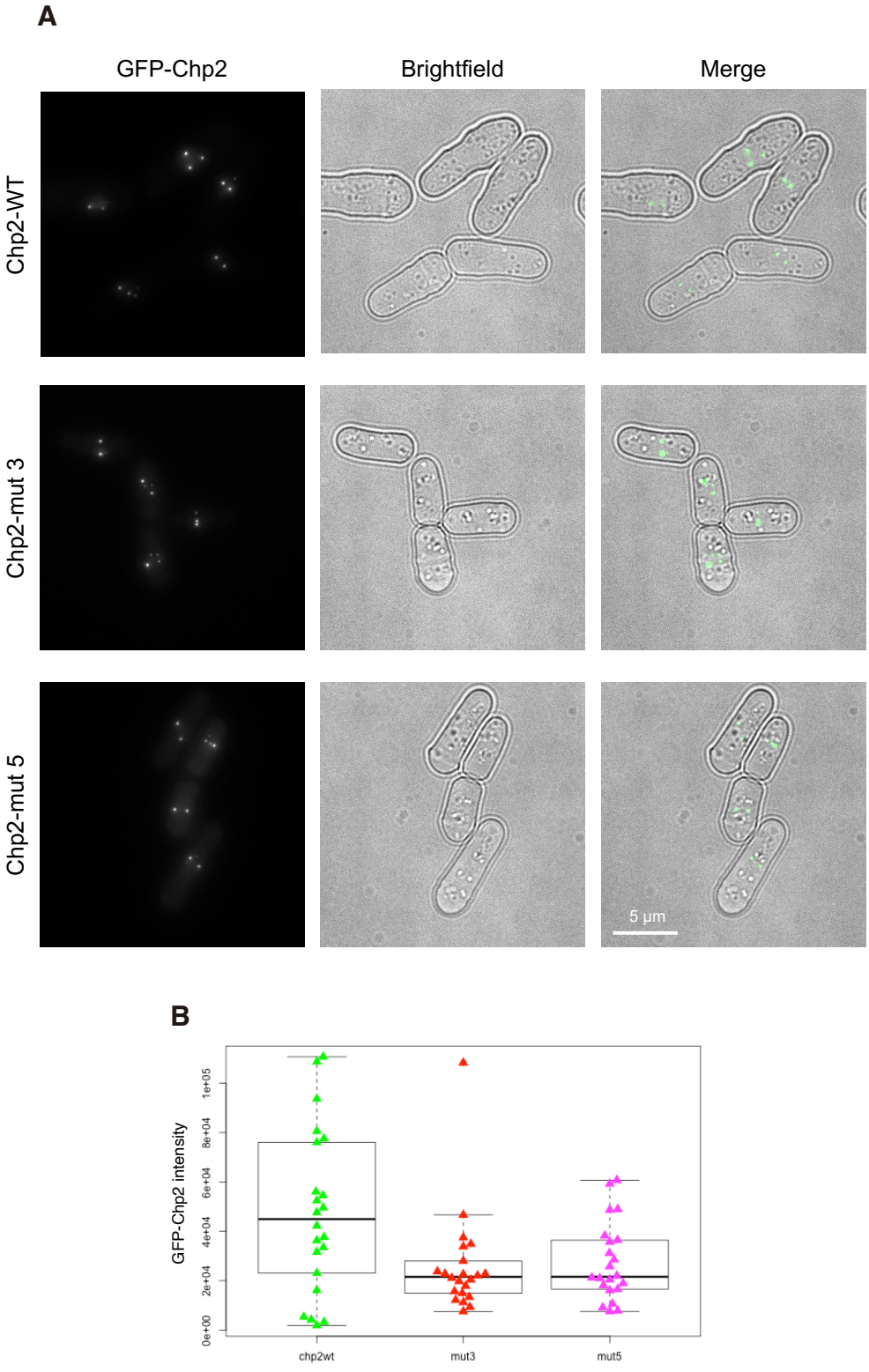

Fig. 14. DNA binding of Chp2 is required to support Chp2 association with heterochromatin. (A) representative of microscopy images of widefield microscopy of GFP-Chp2 foci, wild-type and mutants Chp2. **(B)** Box plot of Chp2 intensity between wild-type, mut3 and mut5 foci calculated by Fiji. (n=22 biological replicates)

Identification of protein interactors by tandem affinity purification (TAP) of N-terminal TAP-tagged Chp2 (NTAP-Chp2)

As described previously, Chp2 persists in the chromatin-enriched fraction even in *clr4*Δ cells, and the intrinsic DNA-binding activities of Chp2 appear to play a minor role in its chromatin association. Although previous studies have identified Mit1 as a direct Chp2 binding partner (Job et al., 2016; Leopold et al., 2019; Motamedi et al., 2008), the chromatin association of Chp2 was not detectably altered by Mit1 mutation ($Mit1^{I11R}$), which has been shown to impair the interaction with Chp2 (Fig. 5B). Additionally, a combination between Clr4 and Mit1 depleted condition was also not altered Chp2 tight association with chromatin (Fig. 5C). Therefore, it is possible that the Chp2-chromatin association is mediated by associating with other complexes through binding with yet unidentified binding partner(s).

While a previous study used a conventional C-terminal TAP strategy, and identified Mit1 and Clr1 as Chp2-interacting proteins (Motamedi et al., 2008), considering that the expression level of Chp2 is low in cells (Sadaie et al., 2008) and the C-terminal tag may interfere with the interaction between Chp2 and binding partner(s), it is possible that the physiological Chp2 binding partner(s) may not be identified by the previous strategy. To identify previously unidentified Chp2 interaction partner(s), *S. pombe* strain expressing N-terminal TAP-tagged (NTAP) Chp2 under *swi6+* promoter was generated which was expressing Chp2 protein in 80-times higher than its endogenous promoter (Fig. 15A), and then tandem affinity purification was performed. Additionally, NTAP-Chp2 was purified from a strain expressing $Mit1^{I11R}$ to increase the possibility of finding new interactor proteins besides Mit1 (Fig. 15B). Immunoblotting using the Chp2 antibody was routinely performed to validate the purification procedures (Fig. 15C). In the two independent NTAP-Chp2 experiments, approximately 915 proteins were identified in association with NTAP-Chp2 and NTAP-Chp2 with $Mit1^{I11R}$. Interactors for NTAP-Chp2 with Δ*CSD* (NTAP-Chp2ΔCSD) were also examined to know which proteins are specifically bound to dimerized Chp2-CSD (Fig. 15D, 15E, and 15F). From approximately 915 interactors, 461 proteins were known to interact through the CSD (Fig. 15F), and the full list of the interactors specifically bound to CSD are listed in Table 4.

LC-MS/MS analyses of two independent NTAP-Chp2 purifications successfully identified candidates for Chp2-interacting proteins, and the summary of selected identified proteins is shown in Table 3. Those proteins were selected based on their functions related to

heterochromatin but the detailed contribution for heterochromatin formation remains unknown. A number of peptides for Mit1 were identified in the NTAP-Chp2 purification and it was listed as the third from the top, indicating the reliability of this strategy. Newly identified potential Chp2 interactors are associated with a variety of cellular processes, including nuclear transport (karyopherin, Sal3), H3K9 methyltransferase (Clr4), RNA polymerase II components (Rpb2, Rpb1, Prf1, Paf1), DNA replication/repair (Rad50 and Mms19), RNA binding protein (Dri1), histone deacetylase (Sir2), nucleosome remodeling (Spt6), and histone chaperone (Hip1 and Ccp1). Although whether these proteins interact directly or indirectly with Chp2 needs to be evaluated by further analysis. Most of the identified proteins appear to be associated with chromosomal processes. A recent study characterizing Swi6 interacting proteins suggests that heterochromatin assembly in *S. pombe* is closely associated with (1) complexes involved in RNAi-mediated process, (2) proteins involved in H3K9me and histone deacetylation, (3) a novel RNA processing complex containing Rix1, and (4) proteins involved in nuclear envelope and nucleoporins (Iglesias et al., 2020). Although the list of proteins identified in the NTAP-Chp2 appears to partially overlap with those identified in the previous study for Swi6, this study also uncovered potential functional interactions between Chp2 and factors involved in transcription and DNA replication/repair, which may be related to the distinct function of Chp2 and Swi6 and also to the tight chromatin association of Chp2.

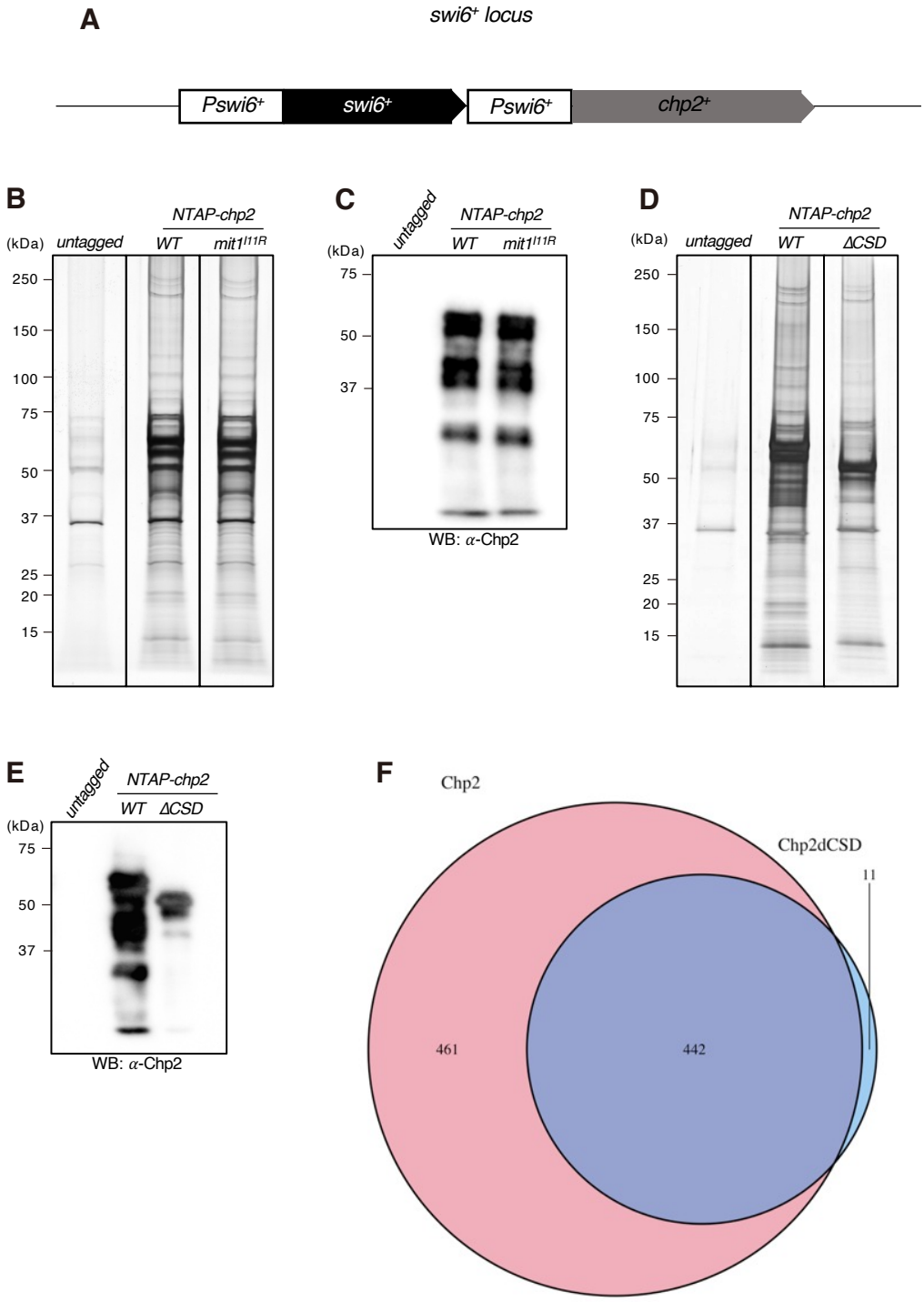

Fig. 15. N-terminus tandem affinity purification (NTAP) of Chp2. (A) N-terminal TAP-tagging Chp2 is expressed at the *swi6*$^{+}$ locus, under the *swi6*$^{+}$ promoter. **(B)** Silver stained-gel showing purification of control (untagged), N-terminal TAP-tagging Chp2 (NTAP-Chp2) in wild-type (WT), and NTAP-Chp2 with Mit1 I11R mutant (*mit1*^{I11R}). **(C)** Western blot analysis of eluted fraction in NTAP-Chp2 purification of WT and *mit1*^{I11R} using anti-Chp2. **(D)** Silver stained-gel showing purification of NTAP-Chp2 wild-type (WT) and NTAP-Chp2 with CSD deletion (Δ*CSD*) was performed as a control experiment of proteins pulled down by WT and *mit1*^{I11R}. **(E)** Western blot analysis of eluted fraction in NTAP-Chp2 purification of WT and Δ*CSD* using anti-Chp2. **(F)** Venn diagram of Chp2-interactor in NTAP-Chp2 wild-type and ΔCSD.

Table 3. Summary of identified proteins associated with Chp2 by NTAP strategy

Identified proteins	sum of peptide count
Sal3 (karyopherin/importin beta family nuclear import signal receptor)	39
Clr4 (histone lysine H3-K9 methyltransferase)	25
Mit1 (SHREC complex ATP-dependent DNA helicase subunit)	21
Rpb2 (RNA polymerase II complex subunit)	12
Rad50 (DNA repair protein)	12
Mms19 (CIA machinery protein)	12
Spt6 (nucleosome remodeling protein/ transcription elongation factor)	9
Hip1 (histone H3.3 H4 chaperone, hira family)	8
Vps4 (AAA family ATPase)	8
Rpb1 (RNA polymerase II large subunit)	7
Prf1 (RNA polymerase II associated Paf1 complex)	7
Ccp1 (histone chaperone, CENP-A nucleosome disassembly)	7
Cut9 (anaphase-promoting complex, TPR lobe subcomplex subunit)	5
Sir2 (histone deacetylase, Sirtuin family, NAD-dependent)	4
Brl2 (ubiquitin-protein ligase E3)	2
Paf1 (RNA polymerase II associated Paf1 complex)	2
Dri1 (RNA-binding protein involved in heterochromatin assembly)	2

Table 4. **List of Chp2's potential binding partners mediated by CSD**

Identified Proteins	Peptide count (tagged-untagged)
Tif302 (translation initiation factor eIF3b [p84])	28
Aro1 (pentafunctional aromatic polypeptide [predicted])	26
Sec26 (coatomer beta subunit [predicted])	25
Sal3 (karyopherin/importin beta family nuclear import signal receptor)	24
Rpc2 (DNA-directed RNA polymerase III complex subunit)	22
Gcn1 (translation initiation regulator)	21
Cam1 (calmodulin)	21
Elf1 (AAA family ATPase)	21
Lys1 (aminoadipate-semialdehyde dehydrogenase)	20
Snd1 (RNA-binding protein, involved in chromatin silencing by small RNA)	20
Rpl301 (60S ribosomal protein L3)	17
Leo1 (RNA polymerase II associated Paf1 complex subunit)	17
Apl4 (AP-1 adaptor complex gamma subunit)	16
Cta4 (P-type ATPase family V, transmembrane protein dislocase/calcium transporting ATPase)	16
Sec24 (coincidence detector Sec24/Sfb2 subunit)	15
ubp5 (ubiquitin C-terminal hydrolase)	15
Cct4 (chaperonin-containing T-complex delta subunit)	14
Ubp15 (ubiquitin C-terminal hydrolase)	14
Ufd2 (ubiquitin-protein ligase E4 Ufd2 [predicted])	14
Rpl2002 (60S ribosomal protein L20 [predicted])	13
Rpc82 (DNA-directed RNA polymerase III complex subunit Rpc82 [predicted])	13
San1 (sir antagonist, ubiquitin-protein ligase E3)	13
Rad50 (DNA repair protein)	12
Rpb2 (RNA polymerase II complex subunit)	12
Leu3 (2-isopropylmalate synthase)	12
Ekc1 (serine/threonine protein phosphatase PP6 regulatory subunit)	12
Tps3 (alpha,alpha-trehalose-phosphate synthase [predicted])	12
Def1 (RNAPII degradation factor Def1 [predicted])	12
Dnm1 (mitochondrial dynamin family scission GTPase)	11
Sds23 (serine/threonine protein phosphatase PP2A inhibitor)	11
Mit1 (SHREC complex ATP-dependent DNA helicase subunit)	11
Erg5 (C-22 sterol desaturase)	10
Grs1 (mitochondrial and cytoplasmic glycine-tRNA ligase)	10
Los1 (karyopherin/importin-beta family nuclear import receptor [predicted])	10
Met10 (sulfite reductase NADPH flavoprotein subunit [predicted])	10
Nmd3 (ribosome export adaptor [predicted])	9
Lrs1 (cytoplasmic leucine-tRNA ligase [predicted])	9
Rpn3 (19S proteasome regulatory subunit)	9
Msh2 (MutS protein homolog 2)	9
Sfb3 (COPII-coated vesicle component [predicted])	9

Clr4 (histone lysine H3-K9 methyltransferase)	9
Apl2 (AP-1 adaptor complex beta subunit)	9
Lcb1 (serine palmitoyltransferase complex subunit [predicted])	9
SPCC14G10.4 (*Schizosaccharomyces* specific protein)	9
Mms19 (CIA machinery protein)	8
Cdc17 (ATP-dependent DNA replication ligase)	8
Rpn6 (19S proteasome regulatory subunit)	8
Frs2 (cytoplasmic phenylalanine-tRNA ligase alpha subunit [predicted])	8
Mtr4 (TRAMP complex ATP-dependent RNA helicase subunit)	8
Vid27 (WD repeat protein, Vid27 family, conserved in fungi and plants)	8
Hip1 (histone H3.3 H4 chaperone, hira family)	8
Puf1 (pumilio family RNA-binding protein)	8
Cwf11 (U2-type spliceosomal complex ATPase)	8
Asp1 (diphosphoinositol pentakisphosphate kinase/InsP8 pyrophosphatase)	8
Rpl3002 (60S ribosomal protein L30 [predicted])	7
Not1 (CCR4-Not complex scaffold subunit 1)	7
Ubp2 (ubiquitin C-terminal hydrolase)	7
Rpl1802 (60S ribosomal protein L18 [predicted])	7
Ppr8 (mitochondrial PPR repeat protein)	7
Nup82 (nucleoporin, WD repeat)	7
Rpn12 (19S proteasome regulatory subunit)	7
Mcm6 (MCM complex subunit)	7
Cwf10 (U5 snRNP GTPase subunit)	7
Kap109 (karyopherin/importin beta family nuclear export signal receptor)	7
Cut14 (condensin complex SMC subunit)	7
Dbl5 (ubiquitin-protein ligase E3)	7
SPAC19B12.01 (TPR repeat protein, human TTC27 ortholog)	7
SPBC1861.05 (bifunctional pseudouridylate synthase/pseudouridine kinase [predicted])	7
Ubp12 (CSN-associated deubiquitinating enzyme)	7
Sty1 (MAP kinase)	6
Uso1 (ER to Golgi tether Uso1 [predicted])	6
Moe1 (translation initiation factor eIF3d)	6
Pol5 (rRNA processing protein)	6
Scs2 (VAP family protein)	6
Fim1 (fimbrin)	6
Cnt5 (Centaurin)	6
Rpb1 (RNA polymerase II large subunit)	6
Psm1 (mitotic/meiotic cohesin complex ATPase subunit Psm1/Smc1)	6
Pmr1 (plasma membrane P-type ATPase, calcium transporting)	6
Usp105 (U1 snRNP-associated protein)	6
Rpn7 (19S proteasome regulatory subunit)	6
Prf1 (RNA polymerase II associated Paf1 complex [predicted])	6
Gnd1 (phosphogluconate dehydrogenase, decarboxylating)	6

Thf1 (C1-5,6,7,8-tetrahydrofolate (THF) synthase, trifunctional enzyme)	6
Puf2 (pumilio family RNA-binding protein)	6
Ags1 (cell wall alpha-1,3-glucan synthase)	6
Srp68 (signal recognition particle subunit [predicted])	6
Npp106 (nucleoporin)	6
Gcs2 (glutamate-cysteine ligase regulatory subunit [predicted])	6
Zpr1 (EF-1 alpha binding zinc finger protein [predicted])	6
Bud6 (nucleation-promoting factor)	6
SPAC30C2.08 (UPF0662 family conserved fungal protein)	6
SPBC1347.09 (hexaprenyldihydroxybenzoate methyltransferase, Coq3 variant [predicted])	6
SPBC1604.12 (*Schizosaccharomyces* specific phosphoprotein)	6
Vrs1 (cytoplasmic valine-tRNA ligase Vrs1/Vas1)	6
Ntp1 (alpha,alpha-trehalase)	6
Ura6 (uridylate kinase)	6
Erg11 (lanosterol 14-demethylase)	5
Rcf2 (cytochrome c oxidase assembly protein)	5
Ssr1 (SWI/SNF and RSC complex subunit)	5
Cka1 (serine/threonine protein kinase)	5
Lsd2 (histone demethylase SWIRM2 [predicted])	5
Ani2 (CENP-A amino terminus domain (NTD) isomerase)	5
End4 (Clathrin adaptor)	5
Met26 (homocysteine methyltransferase)	5
Rpl1002 (60S ribosomal protein L10)	5
Cft2 (cleavage factor two Cft2/polyadenylation factor CPSF-73 [predicted])	5
Cwf3 (Prp19 complex subunit)	5
Gpd1 (glycerol-3-phosphate dehydrogenase)	5
Ppi1 (cyclophilin family peptidyl-prolyl cis-trans isomerase)	5
Uch2 (ubiquitin C-terminal hydrolase)	5
Utp15 (U3 snoRNP-associated WD repeat protein [predicted])	5
Prp1 (U4/U6 x U5 tri-snRNP complex subunit)	5
Prp5 (Prp19 complex WD repeat protein)	5
Phb2 (prohibitin Phb2 [predicted])	5
Mcm3 (MCM complex subunit)	5
Rpc53 (DNA-directed RNA polymerase III complex subunit [predicted])	5
Naa15 (NatA N-acetyltransferase complex regulatory subunit [predicted])	5
Vma4 (V-type ATPase V1 subunit E [predicted])	5
Cdc15 (F-BAR domain protein)	5
Srs1 (cytoplasmic serine-tRNA ligase [predicted])	5
Rps801 (40S ribosomal protein S8 [predicted])	5
Cut9 (anaphase-promoting complex, TPR lobe subcomplex subunit Cut9/Apc6)	5
Vps17 (retromer complex subunit)	5
Tcb3 (tricalbin, C2 domain protein (phospholipid binding) ER-plasma membrane tethering protein)	5

Npa3 (RNA polymerase II binding AAA family ATPase [predicted])	5
Ptr3 (ubiquitin activating enzyme E1)	5
Atp4 (F1-FO ATP synthase subunit [predicted])	5
Rip1 (ubiquinol-cytochrome-c reductase complex subunit 5)	5
Tim50 (TIM23 translocase complex subunit [predicted])	5
Rpl1001 (60S ribosomal protein L10)	5
Cwf7 (Prp19 complex subunit)	5
SPBC2G5.05 (transketolase [predicted])	5
Gtr1 (Gtr1/RagA G protein)	5
Oac1 (mitochondrial carrier, ocaloacetate family anion [predicted])	4
Mce1 (mitochondrial carrier, citrate [predicted])	4
Not3 (CCR4-Not complex NOT box subunit 3/5)	4
Arp42 (SWI/SNF and RSC complex subunit)	4
Rps2801 (40S ribosomal protein S28 [predicted])	4
Sec16 (multidomain vesicle coat component [predicted])	4
Smd2 (Sm snRNP core protein)	4
Abc2 (vacuolar phytochelatin and glutathione S-conjugate ABC family transmembrane transporter)	4
Rpl501 (60S ribosomal protein L5 [predicted])	4
Rpn9 (19S proteasome regulatory subunit)	4
Taf3 (transcription factor TFIID complex subunit Taf3 [predicted])	4
Tif225 (translation initiation factor eIF2B epsilon subunit)	4
Brr2 (U5 snRNP complex subunit)	4
Naa25 (NatB N-acetyltransferase complex regulatory subunit)	4
Ani1 (CENP-A amino terminus domain (NTD) isomerase)	4
Mpg2 (mannose-1-phosphate guanyltransferase [predicted])	4
Sir2 (histone deacetylase, Sirtuin family, NAD-dependent)	4
Smd3 (Sm snRNP core protein)	4
Erg10 (acetyl-CoA C-acetyltransferase Erg10 [predicted])	4
Psy2 (serine/threonine protein phosphatase PP4 regulatory subunit 3 [predicted])	4
Utp6 (U3 snoRNP-associated protein Utp6 [predicted])	4
Spt7 (SAGA complex bromodomain subunit)	4
Rpl2101 (60S ribosomal protein L21 [predicted])	4
Ccp1 (histone chaperone, CENP-A nucleosome disassembly)	4
Tsc13 (enoyl-[acyl-carrier-protein] reductase [predicted])	4
Sec2302 (COPII cargo receptor subunit Sec23b [predicted])	4
Ste13 (ATP-dependent RNA helicase Ste13/Dhh1)	4
Usp107 (U1 snRNP-associated protein)	4
Rpl1601 (60S ribosomal protein L13/L16 [predicted])	4
Irs1 (cytoplasmic isoleucine-tRNA ligase Irs1 [predicted])	4
Ssr4 (SWI/SNF and RSC complex subunit)	4
Pef1 (Pho85/PhoA-like cyclin-dependent kinase)	4
Vid21 (NuA4 histone acetyltransferase complex subunit)	4
Cnd3 (condensin complex non-SMC subunit)	4

Mto1 (gamma tubulin complex linker)	4
Rpl2702 (60S ribosomal protein L27 [predicted])	4
Psi1 (Hsp40 family DNAJ domain protein)	4
Tcb1 (tricalbin, C2 domain protein (phospholipid binding) ER-plasma membrane tethering protein [predicted])	4
Rps1201 [40S ribosomal protein S12 [predicted])	4
Red1 (MTREC (exosome adaptor) complex subunit)	4
Sey1 (ER fusion GTPase, atlastin)	4
Apt1 (adenine phosphoribosyltransferase [APRT])	4
Psd3 (phosphatidylserine decarboxylase)	4
Cwf2 (zf-CCCh type zinc finger protein, Prp19 complex subunit, RNA-binding)	4
Fet5 (predicted GTPase with a role in RNA polymerase localization [predicted])	4
Vma13 (V-type ATPase V1 subunit H [predicted])	4
Dtd1 (D-Tyr-tRNA deacylase Dtd1 [predicted])	4
Gde1 (glycerophosphoryl diester phosphodiesterase Gde1 [predicted])	4
Pre6 (20S proteasome complex subunit alpha 4)	4
Taf51 (transcription factor TFIID complex subunit)	4
SPBC16H5.12c (DUF2433 metallo phosphatase superfamily conserved fungal protein)	4
Tif452 (translation initiation factor eIF4E, 4F complex E subunit isoform 2, stress response factor)	4
Ppk29 (Ark1/Prk1 family protein kinase)	4
Fkh1 (FKBP-type peptidyl-prolyl cis-trans isomerase)	4
Rpn1302 (19S proteasome regulatory subunit)	4
Sly1 (SNARE binding protein [predicted])	4
Get3 (GET complex (ER membrane insertion) ATPase subunit [predicted])	3
Arp2 (ARP2/3 actin-organizing complex subunit)	3
Snf21 (RSC-type complex ATP-dependent DNA helicase)	3
Rga8 (RhoGAP, GTPase activating protein)	3
Utp8 (t-UTP complex subunit [predicted])	3
Fol2 (GTP cyclohydrolase [predicted])	3
Ptr1 (HECT-type ubiquitin-protein ligase E3)	3
Tcd1 (tRNA threonylcarbamoyladenosine dehydratase [predicted])	3
Rpl1602 (60S ribosomal protein L13/L16 [predicted])	3
Fft3 (SMARCAD1 family ATP-dependent DNA helicase)	3
Snz1 (pyridoxal 5'-phosphate synthase [glutamine hydrolysing])	3
Pno1 (KH domain RNA-binding protein [predicted])	3
Kap104 (karyopherin/importin beta family nuclear import signal receptor)	3
Lsm6 (Lsm2-8 complex subunit)	3
Wrs1 (cytoplasmic tryptophan-tRNA ligase Wrs1 [predicted])	3
Sec72 (Arf GEF)	3
Rad52 (DNA recombination protein, Rad51 mediator Rad52 [previously Rad22])	3
Pup2 (20S proteasome complex subunit alpha 5)	3
Cyp1 (cyclophilin family peptidyl-prolyl cis-trans isomerase)	3
Pkp1 (mitochondrial pyruvate dehydrogenase [lipoamide] kinase [predicted])	3

Mrpl9 (mitochondrial ribosomal protein subunit L3 [predicted])	3
Nup155 (nucleoporin, WD repeat)	3
Wos2 (p23 homolog, predicted co-chaperone)	3
Mtr10 (karyopherin/importin-beta family nuclear import receptor Mtr10 [predicted])	3
Cut3 (condensin complex SMC subunit Smc4)	3
Pcl1 (vacuolar ferrous iron/manganese transmembrane transporter)	3
Rps27 (40S ribosomal protein S27 [predicted])	3
Tad2 (tRNA specific adenosine deaminase subunit)	3
Rsc9 (RSC complex subunit)	3
Taf10 (SAGA complex/transcription factor TFIID complex subunit)	3
Ssn6 (transcriptional corepressor)	3
Rga7 (RhoGAP, GTPase activating protein)	3
Rps902 (40S ribosomal protein S9 [predicted])	3
Rrs1 (ribosome biogenesis protein)	3
Rpc25 (DNA-directed RNA polymerase III complex subunit)	3
Cwf4 (Prp19 complex subunit)	3
Cdc6 (DNA polymerase delta catalytic subunit)	3
Hsp16 (heat shock protein)	3
Bag102 (BAG family molecular chaperone regulator)	3
Nop56 (U3 snoRNP protein Nop56 [predicted])	3
Tuf1 (mitochondrial translation elongation factor EF-Tu)	3
Vtc4 (vacuolar transporter chaperone [VTC] complex subunit [predicted])	3
Tef5 (translation elongation factor EF-1 beta subunit, guanyl-nucleotide exchange factor [eEF1B])	3
Hmg1 (3-hydroxy-3-methylglutaryl-CoA reductase)	3
Toa2 (transcription factor TFIIA complex small subunit Toa2 [predicted])	3
Smc6 (Smc5-6 complex SMC P-loop ATPase subunit)	3
Cut15 (importin alpha family nuclear import signal receptor adaptor)	3
Rps1502 (40S ribosomal protein S15 [predicted])	3
Rcl1 (rRNA processing protein [predicted])	3
SPAC13C5.05c (N-acetylglucosamine-phosphate mutase [predicted])	3
Cia2 (CIA machinery protein Cia2 [predicted])	3
SPAC17G6.11c (sphingolipid biosynthesis protein [predicted])	3
Dlp1 (decaprenyl diphosphate synthase subunit 2)	3
Pdc1 (P-body assembly protein)	3
Yfh7 (uridine kinase [predicted])	3
Mug35 (*Schizosaccharomyces* specific protein)	3
Srp102 (signal recognition particle receptor beta subunit [predicted])	3
Mug70 (CBS and PB1 domain protein, conserved in fungi and plants, implicated in signalling)	3
Smd1 (Sm snRNP core protein)	3
SPAC29E6.06c cytoplasmic cysteine-tRNA ligase Crs1 [predicted])	3
Ppk11 (PAK-related GC kinase)	3
SPAC31G5.05c (ribulose phosphate 3-epimerase [predicted])	3

His6 (1-[5-phosphoribosyl]-5-[(5-phosphoribosylamino) methylideneamino]imidazole-4-carboxamide isomerase [predicted])	3
Pan6 (pantoate-beta-alanine ligase)	3
Rps1602 (40S ribosomal protein S16 [predicted])	3
Atg24 (autophagy associated PX/BAR domain sorting nexin)	3
Pre5 (20S proteasome complex subunit alpha 6)	3
SPAC8E11.04c (palmitoyl-[protein] hydrolase [predicted])	3
SPACUNK4.15 (2',3'-cyclic-nucleotide 3'-phosphodiesterase [predicted])	3
Tim21 (TIM23 translocase complex subunit [predicted])	3
Scj1 (Hsp40 family ER-associated DNAJ domain protein [predicted])	3
Trp4 (phosphoribosylanthranilate transferase)	3
SPBC16H5.08c (ribosome biogenesis ATPase, Arb family ABCF2-like [predicted])	3
Met7 (folylpolyglutamate synthase [predicted])	3
Anp1 (mannan polymerase I complex subunit)	3
His5 (imidazoleglycerol-phosphate dehydratase)	3
SPBC29B5.04c (phosphatidate phosphatase converting phosphatidate to diacylglycerol [predicted])	3
SPBC2A9.02 (NADH-dependent glycolaldehyde/furfural/butyraldehyde/propylaldehydealdehyde reductase [predicted])	3
Mrpl35 (mitochondrial ribosomal protein subunit L38 [predicted])	3
SPBC8D2.18c (adenosylhomocysteinase [predicted])	3
Nrk1 (nicotinamide riboside kinase [predicte])	3
SPCC1450.12 (mitochondrial DUF3818 and PXA domain conserved fungal protein)	3
Mrpl22 (mitochondrial ribosomal protein subunit L22 [predicted])	3
SPCC18.17c (proteasome assembly chaperone [predicted])	3
Prp45 (Prp19 complex subunit)	3
Pdr16 (meiotic sec14 cytosolic factor family, phospholipid-intermembrane transfer protein [predicted])	3
Tip41 (TIP41-like type 2a phosphatase regulator)	3
Swp1 (oligosaccharyltransferase delta subunit Swp1 [predicted])	3
Cca2 (ATP 3'tRNA nucleotidyltransferase)	3
SPCC663.15c (DUF3818 and PXA domain conserved fungal protein)	3
Fap7 (nucleoside-triphosphatase involved in SSU-rRNA maturation [predicted])	3
Taf9 (SAGA complex/transcription factor TFIID complex subunit)	2
Mrpl1 (mitochondrial ribosomal protein subunit L1 [predicted])	2
Pro2 (glutamate 5-kinase)	2
Cpy1 (vacuolar carboxypeptidase Y)	2
Nan1 (U3 snoRNP-associated protein [predicted])	2
Rsc58 (RSC complex subunit)	2
Spt6 (nucleosome remodeling protein/ transcription elongation factor)	2
Rpc11 (DNA-directed RNA polymerase III complex subunit)	2
Sap145 (U2 snRNP-associated protein)	2
Kri1 (ribosome biogenesis protein Kri1 [predicted])	2
Kap114 (karyopherin/importin beta family nuclear import signal receptor Kap14)	2
Mpp10 (U3 snoRNP-associated protein [predicted])	2
Rbx1 (SCF complex, Cul4-RING and CLRC ubiquitin ligase ligase E3 subunit)	2

Rfc3 (DNA replication factor C complex subunit)	2
prp10 (U2 snRNP-associated protein SF3B1)	2
Cbf5 (pseudouridine synthase Cbf5 [predicted])	2
Nrd1 (RNA-binding protein)	2
Vps4 (RNA-binding protein)	2
Rpl3802 (60S ribosomal protein L38 [predicted])	2
Rpb11 (RNA polymerase II complex subunit)	2
Sdo1 (SBDS family ribosome assembly protein Sdo1 [predicted])	2
Rpl901(60S ribosomal protein L9)	2
Rpp101 (60S acidic ribosomal protein A1)	2
Paf1 (RNA polymerase II associated Paf1 complex)	2
Rna14 (mRNA cleavage and polyadenylation specificity factor complex subunit)	2
Pro1 (gamma-glutamyl phosphate reductase)	2
Ytm1 (ribosome biogenesis WD repeat WDR12/Ytm1 protein [predicted])	2
Ypt2 (GTPase)	2
Plr1 (pyridoxal reductase)	2
Nop10 (box H/ACA snoRNP complex protein [predicted])	2
Rpc17 (DNA-directed RNA polymerase III complex subunit)	2
Mrt4 (mRNA turnover and ribosome assembly protein Mrt4 [predicted])	2
Pgi1 (glucose-6-phosphate isomerase [predicted])	2
Rix7 (ribosome assembly ATPase Rix7 [predicted])	2
Pwp1 (WD repeat protein Pwp1 [predicted])	2
Krs1 (cytoplasmic lysine-tRNA ligase Krs1 [predicted])	2
Abp2 (unknown protein, may bind replication origins)	2
Rps21 (40S ribosomal protein S21)	2
Lcf1 (long-chain-fatty-acid-CoA ligase)	2
Sac11 (inositol polyphosphate phosphatase [predicted])	2
Utp18 (CGI-48 family [predicted])	2
Rpl26 (60S ribosomal protein L26 [predicted])	2
Gtb1 (gamma-tubulin)	2
Vac8 (vacuolar protein Vac8 [predicted])	2
But2 (But2 family protein, similar to cell surface molecules)	2
Dip2 (U3 snoRNA associated protein Dip2 [predicted])	2
Pdi3 (ER associated protein disulfide isomerase)	2
Rfc5 (DNA replication factor C complex subunit)	2
Rps1701 (40S ribosomal protein S17 [predicted])	2
Rmt3 (type I ribosomal protein arginine N-methyltransferase)	2
Rrp5 (U3 snoRNP-associated protein [predicted])	2
Taf8 (transcription factor TFIID complex subunit 8 [predicted])	2
Sec65 (signal recognition particle subunit [predicted])	2
Fyu1 (UTP-glucose-1-phosphate uridylyltransferase)	2
Rps1501 (40S ribosomal protein S15 [predicted])	2
Oca8 (cytochrome b5 [predicted])	2

Ssb3 (DNA replication factor A subunit)	2
Gad8 (serine/threonine protein kinase [AGC family])	2
Rps1702 (40S ribosomal protein S17 [predicted])	2
Ser3 (D-3 phosphoglycerate dehydrogenase [predicted])	2
Rpl902 (60S ribosomal protein L9)	2
Ssp2 (AMP-activated protein serine/threonine kinase alpha subunit)	2
Vps35 (retromer complex subunit)	2
Mae2 (malic enzyme, malate dehydrogenase [oxaloacetate decarboxylating])	2
Brl2 (ubiquitin-protein ligase E3)	2
Ure7 (urease accessory protein UreG)	2
Mrpl6 (mitochondrial ribosomal protein subunit L6 [predicted])	2
Mrpl19 (mitochondrial ribosomal protein subunit L11 [predicted])	2
Qtr1 (queuine tRNA-ribosyltransferase)	2
Mta1 (S-methyl-5-thioadenosine phosphorylase)	2
Erp2 (COPII-coated vesicle component Erp2/3/4 [predicted])	2
Pck1 (protein kinase C (PKC)-like)	2
Dri1 (RNA-binding protein involved in heterochromatin assembly)	2
Rps3001 (40S ribosomal protein S30 [predicted])	2
SPAC1B3.01c (uracil phosphoribosyltransferase [predicted])	2
Wis2 (cyclophilin family peptidyl-prolyl cis-trans isomerase)	2
Sck1 (serine/threonine protein kinase S6K family)	2
Erv25 (COPII-coated vesicle component Erv25 [predicted])	2
Sds3 (Clr6 histone deacetylase complex subunit)	2
SPAC26A3.14c (DUF1748 family protein)	2
SPAC3A12.08 (acyl-coenzyme A thioesterase)	2
Rrp41 (exosome subunit)	2
Ryh1 (Rab family GTPase)	2
Met8 (siroheme synthase Met8 [predicted])	2
Mtx1 (metaxin 1 [predicted])	2
Gpp74 (Golgi phosphoprotein 3 family Vps74 [predicted])	2
Mug58 (GLYK family kinase of unknown specificity, implicated in nucleotide metabolism [predicted]	2
SPAC644.09 (pyridoxal phosphate homeostasis protein [predicted])	2
Klp2 (kinesin-14 family minus-end directed microtubule motor)	2
Ypt5 (GTPase)	2
Tea3 (cell end marker)	2
SPAC8F11.04 (U3 snoRNP-associated protein Cic1/Utp30 family [predicted])	2
SPAC9.06c (5'-methylthioribulose-1-phosphate dehydratase, adducin Mta3)	2
Rps403 (40S ribosomal protein S4 [predicted])	2
Rps1202 (40S ribosomal protein S12 [predicted])	2
Erp5 (COPII vesicle coat component Erp5/Erp6 [predicted]	2
Mrpl23 (mitochondrial ribosomal protein subunit L13 [predicted])	2
Mtd1 (methylenetetrahydrofolate reductase [predicted])	2
Nup85 (nucleoporin)	2

Prp24 (RNA-binding protein)	2
Rsm10 (mitochondrial ribosomal protein subunit S10 [predicted])	2
Rpn1301 (19S proteasome regulatory subunit Rpn13a)	2
SPBC3E7.07c (DUF757 family protein, human PBDC1 ortholog)	2
Ypt7 (GTPase)	2
Ade7 (phosphoribosylamidoimidazolesuccinocarboxamide synthase, SAICAR synthetase)	2
Rhb1 (Rheb GTPase)	2
Lub1 (WD repeat protein)	2
Snx3 (sorting nexin [predicted])	2
Vps68 (vacuolar sorting protein Vps68 [predicted])	2
Msl1 (U2 snRNP-associated protein Msl1 [predicted])	2
Gsk31 (serine/threonine protein kinase [predicted])	2
Gmh4 (alpha-1,2-galactosyltransferase [predicted])	2
SPBP4H10.07 (ubiquitin-protein ligase E3, unknown specificity [predicted])	2
Tif221 (translation initiation factor eIF2B alpha subunit)	2
SPCC11E10.01 (cystathionine beta-lyase [predicted])	2
Mpc1 (mitochondrial carrier, pyruvate [predicted])	2
Cox9 (cytochrome c oxidase subunit VIIa [predicted])	2
Rpl3402 (60S ribosomal protein L34)	2
Mrpl20 (mitochondrial ribosomal protein subunit L58 [predicted])	2
Coq3 (hexaprenyldihydroxybenzoate methyltransferase)	2
Lsm2 (Lsm2-8 complex subunit)	2
Tim23 (TIM23 translocase complex subunit [predicted])	2
Cti1 (exosome C1D family subunit)	2
Pcs60 (acetyl-CoA ligase [predicted])	2
Hdd1 (GMP 5'-nucleotidase [predicted])	2
Ubc12 (NEDD8-conjugating enzyme)	2
Pda1 (pyruvate dehydrogenase e1 component alpha subunit [predicted])	1.77777778
Pht1 (histone H2A variant H2A.Z)	1.63636364
Gpd3 (glyceraldehyde 3-phosphate dehydrogenase)	1.57803468
Tdh1 (glyceraldehyde-3-phosphate dehydrogenase)	1.37752161
Mcp60 (mitochondrial heat shock protein Hsp60/Mcp60)	1.31683168
Efg1 (rRNA processing protein Efg1 [predicted])	1
Pmm1 (phosphomannomutase)	1
Spb1 (rRNA methyltransferase [predicted])	1
Gsk3 (serine/threonine protein kinase)	1
Yaf9 (YEATS family histone acetyltransferase subunit)	1
Ckb1 (CK2 family regulatory subunit)	1
Irc6 (clathrin coat adaptor)	1
Rpb10 (DNA-directed RNA polymerase I, II, and III subunit)	1
Mde1 (5'-methylthioribulose-1-phosphate dehydratase, adducin Mde1 [predicted])	1
Seb1 (RNA-binding and 3'-end processing protein)	1
Pup1 (20S proteasome complex subunit beta 2)	1

Rnp24 (RNA-binding protein)	1
Rng2 (IQGAP domain cytoskeleton scaffold protein)	1
Atg11 (autophagy associated protein kinase regulator)	1
Ppa1 (serine/threonine protein phosphatase PP2A catalytic subunit)	1
Rpl31 (60S ribosomal protein L31 [predicted])	1
Vas2 (AP-1 adaptor complex sigma subunit)	1
Ost3 (oligosaccharyltransferase gamma subunit [predicted])	1
Lsd1 (histone demethylase SWIRM1)	1
Snx41 (PX domain sorting nexin)	1
Rpl3201 (60S ribosomal protein L32)	1
Las1 (Las1 pre-rRNA processing protein)	1
Srp40 (nucleocytoplasmic transport chaperone [predicted])	1
Rps402 (40S ribosomal protein S4 [predicted])	1
Spt4 (DSIF transcription elongation factor complex subunit)	1
Utp10 (U3 snoRNP-associated protein [predicted])	1
Sec28 (coatomer epsilon subunit [predicted])	1
Cct7 (chaperonin-containing T-complex eta subunit)	1
Mmf1 (mitochondrial matrix protein, YjgF family protein Mmf1, reactive intermediate imine deaminase A homolog)	1
Lsb5 (actin cortical patch component Lsb5 [predicted])	1
Rpl3801 (60S ribosomal protein L38 [predicted])	1
Prp17 (Prp19 complex WD repeat protein)	1
Pwp2 (U3 snoRNP-associated protein Utp1 [predicted])	1
Dis2 (serine/threonine protein phosphatase PP1 catalytic subunit)	1
Sur2 (sphingosine hydroxylase/sphingolipid delta-4 desaturase activity)	1
Alp5 (actin-like protein Arp4)	1
Rpb3 (RNA polymerase II subunit 3)	1
Scw1 (RNA-binding protein)	1
Srp72 (signal recognition particle subunit Srp72 [predicted])	1
Mms2 (ubiquitin conjugating enzyme E2)	1
Not2 (CCR4-Not complex NOT box subunit 2)	1
Rpl35a (60S ribosomal protein L35a)	1
Crn1 (actin binding protein, coronin)	0.63636364
Clc1 (clathrin light chain)	0.33333333
Rps802 (40S ribosomal protein S8 [predicted])	0
Rpl1801 (60S ribosomal protein L18)	0
Rpl401 (60S ribosomal protein L4 [predicted])	0
Nse4 (Smc5-6 complex non-SMC delta-kleisin subunit)	0
Rpb6 (DNA-directed RNA polymerase I, II and III subunit)	0

Potential phosphorylation sites in Chp2

HP1 proteins are subject to post-translational modifications such as phosphorylation, acetylation, or methylation. Among those modifications, the most widely studied modification is phosphorylation, which regulates HP1 association with heterochromatin in *Drosophila*, *S. pombe,* and mammals (Eissenberg et al., 1990; Hiragami-Hamada et al., 2011; Nishibuchi et al., 2019, 2014; Shimada et al., 2009). The phosphorylation state of Chp2 is unknown, but a previous study showed that Chp2 is phosphorylated *in vivo*, but this was not proven by *in vitro* experiments (Shimada et al., 2009). The main reason why the phosphorylation state of Chp2 in cells has not been clarified so far is probably due to the fact that the expression level of Chp2 is very low and it is difficult to prepare Chp2 for phosphorylation analysis. In this study, however, Chp2 expression is driven by the *swi6*$^{+}$ promoter, and NTAP-Chp2 purification allows to obtain sufficient amount of Chp2 for phosphorylation analysis as well as its potential interactors. Using purified NTAP-Chp2, its potential phosphorylation sites were analyzed by LC-MS/MS analysis. This analysis successfully identified 16 phosphorylation sites of Chp2, most of which are located in its disordered N-terminal and hinge regions and were consistently detected in two independent NTAP-Chp2 purifications (Fig. 16).

As with the phosphorylation states of Chp2, the kinases responsible for Chp2 phosphorylation remain unclear. *S. pombe* and mammalian HP1 isoforms, HP1α and HP1β, have been shown to be phosphorylated by casein kinase II (CK2) (Ayoub et al., 2008; Hiragami-Hamada et al., 2011; Nishibuchi et al., 2014; Shimada & Murakami, 2010). Among the Chp2 phosphorylation sites identified in this study, 6 sites match the consensus sequence of CK2 (S-X-X-[E/D], SX[E/D], SD) (Fig. 16). Human HP1 proteins are also phosphorylated by Aurora B kinase (AURKB) during mitosis (Nishibuchi et al., 2019). Although it is still unknown if Swi6 is phosphorylated by Ark1 (a homolog of AURKB in fission yeast), two sites match the consensus sequences of Ark1 (Fig. 16). Phosphorylation of HP1 proteins has been shown to decrease their DNA/RNA binding while increasing selective binding to H3K9me2/3 (Hiragami-Hamada et al., 2011; Nishibuchi et al., 2014; Shimada & Murakami, 2010). This finding suggests that the chromatin association of Chp2 may be controlled by its phosphorylation and that phosphorylated Chp2, like other HP1 proteins, would be dissociated from chromatin during chromosome condensation and segregation.

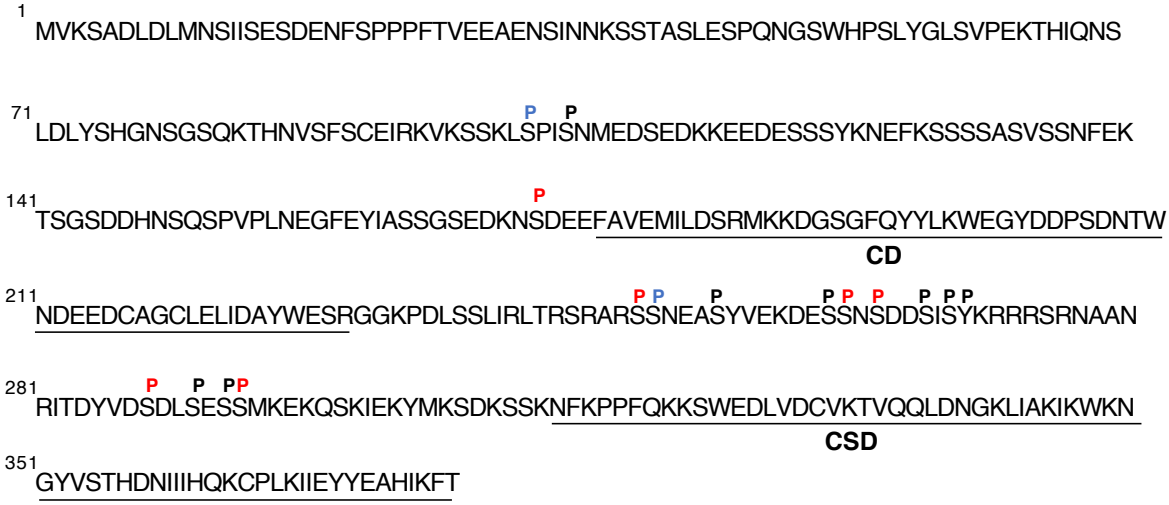

Fig. 16. Identification of phosphorylation sites in Chp2. Summary of phosphorylation sites of Chp2 detected by mass spectrometry analysis. These sites were consistently detected in two independent NTAP-Chp2 WT purifications. **P**; phosphorylation by unknown kinase, **P**; containing aurora kinase (Ark1) consensus sequence, **P**; containing casein kinase II (CK2) consensus sequence.

Chp2 interacts with methyltransferase Clr4

Clr4 is a member of the Su(var)3-9 family H3K9 methyltransferases in fission yeast. Clr4 consists of an N-terminal chromodomain (CD) and a C-terminal catalytic domain connected by a disorder region. The C-terminal catalytic domain is further subdivided into N-terminal SET (N), pre-SET (Pre), catalytic SET with auto-regulatory loop (ARL) region, and post-SET domains (Fig. 17A) (Min et al., 2002; Yeates, 2002). Clr4 methylates histone H3 lysine 9 (H3K9) through its catalytic SET domain using S-adenosyl-L-methionine (SAM) as a cofactor.

NTAP-Chp2 purification identified Clr4 as the second from the top on the list of Chp2 candidate interactors (Table 3). Among the Su(var)3-9 family members, mammalian SUV39H1 (Muramatsu et al., 2016) and *Drosophila* Su(var)3-9 (Schotta et al., 2002; Vermaak & Malik, 2009) have been shown to interact with HP1 proteins in their respective species, and the interaction is important for their distinct heterochromatic localization. However, a potential interaction between Clr4 and two HP1 proteins in fission yeast has not yet been defined. To investigate whether Chp2 directly interacts with Clr4, a yeast two-hybrid assay was used (Fig. 2B). In this assay, Chp2 and Clr4 were expressed as bait and prey, respectively, similar to what was done to study the interaction between Chp2 and Mit1 (Fig. 2A). A small number of diploid cells expressing Chp2 (bait) and Clr4 (prey) grew on the medium without histidine (SD-TLH) but not on the medium with the addition of 3AT (Fig. 17B). The number of diploid cells growing on the SD-TLH medium was apparently higher than that of the negative control expressing an empty vector, suggesting that Chp2 interacts weakly with Clr4. The protein expression for the yeast two-hybrid assay was also examined by Western blotting (Fig. 17C).

To understand the physical interaction between Chp2 and Clr4, mutant Clr4 proteins lacking each domain were expressed and examined in the yeast two-hybrid assay (Fig. 18A). Interestingly, diploid cells expressing Chp2 with mutant Clr4 lacking N and Pre (NpreΔ) or SET (SETΔ) grew well on SD-TLH medium as well as SD-TLH medium containing 3AT, whereas mutant Chp2 lacking CD (CDΔ) failed to grow even in SD-TLH medium (Fig. 18B). The protein expression of each deletion construct was examined by Western blotting (Fig. 18C). These results indicate that the mutant Clr4 with NpreΔ or SETΔ interacts strongly with Chp2, even more strongly than the full-length Clr4, and also suggest that the N-Pre and SET domains may inhibit the interaction between Chp2 and Clr4.

To gain further insight into the interaction between Chp2 and Clr4, a series of Clr4 truncated mutants were examined in the yeast two-hybrid assay (Fig. 19A). Diploid cells expressing Chp2 with the N-terminus of Clr4 containing the CD and the disorder region (N-H) grew well on the SD-TLH medium but not on the SD-TLH medium containing 3AT (Fig. 19B). However, further addition of the C-terminal domain N- and pre-SET (Npre) to the N-terminus resulted in no growth of diploid cells on the selective medium. On the other hand, cells expressing Chp2 with the C-terminus of Clr4 containing the SET and the distal C-terminal regions (SET) grew well on the SD-TLH medium as well as on the SD-TLH medium containing 3AT, but further addition of the Npre blocked the growth of the diploid cells (Fig. 19B). The expression of each truncated Clr4 was confirmed by Western blotting (Fig. 19C). Taken together, these results suggest that Clr4 may interact with Chp2 through at least two distinct domains: one in the N-terminus of Clr4 containing the CD and the disordered region, and the other in the C-terminus of Clr4 containing the SET and the distal C-terminal regions, and also that these interactions are similarly blocked by the presence of the central Npre domain. Since diploid cells expressing Chp2 with mutant Clr4 lacking the CD no longer grew on the selective medium (Fig. 18B), it is likely that the Clr4-CD plays a critical role in the interaction between Chp2 and the Clr4 N-terminus. In addition, the result showed a positive interaction between SETΔ and Chp2 that needs to be considered carefully (Fig. 17B). Deletion of the SET domain may alter the overall structure of Clr4, thereby suppressing the inhibitory function of the Npre domains. Further analysis of Chp2-Clr4 interaction may help to understand how the physical interaction between them is regulated in the cellular context.

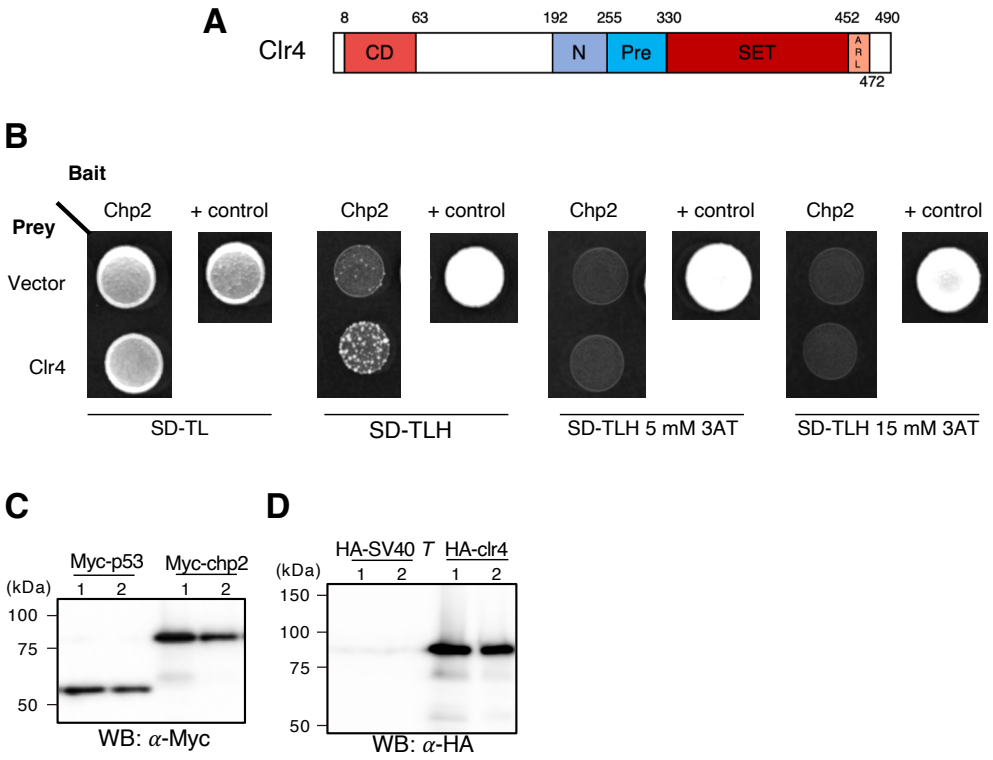

Fig. 17. Chp2 interacts weakly with methyltransferase Clr4. (A) Schematic illustration of Clr4 protein domains. Clr4 protein consists of a chromodomain (CD), N-terminus of SET domain (N), Pre-SET domain (Pre), SET domain (SET), and auto-regulatory loop (ARL). **(B)** Yeast two-hybrid assay of full-length Chp2 and Clr4. The positive control was p53 and SV40 T-antigen. Yeast cells were spotted on SD-TL: SD/-Trp/-Leu, SD-TLH: SD/-Trp/-Leu/-His, SD-TLH with 3AT: 3-amino-1,2,4-triazole. **(C)** Western blot analysis of Chp2 and Clr4, including the positive control used in this assay. Proteins in bait were detected by anti-myc, while proteins in prey were detected by anti-HA.

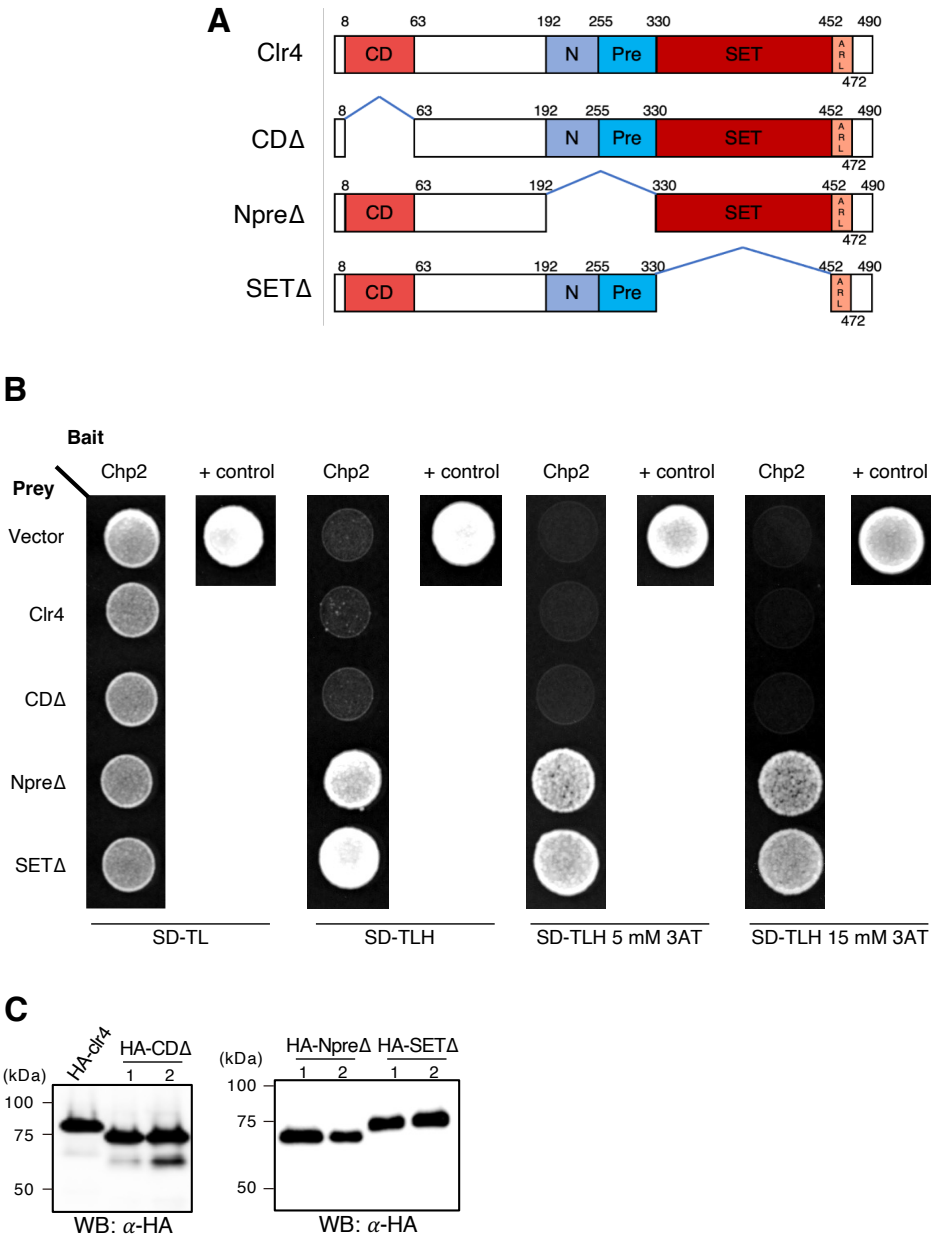

Fig. 18. The interaction site of Chp2 may lie at the C-terminus of Clr4. (A) Schematic illustration of Clr4 mutants used in yeast two-hybrid assay. The deletion series of chromodomain (CDΔ), N-terminus and Pre-SET (NpreΔ), and SET domain (SETΔ) were constructed. **(B)** Yeast two-hybrid assay of full-length Chp2 and deleted domains of Clr4. Chp2-Clr4 interaction was also included as a comparison, and empty vectors as prey were used as a negative control. The positive control was p53 and SV40 T-antigen. Yeast cells were spotted on SD-TL: SD/-Trp/-Leu, SD-TLH: SD/-Trp/-Leu/-His, SD-TLH with 3AT: 3-amino-1,2,4-triazole. **(C)** Western blot analysis of Clr4 mutants used in the yeast two-hybrid assay.

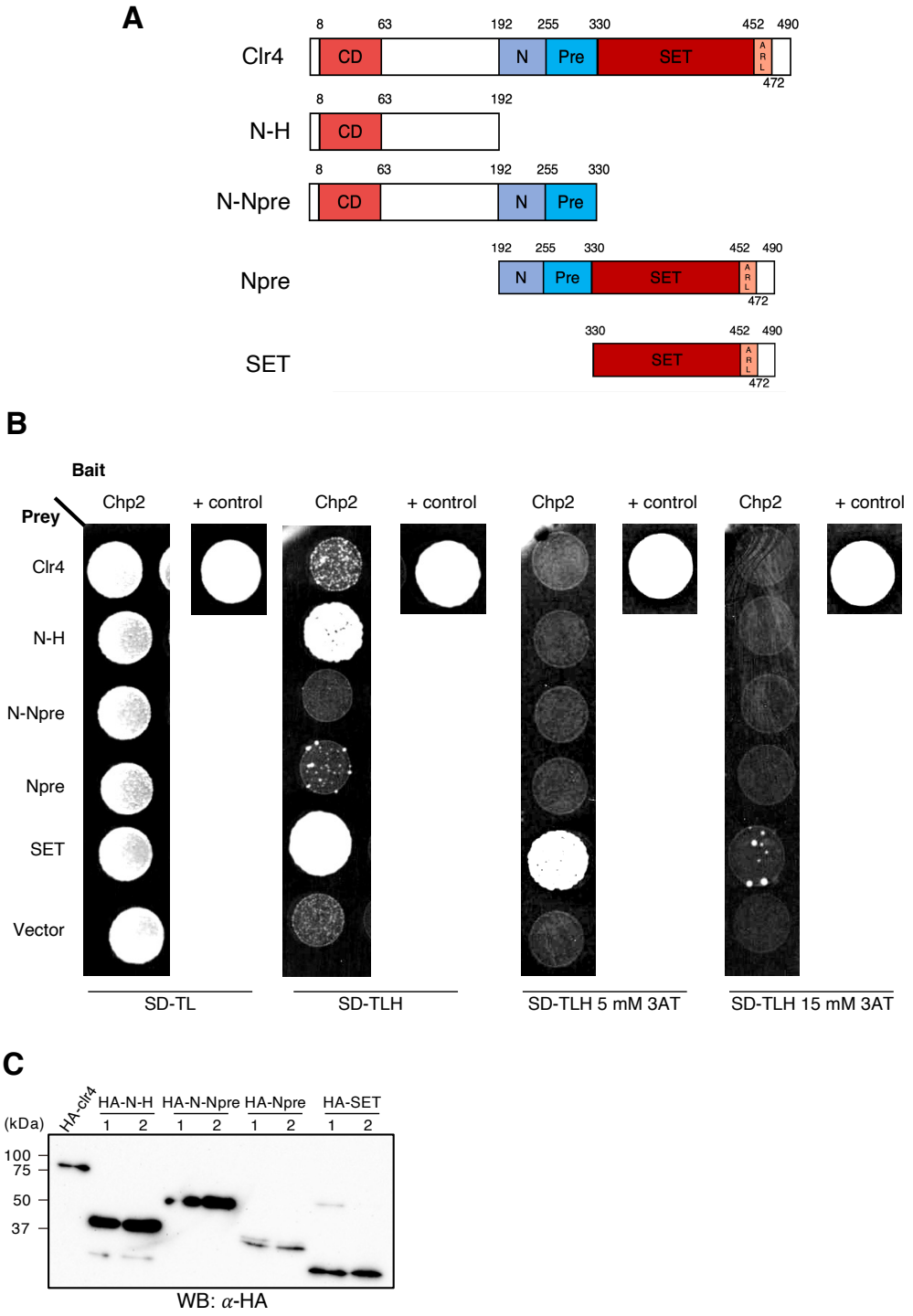

Fig. 19. Interaction site of Chp2 may be located at the N-terminus and C-terminus region of Clr4. **(A)** Schematic illustration of truncated domains of Clr4 used in yeast two-hybrid assay. N-H: N-terminus until hinge region, N-Npre: N-terminus until N-terminus of SET and Pre-SET domain, Npre: N-terminus of SET domain until C-terminus of Clr4, SET: SET domain until C-terminus of Clr4. **(B)** Yeast two-hybrid assay of full-length Chp2 and truncated domains of Clr4. Chp2-Clr4 interaction was also included as a comparison and empty vectors as prey were used as a negative control. The positive control was p53 and SV40 T-antigen. Yeast cells were spotted on SD-TL: SD/-Trp/-Leu, SD-TLH: SD/-Trp/-Leu/-His, SD-TLH 3AT: 3-amino-1,2,4-triazole. **(C)** Western blot analysis of truncated domains of Clr4 used in the yeast two-hybrid assay.

Discussion

Although many eukaryotic cells express HP1 isoforms, the distinct and/or overlapping roles of these isoforms have not been fully elucidated. In this study, I focus on Chp2, one of the two HP1 isoforms in the fission yeast *S. pombe*, and demonstrate that Chp2 recognizes the N-terminus of Mit1 in agreement with a paper published in 2019 with specifically identified CkIvV motif. Furthermore, this study also showed that Chp2's DNA binding mediated by the hinge and the N-terminus of the CSD is critical for the Chp2 function in heterochromatic silencing. Previously, mammalian HP1 proteins are known to bind DNA or RNA primarily through their unstructured hinge regions (Mishima et al., 2013; Nishibuchi et al., 2014), and several studies have also shown that the unstructured N-terminal region also contributes to the binding. Similar to other HP1 proteins, Chp2 also binds to DNA through its hinge and the N-terminal regions (Fig. 7), but Chp2 also has a unique DNA-binding activity through the N-terminus of the CSD, which has not been described for other HP1 proteins. Importantly, mutant Chp2 containing either the hinge or the N-terminus of CSD retains silencing function, but mutant Chp2 with a combined mutations shows a clear silencing defects (Fig. 11C) and impaired heterochromatin localization (Fig. 13A and 14), suggesting that DNA binding activities involving these regions contribute to proper Chp2 function in heterochromatin assembly. How these DNA binding activities are coordinated with the recognition by the CD and/or interaction with other binding partners by dimerized CSD in the nucleosomal context remains to be elucidated by further structural analysis.

To analyze the DNA binding activity of the Chp2-CSD, we identified three residues, Q320, K321, K322, that are critical for the DNA binding (Fig. 20). These three residues are followed by four evolutionarily conserved hydrophobic residues, F315, P317, P318, and F319. These hydrophobic residues interact with other hydrophobic residues of the CSD, which makes the residues of Q320, K321, and K322, face the solvent region, an environment where the side chains can behave flexibly (Fig. 20). This structure seems unique compared to N-terminal part of Swi6-CSD. In addition, such a unique structure may also be related to the unstable nature of full-length Chp2 *in vitro* and *in vivo*. To study about these residues function in DNA binding, I generated two different mutants on the N-terminal part of CSD, mut3 and mut5. The differences are only in the Q320A which is also mutated in mut5. In a previous study, it has been shown that Q320 is shifted due to the structural change when Chp2 binds Mit1. In fact, the N-terminus of CSD in Chp2 provides a binding surface when

interacting with Mit1 compared to Swi6 (Leopold et al., 2019). This N-terminus of CSD in Chp2 may also contribute to selective binding with other chromosomal proteins. I suggest Q320A may increase the hydrophobicity of the N-terminal part of CSD and presumably benefit from the interaction with Mit1 or other binding partners. A previous study has shown that mutant Chp2 with an amino acid substitution at S323, next to the residues required for the DNA binding, showed marked instability *in vivo* (Shimada et al., 2009). These results also support the idea that the N-terminal region of CSD in Chp2 has a unique structural property that is closely related to its protein stability since mut3 and mut5 are unstable both *in vitro* and *in vivo* (Fig. 12). Although Chp2 Q320 does not appear to be directly involved in the interaction with Mit1, it is possible that Q320A increases regional hydrophobicity to support the interaction with Mit1, thereby rescuing the heterochromatic localization of Chp2 in mut5 via the enhanced interaction with Mit1.

In agreement with a previous report (Sadaie et al., 2008), we confirmed that in the chromatin fractionation assay, Chp2 is tightly associated with the chromatin-enriched fraction, and this association is maintained in Clr4-depleted cells or cells expressing mutant Mit1 ($Mit1^{I11R}$) and a combination of both mutants. Based on these observations, DNA binding activities associated with Chp2 seems to be a good explanation. However, mutant Chp2 defective in DNA binding is still tightly associated with the chromatin-enriched fraction (Fig. 12). How does Chp2 bind tightly to the chromatin-enriched fractions? It is possible that Chp2 uses multiple modes in addition to the H3K9me2/3 recognition, DNA binding activities, protein modifications, and the interaction with Mit1/other proteins to maintain a stable association with chromatin. It is also possible that Chp2 dissociated from the chromatin is susceptible to degradation, which may correlate with the observations that Chp2 expression levels appear to be kept low and that overexpression of Chp2 results in a silencing defect (Sadaie et al., 2008).

This study further identified other potential binding partners of Chp2 that may contribute to the stable association of Chp2 with chromatin. NTAP-Chp2 strategy combined with LC-MS/MS analysis successfully identified the potential binding partners. Furthermore, I confirmed the reliability of this strategy, since Mit1 is at the top of the list of interactors in the NTAP-Chp2 wild type. Additionally, direct interaction between those candidates and Chp2 needs to be examined by yeast two-hybrid assays, pull-down experiments, or other techniques. From the list, Sal3, Clr4, Rpb2, Rad50, and Mms19 are highlighted as the top

potential binding partners. From the perspective of Chp2's associated proteins, the function of those proteins suggests that heterochromatin may link with a variety of cellular processes, including nuclear transport (Karyopherin, Sal3), H3K9 methyltransferase (Clr4), RNA polymerase II components (Rpb2, Rpb1, Prf1, Paf1), DNA replication/repair (Rad50 and Mms19), RNA binding protein (Dri1), histone deacetylase (Sir2), nucleosome remodeling (Spt6), and histone chaperones (Hip1 and Ccp1). In a recent paper, Swi6 immunoprecipitation revealed that heterochromatin is closely associated with (1) RNAi protein complexes, (2) proteins involved in H3K9me and histone deacetylation, (3) Rix1 RNA processing complex, and (4) nuclear envelope proteins and nucleoporins. Indeed, previous TAP-Swi6 identified DNA replication/repair proteins associated with Swi6 (Fischer et al., 2009). Although the list of proteins identified in the NTAP-Chp2 appears to partially overlap with those identified in the previous study for Swi6, this study also uncovered potential functional interactions between Chp2 and factors involved in various cellular processes and complex outside SHREC. By the interactions with Rpb2, Chp2 may also be associated with the RNAi processing complex. Rpb2, the largest member of the RNA polymerase II complex, is responsible for RNAi transcription of pericentromeric in *cis*-PTGS rather than RNA polymerase III (Kato et al., 2005). Yet, it is still unknown how Chp2 functions in other chromosomal complexes inside cells to regulate heterochromatin. Moreover, it is also unclear how such binding partners contribute to Chp2-chromatin binding. One of the binding partners may be required for Chp2-chromatin association.

On the other hand, HP1 proteins are known to be regulated by post-translational modification. The most widely studied is phosphorylation. HP1 proteins, in general, are known to be phosphorylated, and the phosphorylation is important for targeting H3K9me, DNA/RNA binding, and also dissociation from chromatin during mitosis (Hiragami-Hamada et al., 2011; Nishibuchi et al., 2019, 2014; Nozawa et al., 2010). While Swi6 has previously been shown to be phosphorylated by CK2 (Nishibuchi et al., 2014; Shimada et al., 2009; Shimada & Murakami, 2010), this study also shows that Chp2 may be subjected to phosphorylation within its disordered region at the N-terminus and hinge. I suggest that phosphorylation may regulate Chp2 function in the same way as other HP1 proteins. However, it is still unknown what kind of kinase is responsible for Chp2 phosphorylation. At least, from the result of LC-MS/MS analysis, CK2, and Ark1 are presumably responsible for Chp2 phosphorylation. Further, the effect of phosphorylated Chp2 on the Chp2-chromatin association and the regulation of its function needs to be confirmed.

Meanwhile, it is unknown previously that Chp2 interacts with H3K9 methyltransferase Clr4 as shown by the NTAP-Chp2 result. The relationship between Chp2-Clr4 is intriguing to study since the dependency and direct interaction between them have been reported in higher organisms but are unknown in the fission yeast (Muramatsu et al., 2016; Schotta et al., 2002; Vermaak & Malik, 2009). Raising the possibility that the interaction between HP1 proteins and methyltransferase is a conserved mechanism in eukaryotes. In the higher eukaryotes, the interaction between the N-terminus of H3K9 methyltransferase Su(var)3-9 in *Drosophila* or SUV39H1 in mammals with HP1 proteins is critical for heterochromatin localization of both proteins (Muramatsu et al., 2016; Schotta et al., 2002). But the role of Chp2 in Clr4 targeting heterochromatin is unclear yet since Clr4 seems to rely on its CD to associate with H3K9me and further di-methylate and tri-methylate heterochromatin regions in fission yeast (Iglesias et al., 2018; Jih et al., 2017). In this study, the yeast two-hybrid assay was used to clarify the direct interactions between Chp2-Clr4. While full-length Chp2 and Clr4 interaction was relatively weak, subsequent confirmation by Clr4 mutations and truncations suggested that Clr4 may interact with Chp2 through at least two distinct domains: one in the N-terminus of Clr4 containing the CD and the disordered region, and the other in the C-terminus of Clr4 containing the SET and the distal C-terminal regions, and also that these interactions are presumably blocked by the presence of the central N-and Pre-SET domain.

Further research is needed to clarify how DNA-binding activities, binding partners, and phosphorylation work together to contribute to Chp2's involvement in heterochromatin assembly and protein stability. Dysregulation of HP1 proteins or heterochromatin is linked to the development of disease in humans. Decreased HP1α has been reported in invasive breast cancer while HP1c is known as one of the high-risk genes in colorectal cancer and gastric cancer using *Drosophila* gut as a model (Hahn et al., 2010; Sun et al., 2021). Taken together, understanding the complexity of Chp2 biochemical properties and function as one of the HP1 protein homologs, will help to understand HP1 protein function in higher organisms.

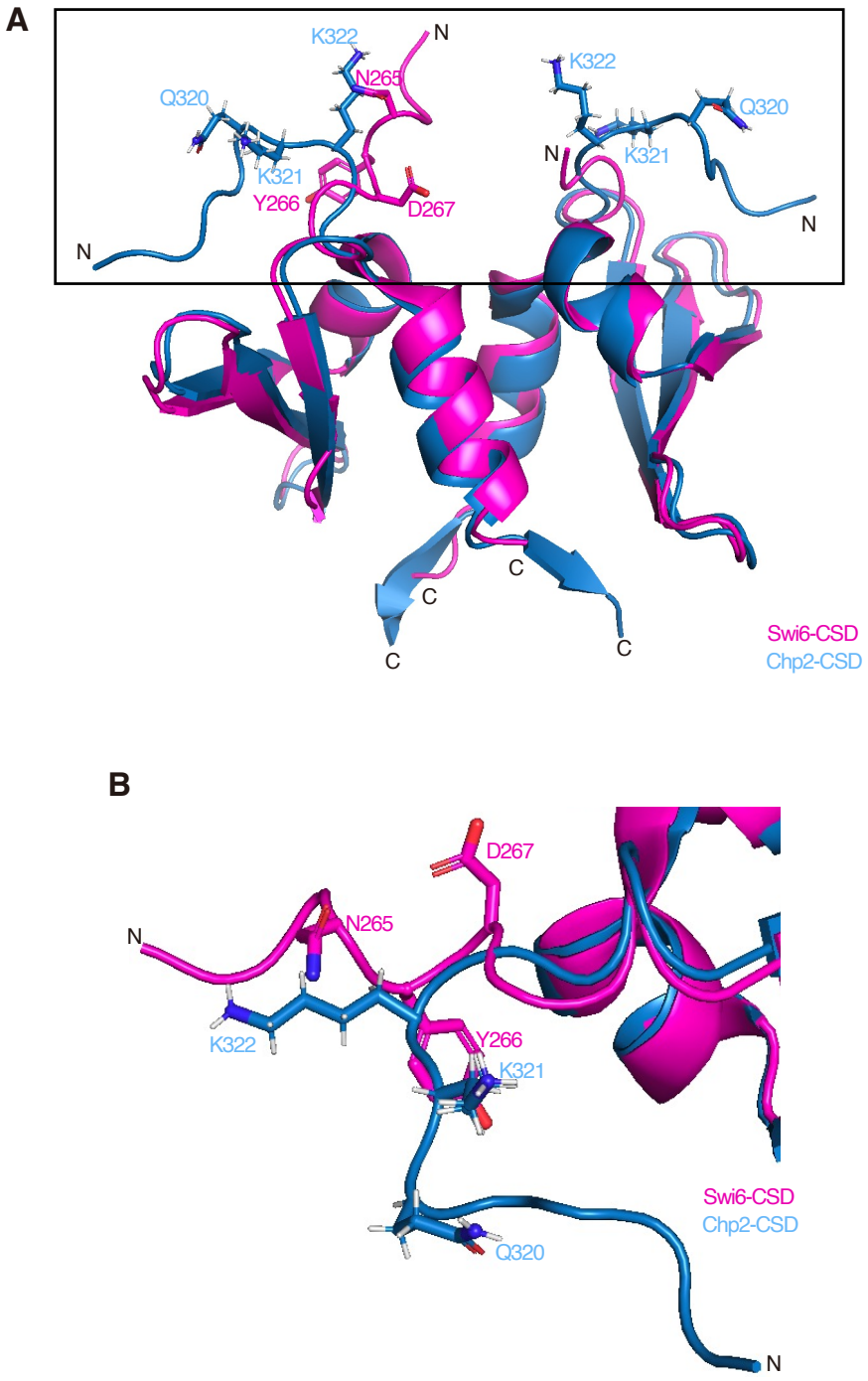

Fig. 20. The chromoshadow domain of Chp2 and Swi6 have different structures at the N-terminus. (A) Superimposition of Chp2-CSD (PDB, ID: 6FTO) in light blue and Swi6-CSD (PDB, ID: 1E0B) in pink. The N-terminus part of CSD (N) is shown inside a black square. The important residues for DNA binding in Chp2 are shown as Q320, K321, and K322. Swi6's residues in equal positions are also shown as N265, Y266, and D267. **(B)** N-terminus of Chp2-CSD and Swi6-CSD.

Concluding remarks

The purpose of this study is to gain insight into the distinct function of HP1 proteins in fission yeast. I focused on fission yeast or *S. pombe* Chp2 and investigated the connection between its biochemical properties and its function, in particular its DNA binding ability, and tried to identify Chp2-specific interacting partners by affinity purification.

This study showed that Chp2 has a similar affinity to bind DNA compared with Swi6, and the basic residues on its hinge and CSD contribute to this binding. These residues are critical in regulating Chp2-chromatin binding and silencing of heterochromatin. Nonetheless, chromatin fractionation experiments revealed that Chp2's DNA-binding defect remains fully associated with chromatin. The persistence of Chp2's chromatin-binding is also observed in Clr4- and Mit1-depleted conditions, which is thought to be related to Chp2's distinct roles. However, how the distinct function of Chp2 contributes to the formation of a fully repressed chromatin state remains incompletely understood. Therefore, this study also further identifies Chp2's potential binding partners and phosphorylation sites, to gain more insight on how Chp2 works with those different modes in the cell context. NTAP-Chp2 purification following LC-MS/MS analysis identified a number of novel Chp2 binding partners, including importin/karyopherin family proteins, RNA polymerase II components, factors involved in DNA replication/repair, and the H3K9 methyltransferase Clr4. In this study, only Chp2-Clr4 and Chp2-Mit1 are confirmed to have direct interactions by a yeast two-hybrid assay. How other candidates associate with Chp2, in a direct or indirect manner or how they affect Chp2-chromatin binding must be examined in the future.

Acknowledgments

I would like to express my sincere gratitude to Prof. Dr. Jun-ichi Nakayama for his patience, continuous advice, and guidance during my Ph.D study. I would like to express my sincere gratitude to Dr. Aki Hayashi for her patience, advice, and all the jokes in her calm advice when I make a mistake during experiments, it helps me to reduce my panic.

I want to express my gratitude to the Japan Ministry of Education, Culture, Sports, Science, and Technology (MEXT) for the scholarship during my five years doctoral course and SOKENDAI Student Dispatch Program, which supported my trip to attend a conference and visit a lab.

I would like to thank Dr. Genevieve Thon for the original yeast strains that I used in this research. Yamashita lab for lending me the scanner to capture images. I also want to thank my life science progress committee advisors for all the advice during my study, also Prof. Dr. Tomomi Tsubouchi for all the advice about research, and our talk on how to navigate a career path after Ph.D.

I would like to thank Nakayama lab members including former lab members, Aki Hachisuka and Megumi Kiyohara for their kind help with my research and with my life in Japan. I would like to thank Dwi Wahyu Indriani, Rizki Tsari, Nur Ika Puji Ayu as my Indonesian seniors here, for the help, friendship, sisterhood, and all of our Japan trip together. I would like to thank all of my friends in Okazaki and Riri in Okayama for their friendship, and for the good foods that we enjoyed together.

I would like to thank Slamet Mudjio family, my fiancée, and all of my friends in Indonesia that have been really supportive. Without their support, their reminder, and their prayer, I don’t think I am strong enough to still stand up through the days and finish my Ph.D. “Remember your idea, your goals, and the reason why you chose to study abroad. Study well and be strong!” is an unforgettable quote in every phone call.

Finally, many thanks to all of the musicians on my music playlist who have provided me with fantastic music to enjoy Ph.D journey. Linkin Park, BMTH, A7X, Saosin, SWS, Paramore, MCR, Radiohead, Incubus, Tame Impala, Murphy Radio, Payung Teduh, Kilms, For Revenge, BTS, Twice, and NewJeans, all of your songs saved my day.

Anisa Fitri Rahayu

References

Akoury, E., Ma, G., Demolin, S., Brönner, C., Zocco, M., Cirilo, A., Ivic, N., & Halic, M. (2019). Disordered region of H3K9 methyltransferase Clr4 binds the nucleosome and contributes to its activity. *Nucleic Acids Research*, *47*(13), 6726–6736. https://doi.org/10.1093/nar/gkz480

Allshire, R. C., & Ekwall, K. (2015). Epigenetic regulation of chromatin states in Schizosaccharomyces pombe. *Cold Spring Harbor Perspectives in Biology*, *7*(7), 1–25. https://doi.org/10.1101/cshperspect.a018770

Allshire, R. C., & Madhani, H. D. (2018). Ten principles of heterochromatin formation and function. *Nature Reviews Molecular Cell Biology*, *19*(4), 229–244. https://doi.org/10.1038/nrm.2017.119

Ayoub, N., Jeyasekharan, A. D., Bernal, J. A., & Venkitaraman, A. R. (2008). HP1-β mobilization promotes chromatin changes that initiate the DNA damage response. *Nature*, *453*(7195), 682–686. https://doi.org/10.1038/nature06875

Buker, S. M., Iida, T., Bühler, M., Villén, J., Gygi, S. P., Nakayama, J. I., & Moazed, D. (2007). Two different Argonaute complexes are required for siRNA generation and heterochromatin assembly in fission yeast. *Nature Structural and Molecular Biology*, *14*(3), 200–207. https://doi.org/10.1038/nsmb1211

Canzio, D., Liao, M., Naber, N., Pate, E., Larson, A., Wu, S., Marina, D. B., Garcia, J. F., Madhani, H. D., Cooke, R., & Schuck, P. (2014). *NIH Public Access*. *496*(7445), 377–381. https://doi.org/10.1038/nature12032.A

Cowieson, N. P., Partridge, J. F., Allshire, R. C., & McLaughlin, P. J. (2000). Dimerisation of a chromo shadow domain and distinctions from the chromodomain as revealed by structural analysis. *Current Biology*, *10*(9), 517–525. https://doi.org/10.1016/S0960-9822(00)00467-X

Eissenberg, J. C., James, T. C., Foster-Hartnett, D. M., Hartnett, T., Ngan, V., & Elgin, S. C. R. (1990). Mutation in a heterochromatin-specific chromosomal protein is associated with suppression of position-effect variegation in Drosophila melanogaster. *Proceedings of the National Academy of Sciences of the United States of America*, *87*(24), 9923–9927. https://doi.org/10.1073/pnas.87.24.9923

Fennessy, D., Grallert, A., Krapp, A., Cokoja, A., Bridge, A. J., Petersen, J., Patel, A., Tallada, V. A., Boke, E., Hodgson, B., Simanis, V., & Hagan, I. M. (2014). Extending the Schizosaccharomyces pombe molecular genetic toolbox. *PLoS ONE*, *9*(5). https://doi.org/10.1371/journal.pone.0097683

Fischer, T., Cui, B., Dhakshnamoorthy, J., Zhou, M., Rubin, C., Zofall, M., Veenstra, T. D., & Grewal, S. I. S. (2009). Diverse roles of HP1 proteins in heterochromatin. *Pnas*, *106*(22), 1–6.

Goto, D. B., & Nakayama, J. I. (2012). RNA and epigenetic silencing: Insight from fission yeast. *Development Growth and Differentiation*, *54*(1), 129–141. https://doi.org/10.1111/j.1440-169X.2011.01310.x

Grewal, S. I. S., & Elgin, S. C. R. (2002). Heterochromatin: New possibilities for the inheritance of structure. *Current Opinion in Genetics and Development*, *12*(2), 178–187. https://doi.org/10.1016/S0959-437X(02)00284-8

Hahn, M., Dambacher, S., & Schotta, G. (2010). Heterochromatin dysregulation in human diseases. *Journal of Applied Physiology*, *109*(1), 232–242. https://doi.org/10.1152/japplphysiol.00053.2010

Hiragami-Hamada, K., Shinmyozu, K., Hamada, D., Tatsu, Y., Uegaki, K., Fujiwara, S., & Nakayama, J. (2011). *N-Terminal Phosphorylation of HP1α Promotes Its Chromatin Binding*. *31*(6), 1186–1200. https://doi.org/10.1128/MCB.01012-10

Iglesias, N., Currie, M. A., Jih, G., Paulo, J. A., Siuti, N., Kalocsay, M., Gygi, S. P., & Moazed, D. (2018). Automethylation-induced conformational switch in Clr4 (Suv39h) maintains epigenetic stability. *Nature*, *560*(7719), 504–508. https://doi.org/10.1038/s41586-018-0398-2

Iglesias, N., Paulo, J. A., Tatarakis, A., Haas, W., Gygi, S. P., Moazed, D., Iglesias, N., Paulo, J. A., Tatarakis, A., Wang, X., Edwards, A. L., & Bhanu, N. V. (2020). Native Chromatin Proteomics Reveals a Role for Specific Nucleoporins in Heterochromatin Organization and Maintenance Article Native Chromatin Proteomics Reveals a Role for Specific Nucleoporins in Heterochromatin Organization and Maintenance. *Molecular Cell*, 1–16. https://doi.org/10.1016/j.molcel.2019.10.018

Isaac, R. S., Sanulli, S., Tibble, R., Hornsby, M., Ravalin, M., Craik, C. S., Gross, J. D., & Narlikar, G. J. (2017). Biochemical Basis for Distinct Roles of the Heterochromatin Proteins Swi6 and Chp2. *Journal of Molecular Biology*, *429*(23), 3666–3677. https://doi.org/10.1016/j.jmb.2017.09.012

Jacobs, S. A., & Khorasanizadeh, S. (2002). Structure of HP1 chromodomain bound to a lysine 9-methylated histone H3 tail. *Science*, *295*(5562), 2080–2083. https://doi.org/10.1126/science.1069473

James, P., Halladay, J., & Craig, E. a. (1996). Genomic Libraries and a Host. *Genetics*, *144*, 1425–1436.

James, T. C., & Elgin, S. C. (1986). Identification of a nonhistone chromosomal protein associated with heterochromatin in Drosophila melanogaster and its gene. *Molecular and Cellular Biology*, *6*(11), 3862–3872. https://doi.org/10.1128/mcb.6.11.3862

Jih, G., Iglesias, N., Currie, M. A., Bhanu, N. V., Paulo, J. A., Gygi, S. P., Garcia, B. A., & Moazed, D. (2017). Unique roles for histone H3K9me states in RNAi and heritable silencing of transcription. *Nature*, *547*(7664), 463–467. https://doi.org/10.1038/nature23267

Job, G., Brugger, C., Xu, T., Lowe, B. R., Pfister, Y., Qu, C., Shanker, S., Baños Sanz, J. I., Partridge, J. F., & Schalch, T. (2016). SHREC Silences Heterochromatin via Distinct Remodeling and Deacetylation Modules. *Molecular Cell*, *62*(2), 207–221. https://doi.org/10.1016/j.molcel.2016.03.016

Kato, H., Goto, D. B., Martienssen, R. A., Urano, T., Furukawa, K., & Murakami, Y. (2005). Molecular Biology: RNA polymerase II is required for RNAi-dependent

heterochromatin assembly. *Science*, *309*(5733), 467–469. https://doi.org/10.1126/science.1114955

Keller, C., Adaixo, R., Stunnenberg, R., Woolcock, K. J., Hiller, S., & Bühler, M. (2012). HP1 Swi6 Mediates the Recognition and Destruction of Heterochromatic RNA Transcripts. *Molecular Cell*, *47*(2), 215–227. https://doi.org/10.1016/j.molcel.2012.05.009

Leopold, K., Stirpe, A., & Schalch, T. (2019). Transcriptional gene silencing requires dedicated interaction between hp1 protein chp2 and chromatin remodeler mit1. *Genes and Development*, *33*(9–10), 565–577. https://doi.org/10.1101/gad.320440.118

LeRoy, G., Weston, J. T., Zee, B. M., Young, N. L., Plazas-Mayorca, M. D., & Garcia, B. A. (2009). Heterochromatin protein 1 is extensively decorated with histone code-like post-translational modifications. *Molecular and Cellular Proteomics*, *8*(11), 2432–2442. https://doi.org/10.1074/mcp.M900160-MCP200

Maison, C., Bailly, D., Roche, D., De Oca, R. M., Probst, A. V., Vassias, I., Dingli, F., Lombard, B., Loew, D., Quivy, J. P., & Almouzni, G. (2011). SUMOylation promotes de novo targeting of HP1 ± to pericentric heterochromatin. *Nature Genetics*, *43*(3), 220–227. https://doi.org/10.1038/ng.765

Maksimov, V., Oya, E., Tanaka, M., Kawaguchi, T., Hachisuka, A., Ekwall, K., Bjerling, P., & Nakayama, J. I. (2018). The binding of Chp2's chromodomain to methylated H3K9 is essential for Chp2's role in heterochromatin assembly in fission yeast. *PLoS ONE*, *13*(8), 1–20. https://doi.org/10.1371/journal.pone.0201101

Meehan, R. R., Kao, C. F., & Pennings, S. (2003). HP1 binding to native chromatin in vitro is determined by the hinge region and not by the chromodomain. *EMBO Journal*, *22*(12), 3164–3174. https://doi.org/10.1093/emboj/cdg306

Min, J., Zhang, X., Cheng, X., Grewal, S. I. S., & Xu, R. M. (2002). Structure of the SET domain histone lysine methyltransferase Clr4. *Nature Structural Biology*, *9*(11), 828–832. https://doi.org/10.1038/nsb860

Mishima, Y., Watanabe, M., Kawakami, T., Jayasinghe, C. D., Otani, J., Kikugawa, Y., Shirakawa, M., Kimura, H., Nishimura, O., Aimoto, S., Tajima, S., & Suetake, I. (2013). Hinge and chromoshadow of HP1α participate in recognition of K9 methylated histone H3 in nucleosomes. *Journal of Molecular Biology*, *425*(1), 54–70. https://doi.org/10.1016/j.jmb.2012.10.018

Moreno, S., Klar, A., & Nurse, P. (1991). Molecular genetic analysis of fission yeast Schizosaccharomyces pombe. *Methods in Enzymology*, *194*(C), 795–823. https://doi.org/10.1016/0076-6879(91)94059-L

Motamedi, M. R., Hong, E. J. E., Li, X., Gerber, S., Denison, C., Gygi, S., & Moazed, D. (2008). HP1 Proteins Form Distinct Complexes and Mediate Heterochromatic Gene Silencing by Nonoverlapping Mechanisms. *Molecular Cell*, *32*(6), 778–790. https://doi.org/10.1016/j.molcel.2008.10.026

Motamedi, M. R., Verdel, A., Colmenares, S. U., Gerber, S., Gygi, S. P., & Moazed, D. (2004). Two RNAi Complexes, RITS and RDRC, Physically Interact and Localize to

Noncoding Centromeric RNAs. *Cell*, *119*(5), 603–614. https://doi.org/10.1016/j.cell.2004.11.009

Muramatsu, D., Kimura, H., Kotoshiba, K., Tachibana, M., & Shinkai, Y. (2016). Pericentric H3k9me3 formation by HP1 interaction-defective histone methyltransferase suv39h1. *Cell Structure and Function*, *41*(2), 145–152. https://doi.org/10.1247/csf.16013

Nakayama, J. I., Klar, A. J. S., & Grewal, S. I. S. (2000). A chromodomain protein, Swi6, perform imprinting functions in fission yeast during mitosis and meiosis. *Cell*, *101*(3), 307–317. https://doi.org/10.1016/S0092-8674(00)80840-5

Nakayama, J., Rice, J. C., Strahl, B. D., Allis, C. D., & Grewal, S. I. S. (2001). Role of histone H3 lysine 9 methylation in epigenetic control of heterochromatin assembly. *Science*, *292*(5514), 110–113. https://doi.org/10.1126/science.1060118

Nishibuchi, G., Machida, S., Nakagawa, R., Yoshimura, Y., Hiragami-Hamada, K., Abe, Y., Kurumizaka, H., Tagami, H., & Nakayama, J. I. (2019). Mitotic phosphorylation of HP1a regulates its cell cycle-dependent chromatin binding. *Journal of Biochemistry*, *165*(5), 433–446. https://doi.org/10.1093/jb/mvy117

Nishibuchi, G., Machida, S., Osakabe, A., Murakoshi, H., Hiragami-Hamada, K., Nakagawa, R., Fischle, W., Nishimura, Y., Kurumizaka, H., Tagami, H., & Nakayama, J. I. (2014). N-terminal phosphorylation of HP1α increases its nucleosome-binding specificity. *Nucleic Acids Research*, *42*(20), 12498–12511. https://doi.org/10.1093/nar/gku995

Nozawa, R. S., Nagao, K., Masuda, H. T., Iwasaki, O., Hirota, T., Nozaki, N., Kimura, H., & Obuse, C. (2010). Human POGZ modulates dissociation of HP1α from mitotic chromosome arms through Aurora B activation. *Nature Cell Biology*, *12*(7), 719–727. https://doi.org/10.1038/ncb2075

Paro, R., & Hogness, D. S. (1991). The Polycomb protein shares a homologous domain with a heterochromatin-associated protein of Drosophila. *Proceedings of the National Academy of Sciences of the United States of America*, *88*(1), 263–267. https://doi.org/10.1073/pnas.88.1.263

Rea, S., Eisenhaber, F., O'Carroll, D., Strahl, B. D., Sun, Z. W., Schmid, M., Opravil, S., Mechtier, K., Ponting, C. P., Allis, C. D., & Jenuwein, T. (2000). Regulation of chromatin structure by site-specific histone H3 methyltransferases. *Nature*, *406*(6796), 593–599. https://doi.org/10.1038/35020506

Sadaie, M., Kawaguchi, R., Ohtani, Y., Arisaka, F., Tanaka, K., Shirahige, K., & Nakayama, J. -i. (2008). Balance between Distinct HP1 Family Proteins Controls Heterochromatin Assembly in Fission Yeast. *Molecular and Cellular Biology*, *28*(23), 6973–6988. https://doi.org/10.1128/mcb.00791-08

Sadaie, Mahito, Iida, T., Urano, T., & Nakayama, J. I. (2004). A chromodomain protein, Chp1, is required for the establishment of heterochromatin in fission yeast. *EMBO Journal*, *23*(19), 3825–3835. https://doi.org/10.1038/sj.emboj.7600401

Schotta, G., Ebert, A., Krauss, V., Fischer, A., Hoffmann, J., Rea, S., Jenuwein, T., Dorn, R., & Reuter, G. (2002). Central role of Drosophila SU(VAR)3-9 in histone H3-K9 methylation and heterochromatic gene silencing. *EMBO Journal*, *21*(5), 1121–1131.

https://doi.org/10.1093/emboj/21.5.1121

Shimada, A., Dohke, K., Sadaie, M., Shinmyozu, K., Nakayama, J. I., Urano, T., & Murakami, Y. (2009). Phosphorylation of Swi6/HP1 regulates transcriptional gene silencing at heterochromatin. *Genes and Development*, *23*(1), 18–23. https://doi.org/10.1101/gad.1708009

Shimada, A., & Murakami, Y. (2010). Dynamic regulation of heterochromatin function via phosphorylation of HP1-family proteins. *Epigenetics*, *5*(1), 30–33. https://doi.org/10.4161/epi.5.1.10605

Singh, P. B., Miller, J. R., Pearce, J., Kothary, R., Burton, R. D., Paro, R., James, T. C., & J.gaunt, S. (1991). A sequence motif found in a Drosophila heterochromatin protein is conserved in animals and plants. *Nucleic Acids Research*, *19*(4), 789–794. https://doi.org/10.1093/nar/19.4.789

Smothers, J. F., & Henikoff, S. (2001). The Hinge and Chromo Shadow Domain Impart Distinct Targeting of HP1-Like Proteins. *Molecular and Cellular Biology*, *21*(7), 2555–2569. https://doi.org/10.1128/mcb.21.7.2555-2569.2001

Sugimoto, K., Yamada, T., Muro, Y., & Himeno, M. (1996). Human homolog of Drosophila heterochromatin-associated protein 1 (HP1) is a DNA-binding protein which possesses a DNA-binding motif with weak similarity to that of human centromere protein C (CENP-C). *Journal of Biochemistry*, *120*(1), 153–159. https://doi.org/10.1093/oxfordjournals.jbchem.a021378

Sugiyama, T., Cam, H. P., Sugiyama, R., Noma, K. ichi, Zofall, M., Kobayashi, R., & Grewal, S. I. S. (2007). SHREC, an Effector Complex for Heterochromatic Transcriptional Silencing. *Cell*, *128*(3), 491–504. https://doi.org/10.1016/j.cell.2006.12.035

Sun, J., Wang, X., Xu, R., Mao, D., Shen, D., Wang, X., Qiu, Y., Han, Y., Lu, X., Li, Y., Che, Q., Zheng, L., Peng, P., Kang, X., Zhu, R., Jia, Y., Wang, Y., Liu, L., Chang, Z., … Ni, J. (2021). HP1c regulates development and gut homeostasis by suppressing Notch signaling through Su(H). *EMBO Reports*, *22*(4), 1–16. https://doi.org/10.15252/embr.202051298

Suso Platero, J., Hartnett, T., & Eissenberg, J. C. (1995). Functional analysis of the chrome domain of HP1. *EMBO Journal*, *14*(16), 3977–3986. https://doi.org/10.1002/j.1460-2075.1995.tb00069.x

Thiru, A., Nietlispach, D., Mott, H. R., Okuwaki, M., Lyon, D., Nielsen, P. R., Hirshberg, M., Verreault, A., Murzina, N. V., & Laue, E. D. (2004). Structural basis of HP1/PXVXL motif peptide interactions and HP1 localisation to heterochromatin. *EMBO Journal*, *23*(3), 489–499. https://doi.org/10.1038/sj.emboj.7600088

Thon, G., & Verhein-Hansen, J. (2000). Four chromo-domain proteins of Schizosaccharomyces pombe differentially repress transcription at various chromosomal locations. *Genetics*, *155*(2), 551–568. https://doi.org/10.1093/genetics/155.2.551

Tien, C. L., Mohammadparast, S., & Chang, C. (2021). Heterochromatin protein 1 beta regulates neural and neural crest development by repressing pluripotency-associated

gene pou5f3.2/oct25 in Xenopus. *Developmental Dynamics*, *250*(8), 1113–1124. https://doi.org/10.1002/dvdy.319

Vermaak, D., & Malik, H. S. (2009). Multiple Roles for Heterochromatin Protein 1 Genes in Drosophila . *Annual Review of Genetics*, *43*(1), 467–492. https://doi.org/10.1146/annurev-genet-102108-134802

Wade Harper, J., Adami, G. R., Wei, N., Keyomarsi, K., & Elledge, S. J. (1993). The p21 Cdk-interacting protein Cip1 is a potent inhibitor of G1 cyclin-dependent kinases. *Cell*, *75*(4), 805–816. https://doi.org/10.1016/0092-8674(93)90499-G

Yeates, T. O. (2002). Structures of SET domain proteins: Protein lysine methyltransferases make their mark. *Cell*, *111*(1), 5–7. https://doi.org/10.1016/S0092-8674(02)01010-3

Zhao, T., Heyduk, T., Allis, C. D., & Eissenberg, J. C. (2000). Heterochromatin protein 1 binds to nucleosomes and DNA in vitro. *Journal of Biological Chemistry*, *275*(36), 28332–28338. https://doi.org/10.1074/jbc.M003493200